# ADDED MASSES AND FORCES ON TWO BODIES APPROACHING CENTRAL IMPACT IN AN INVISCID FLUID

Louis Landweber and Ali Shahshahan

IIHR Report No. 346

Iowa Institute of Hydraulic Research
The University of Iowa
Iowa City, Iowa 52242

January 1991

# Report Documentation Page

*Form Approved*
*OMB No. 0704-0188*



| 1. REPORT DATE | 2. REPORT TYPE | 3. DATES COVERED |
|---|---|---|
| **JAN 1991** | | **00-00-1991 to 00-00-1991** |

| 4. TITLE AND SUBTITLE | 5a. CONTRACT NUMBER |
|---|---|
| **Added Masses and Forces on Two Bodies Approaching Central Impact in an Inviscid Fluid** | 5b. GRANT NUMBER |
| | 5c. PROGRAM ELEMENT NUMBER |
| 6. AUTHOR(S) | 5d. PROJECT NUMBER |
| | 5e. TASK NUMBER |
| | 5f. WORK UNIT NUMBER |
| 7. PERFORMING ORGANIZATION NAME(S) AND ADDRESS(ES) **The University of Iowa,College of Engineering,IIHR - Hydroscience & Engineering,Iowa City,IA,52242-1585** | 8. PERFORMING ORGANIZATION REPORT NUMBER |
| 9. SPONSORING/MONITORING AGENCY NAME(S) AND ADDRESS(ES) | 10. SPONSOR/MONITOR'S ACRONYM(S) |
| | 11. SPONSOR/MONITOR'S REPORT NUMBER(S) |

12. DISTRIBUTION/AVAILABILITY STATEMENT
**Approved for public release; distribution unlimited**

13. SUPPLEMENTARY NOTES

14. ABSTRACT

15. SUBJECT TERMS

| 16. SECURITY CLASSIFICATION OF: | | | 17. LIMITATION OF ABSTRACT | 18. NUMBER OF PAGES | 19a. NAME OF RESPONSIBLE PERSON |
|---|---|---|---|---|---|
| a. REPORT **unclassified** | b. ABSTRACT **unclassified** | c. THIS PAGE **unclassified** | | **91** | |

# ADDED MASSES AND FORCES ON TWO BODIES APPROACHING CENTRAL IMPACT IN AN INVISCID FLUID

## ABSTRACT

In several papers, which will be referenced, a procedure based on integral equations has been developed and applied for determining the interaction forces on two bodies approaching central impact in an inviscid fluid. The present work was undertaken to evaluate the accuracy of the results from that procedure by applying it to a pair of circles and a pair of spheres with which one could obtain solutions, as accurate as desired, by the method of successive images. A second purpose was to refine the procedure so that accurate solutions could be obtained at closer distances than heretofore.

Solutions by the method of images, given by Hicks and Herman over 100 years ago, are not very clear, and since we have significantly extended their theory in the present work, it seemed appropriate to include a new derivation which we consider more rational. The extensions of the theory consists of:

1) a truncation correction of the infinite series of the doublet strengths for the added masses and their derivatives, which can then be calculated accurately with a moderate number of terms even when the gap between the bodies is very small;

2) asymptotic formulas for the added masses and their derivatives at small gaps which show that, for circles, the derivatives with respect to a parameter asymptotically proportional to the square root of the gap, are finite, and that derivatives with respect to the gap approach infinity inversely as the square root of the gap;

3) a treatment of the case of a circular cylinder or a sphere, or bodies of arbitrary shape approaching a wall, showing that the forces on the body and wall are repulsive and of equal magnitude;

4) a treatment of uniform convergence of the series for the added masses and their derivatives, which shows that the infinite series for the added-mass coefficients converge uniformly for all values of the gap in the closed region from zero to infinity; and that the series of the derivatives with respect to the parameter of item 2) converge uniformly for all values of the gap except zero, where the series converges but its sum is discontinuous.

In Part II, refinements of the integral-equation procedure are presented. Two problems required resolution for small gaps. One is the sharp peaks of the kernels of the

integral equations and of the source distributions on the body surfaces (the unknown functions of the integral equations) in the neighborhood of the gap. The other is that, previously, derivatives of the added masses, obtained by numerical differentiation, were inaccurate and gave large errors in the calculated forces. Simple solutions of both problems with the latter still using numerical differentiation, are presented. Applications to various combinations of circle pairs and to equal spheres gave agreement with exact values to six decimals for the added-mass coefficients and to five for their derivatives. To illustrate the applicability of the new procedures to a noncircular cylinder, the two cases of a 2 to 1 ellipse approaching a circle in the direction of its major or minor axes are also presented.

It is concluded that we now have the capability of obtaining accurate results for interaction forces for two-dimensional forms and bodies of revolution in an inviscid fluid.

## Table of Contents

## List of Tables

## List of Figures

## NOMENCLATURE

| | |
|---|---|
| $a$ | radius of circle or sphere |
| $a_1,a_2$ | lengths of semi-arcs of an ellipse |
| $a_n$ | nth term of a series |
| $b$ | radius of circle or sphere |
| $c$ | distance between centers of circles or spheres |
| $c'$ | derivative of c with respect to $\zeta$ |
| $c_1,c_2$ | closed curves of section of cylinders 1 and 2 |
| $d_n,d_n^*$ | distance of nth doublet within one cylinder or sphere from center of other |
| $g$ | gap or minimum distance between two bodies |
| $k_1,k_{12},k_2$ | added-mass coefficients |
| $\dot{k}_1,\dot{k}_{12},\dot{k}_2$ | derivatives of added-mass coefficients with respect to c or g |
| $k_1',k_{12}',k_2'$ | derivatives of added-mass coefficients with respect to $\zeta$ |
| $n$ | an index |
| $n_P,n_Q$ | outward normal distance at point P or Q of a body surface |
| $\hat{n}$ | unit vector along outward normal to a surface |
| $p_n$ | numerator of nth convergent of a continued fraction |
| $q_n$ | denominator of nth convergent of a continued fraction |
| $r_1,r_2$ | radial distances from center of circles 1 or 2 |
| $r_{PQ}$ | distance between points P and Q |
| $s$ | a+b; also arc length along $c_1$ or $c_2$ |
| $x_1,x_2$ | x-coordinates of centers of two circles or spheres |
| $A$ | area of section of a cylinder |
| $A_{11},A_{12},A_{22}$ | added masses |
| $C_1,C_2$ | curvatures of curves $c_1$ and $c_2$ |
| $C_{F1},C_{F2}$ | force coefficients for body 1 moving and body 2 and fluid at rest |
| $C_{F1}^*,C_{F2}^*$ | force coefficients for body 2 moving and body 1 and fluid at rest |
| $D$ | a factor of $r_{PQ}$ for two spheres |
| $E(\xi)$ | complete elliptic integral of second kind |
| $F_1,F_2$ | interaction forces on bodies |
| $K(\xi)$ | complete elliptic integral of first kind |
| $K(P,Q)$ | kernel of integral equation |

| | |
|---|---|
| $M_1$, $M_2$ | masses of displaced fluid |
| N | the number of terms of a truncated infinite series |
| P,Q | fixed and varying points on a body |
| $P_1', P_2'$ | point of minimum distance on body 1 from point $P_2$ on body 2, and on body 2 from point $P_1$ on body 1 |
| R*(N) | remainder due to truncating an infinite series at Nth term |
| R(N) | approximation to R*(N) by a trapezoidal integral |
| $R_1, R_2$ | radial distance from center of sphere 1 or sphere 2 |
| S | surface area of a three-dimensional body |
| T | kinetic energy of fluid |
| $U_1, U_2$ | velocity of translation of body 1 or 2 in direction of x-axis |
| | |
| $\alpha$ | defined by $\alpha^2 = c^2 - a^2 - b^2$ |
| $\beta$ | defined by $\beta^2 = ab$ |
| $\gamma$ | defined by $\gamma^2 = 2gs/\beta^2$ |
| $\delta_n, \delta_n^*$ | doublet strengths at distances $d_n$ or $d_n^*$ from centers of circles or spheres |
| $\zeta$ | parameter for expressing Herman's formulas in parametric form |
| $\eta$ | defined by $\eta = \alpha^2/\beta^2$ |
| $\theta_1, \theta_2$ | polar angle in circle 1 or 2; also angle with x-axis in spheres |
| $\theta_2'$ | supplement to $\theta_2$, i.e. $\theta_2' = \pi - \theta_2$ |
| $\theta_{P1'}, \theta_{P2'}$ | angles $\theta$ at points $P_1', P_2'$ for circles or spheres |
| $\lambda_1, \lambda_2$ | roots of quadratic equation $\lambda^2 - \alpha^2\lambda + \beta^2 = 0$ |
| $\mu$ | defined by $\mu = \beta/s$ |
| $\nu_1, \nu_2$ | defined by $\nu_1 = \frac{1}{2}(\pi - \psi_1)$, $\nu_2 = \frac{1}{2}(\pi - \psi_2)$ |
| $\xi, \xi'$ | parameter of elliptic integrals, $\xi^2 + \xi'^2 = 1$ |
| $\rho$ | mass density of fluid; also used as argument of power series |
| $\sigma_n$ | defined by $\lambda_1^n - \lambda_2^n$; $\sigma_1$, $\sigma_2$ also used as source strengths on bodies |
| $\sigma_{ij}$ | source distribution on the j-th body due to motion of the i-th |
| $\tau_n$ | defined by $\tau_n = \sigma_n/(\sigma_1\beta^{2n-2})$ |
| $\phi_1, \phi_2$ | unit potentials, defined by $\Phi = U_1\phi_1 + U_2\phi_2$ |
| $\psi_1, \psi_2$ | third coordinate of spherical coordinates in spheres 1 and 2 |
| $\omega$ | a function of $\theta_1$ or $\theta_2'$ used to apply the 'most accurate quadrature formula' with nonuniform intervals in $\theta$ |

| | |
|---|---|
| $\Sigma_2, \Sigma_3$ | defined in eqs. (41b) and (76) |
| $\Phi$ | total velocity potential due to translational motion of two bodies along their line of centroids when the fluid is at rest at infinity |

# Added Masses and Forces on Two Bodies Approaching Central Impact in an Inviscid Fluid

## Introduction

In connection with the problem of an ice mass approaching central impact with an offshore structure, it is important, for design purposes, to estimate the magnitude of the interaction force on the structure prior to and during impact. Previous literature on this problem was reviewed in papers by Landweber, Chwang, and Guo [1], and more recently by Guo and Chwang [2], [3], the latter two mainly on the broader problem of oblique impact, with some contributions on central-impact. In all of these papers, the fluid was assumed to be inviscid and the flow irrotational, so that the forces were entirely due to the inertia of the two bodies and the fluid.

As is shown in [1], for central impact, the interaction forces on the bodies due to the fluid can be expressed in terms of three added masses and their time derivatives. The added masses, at each of a succession of instants, are then obtained by applying generalizations of the Taylor added-mass formula, given by Landweber [4], Landweber & Yih [5], and Landweber and Chwang [6] to the sources and doublets on or in each body. The latter were obtained by solving, numerically and simultaneously, a pair of Fredholm integral equations of the second kind. These were solved by discretizing each integral equation into a set of linear equations.

Two major difficulties were encountered which affected the accuracy of the numerical results when the minimum distance between the bodies was small. One is due to the property that the integrands of the integral equations peak sharply at points of the body surfaces which are in the neighborhood of the eventual contact point when the bodies have nearly met; the other that the absolute value of the time derivatives of the added masses approach infinity as the bodies approach contact. Consequently, accurate results for the added-mass derivatives could not be obtained by direct application of numerical differentiation.

Techniques proposed for overcoming these two difficulties, described in three papers, were developed for a pair of circular cylinders, because, for

this case, results from the integral-equation solution can be compared against those from the method of successive images, which can be made as accurate as one desires. Isaacson and Cheung [7] resolved the peaking problem by increasing the number of points in the neighborhood of the peak, but gave no details concerning the quadrature formulas used. Nor was the problem of numerical differentiation of added masses mentioned.

In Ref. [1], "the most accurate quadrature formula" [8], hereafter called the MAQF, which requires a smooth, cyclic integrand and uniform intervals, was applied, with the number of points used increased as the gap between the bodies decreased. This procedure was inefficient, requiring a huge number of points at the smallest gaps, where the Cray supercomputer had to be used. The added-mass derivatives were obtained by using computer software to "smooth" the added-mass data before the numerical differentiation.

In Ref. [2], the peak was partially removed by a technique which is available when the kernel can be integrated exactly; see Miloh and Landweber [9]. Also, as in [7], the points on the circles were distributed so that at least half of their total number were concentrated in the small region of the peaks. This combination yielded good agreement with the results by successive images, but has the disadvantage that the procedure used to partially remove the peak of the kernel is not an option for bodies of arbitrary shape. To overcome the second difficulty, numerical differentiation was avoided by differentiating the integral equation pair and solving the set of four integral equations simultaneously for the source strengths and their derivatives. The kernels of these new integral equations and their solutions for the source-strength derivatives have much stronger peaks as the gap approaches zero, so that four Gauss quadrature formulas, each of order 40 were used to obtain accurate results at small gaps. The Cray supercomputer was required to perform these calculations. Since the solution of the original pair of integral equations had required most of the computer time, this procedure for avoiding numerical differentiation has more than doubled the computing effort on this problem.

In the present paper, simple resolutions of both difficulties are presented. For the first, the peak is removed by a procedure suitable for arbitrary shapes, and the variable of integration is changed so that many more points

are concentrated in the neighborhood of the peak, without sacrificing either the periodicity or the interval-uniformity condition for applying the MAQF. For the second, the variable of differentiation is changed so that the added masses vary nearly linearly with that parameter when the gap is small. In terms of that variable, the errors of numerical interpolation and differentiation are much less than with the original one.

The aforementioned change of differentiation variable is suggested by a parametric form of Herman's result [10] for the successive doublet strengths in the circles, which was also used, but for other purposes, by Mitra [11], and for a special case which will be described subsequently, by Shail [12]. By applying this form, efficient procedures for summing the doublet series for the added masses, and asymptotic formulas for the added masses and their derivatives at small gaps were developed. These are new results in the classical theory of successive images, which was considered to have been solved completely by Hicks [13, 14] and Herman [10] over one hundred years ago. Their papers on the motions of two spheres along the line of centers present two different closed-form solutions for the positions and strengths of the successive doublets. Their results for the positions are also valid for the motions of two circular cylinders, and, by a slight modification of their analysis, the strengths of the corresponding doublets can also be obtained. However, their derivations are difficult to comprehend, especially that of Hicks, partly because they did not take full advantage of the theory of continued fractions and recurring series which was well known at the time of their papers. Although a clearer derivation, based on these algebraic theories, had been devised by one of the present authors several years ago, it was not considered worth publishing at the time; but now that we have significantly extended the classical theory, it appears appropriate to include these developments as part of a new derivation of the successive-image formulas. Guo and Chwang [2] also show Herman's solution [8], but without derivation or attribution or any new results in the successive-image theory of circles or spheres moving along their line of centers. They also claim, that a "closed-form" solution for the added masses "will be derived", but that did not appear and, probably, does not exist.

The plan of the present paper is as follows. In Part I, a new derivation of Herman's formulas for the added-masses by the method of successive images will be presented, including a new, efficient, and accurate procedure for computing the added masses, which also yields their asymptotic formulas when the gap between the bodies is small. Since the added masses are obtained from an infinite series of doublet strengths, and this series must be differentiated term-by-term, it is important to investigate its uniform convergence. This was undertaken by Guo and Chwang [2,3], but their treatment is incomplete, proving only a necessary condition for ordinary convergence. Hence proofs of uniform convergence will be presented.

In Part II, the method of integral equations for obtaining the added masses will be treated. Procedures for reducing the peaks of the kernel and discretizing the integral equations by means of the MAQF, but with nonuniform intervals which concentrate points in the neighborhood of the peaks, will be presented. Lastly, a procedure for obtaining accurate results for the added-mass derivatives by numerical differentiation will be described. Added masses, their derivatives, and interaction forces for various cases will be computed and compared with the 'exact' results from Part I.

## Part I: Solution for a Pair of Circles or Spheres by Method of Successive Images

### 1. Recurrence formulas for doublet strengths; added masses

Circles of radii a and b are moving with velocities $U_1$ and $U_2$ along their line of centers which will be taken at the x-axis. Denote the centers of the circles by A and B, and their x-coordinates by $x_1$ and $x_2$. Put $c = x_2 - x_1$; see Fig. 1.

The fluid is assumed to be inviscid and incompressible and the flow irrotational. The velocity potential for the fluid, which is assumed to be at rest at infinity, and contain no other stationary or moving boundaries, may be written in the form

$$\Phi = U_1\phi_1 + U_2\phi_2 \tag{1}$$

where $\phi_1$ is the velocity potential when $U_1 = 1$ and $U_2 = 0$, and $\phi_2$ that when $U_2 = 1$ and $U_1 = 0$. In terms of separate polar coordinate systems $(r_1,\theta_1)$ and $(r_2,\theta_2)$ with centers at points A and B and $\theta_1$ and $\theta_2$ measured from the x-axis, the boundary conditions are

$$\left(\frac{\partial\phi_1}{\partial r_1}\right)_{r_1=a} = \cos\theta_1, \quad \left(\frac{\partial\phi_1}{\partial r_2}\right)_{r_2=b} = 0; \quad \left(\frac{\partial\phi_2}{\partial r_1}\right)_a = 0, \quad \left(\frac{\partial\phi_2}{\partial r_2}\right)_b = \cos\theta_2 \tag{2}$$

We shall apply the well-known method of successive doublet images at alternate inverse points in the circles to determine added masses and forces. For this purpose, we need to derive analytical expressions only for the case $U_1 = 1$, $U_2 = 0$, since that for $U_1 = 0$, $U_2 = 1$ could be obtained by permuting indices. For the doublets within the circle about A, let $d_{2n}$, $\delta_{2n}$, $n = 0, 1, 2,...$, denote the distances from B and their strengths, respectively. Also, for the doublets within the circle about B, let $d_{2n-1}$, $\delta_{2n-1}$, $n = 1, 2, 3,...$ denote the distances from A and their strengths. Then we have, successively,

$$d_o = c, \quad \delta_o = a^2, \quad \delta_{2n} = -\delta_{2n-1}\left(\frac{a}{d_{2n-1}}\right)^2, \quad \delta_{2n-1} = -\delta_{2n-2}\left(\frac{b}{d_{2n-2}}\right)^2 \tag{3}$$

which gives

$$\delta_{2n} = \delta_{2n-2}\left(\frac{ab}{d_{2n-2}d_{2n-1}}\right)^2 = \ldots = \frac{\delta_0(ab)^{2n}}{(d_0d_1d_2\ldots d_{2n-1})^2} \quad n = 0,1,2,\ldots \tag{4}$$

Then we obtain from (3)

$$\delta_{2n-1} = -\frac{(ab)^{2n}}{(d_0d_1d_2\ldots d_{2n-2})^2} \tag{5}$$

Here the d's are successively given by the inversion formulas

$$d_{2n} = c - \frac{a^2}{d_{2n-1}} \qquad d_{2n-1} = c - \frac{b^2}{d_{2n-2}} \tag{6}$$

The doublet strengths can then be computed successively from (3).

When circle B is moving with unit velocity in the positive x - direction and circle A is at rest, new sets of d's and δ's are generated. Let $d^*_{2n-1}$, $\delta^*_{2n-1}$, n = 1,2,3,... denote distances from A and the doublet strengths at those locations within circle B, and $d^*_{2n}$, $\delta^*_{2n}$, n = 0,1,2,... the distances from B and doublet strengths within circle A. Then (3) and (6) are modified, by interchanging a and b, to become

$$d^*_0 = c, \quad \delta^*_0 = b^2, \quad \delta^*_{2n} = -\delta^*_{2n-1}\left(\frac{b}{d^*_{2n-1}}\right)^2, \quad \delta^*_{2n-1} = -\delta^*_{2n-2}\left(\frac{a}{d^*_{2n-2}}\right)^2 \tag{7a}$$

$$d^*_{2n} = c - \frac{b2}{d^*_{2n-1}} \qquad d^*_{2n-1} = c - \frac{a2}{d^*_{2n-2}} \tag{7b}$$

Similarly,

$$\delta^*_{2n} = \frac{\delta^*_0(ab)^{2n}}{(d^*_0\, d^*_1\, d^*_2\ldots d^*_{2n-1})^2} \qquad \delta^*_{2n-1} = -\frac{(ab)^{2n}}{(d^*_0\, d^*_1\, d^*_2\ldots d^*_{2n-2})^2} \tag{8}$$

Although the recurrence formulas are identical with those of (3) and (6), the change in the initial values yields different sets of numbers for the d's and δ's.

As is shown in [1], three added masses, $A_{11}$, $A_{22}$ and $A_{12}$, occur in the equation of motion of a pair of bodies along their line of centroids when the fluid is at rest at infinity. Here $A_{11}$ and $A_{22}$ can be obtained from the generalized Taylor formulas of Landweber [4] for the three dimensional case, or of Landweber and Yih [5] for the two- and three-dimensional cases. These give expressions for the added masses of a moving body, when all other bodies and boundaries are at rest, in terms of the sum (or integrals) of the source moments and doublet strengths within or on the surface of the moving body. Reference [6], by Landweber and Chwang, gives a similar expression for $A_{12}$ in terms of the sources in or on a stationary body induced by the moving one. Guo and Chwang [2] noted that the contribution from the doublet strengths was not shown explicitly in [6] and included it in their formulation. That was an oversight in [6], although the source-moment formula could be considered to include the doublet strengths since the strength of a doublet is defined by the moment of its source-sink pair. The resulting expressions for the added masses for the two circular cylinders are then

$$A_{11} = \pi\rho\,(2\Sigma_0^{\infty}\,\delta_{2n} - a^2) = \pi\rho\,(a^2 + 2\Sigma_1^{\infty}\,\delta_{2n}) \tag{9}$$

$$A_{22} = \pi\rho\,(2\Sigma_0^{\infty}\,\delta^*_{2n} - b^2) = \pi\rho\,(b^2 + 2\Sigma_1^{\infty}\,\delta^*_{2n}) \tag{10}$$

$$A_{12} = 2\pi\rho\,\Sigma_1^{\infty}\,\delta^*_{2n-1} = 2\pi\rho\,\Sigma_1^{\infty}\,\delta_{2n-1} \tag{11}$$

Here ρ is the two-dimensional (2-D) mass density of the fluid.

If the bodies are spheres instead of circular cylinders, then the positions of the successive doublet images are also given by (6) and (7), but the strengths of the doublets are altered. Instead of (3), (4), (5), (7) and (8), we would have

$$d_o = c \quad \delta_o = \frac{1}{2}a^3 \quad \delta_{2n} = -\,\delta_{2n-1}\left(\frac{a}{d_{2n-1}}\right)^3 \quad \delta_{2n-1} = -\,\delta_{2n-1}\left(\frac{b}{d_{2n-2}}\right)^3 \tag{3'}$$

Then

$$\delta_{2n} = \delta_o \left[\frac{(ab)^n}{d_o d_1 \ldots d_{2n-1}}\right]^3 \tag{4'}$$

$$\delta_{2n-1} = -\delta_o \left[\frac{b(ab)^{n-1}}{d_o d_1 \ldots d_{2n-2}}\right]^3 = -\frac{1}{2}\left[\frac{(ab)^n}{d_o d_1 \ldots d_{2n-2}}\right]^3 \tag{5'}$$

and

$$d_o^* = c \quad \delta_o^* = \frac{1}{2}b^3 \quad \delta_{2n}^* = -\delta_{2n-1}^* \left(\frac{b}{d_{2n-1}^*}\right)^3 \quad \delta_{2n-1}^* = -\delta_{2n-2}^* \left(\frac{a}{d_{2n-2}^*}\right)^3 \tag{7'}$$

$$\delta_{2n}^* = \delta_o^* \left[\frac{(ab)^n}{d_o^* d_1^* \ldots d_{2n-1}^*}\right]^3 \quad \delta_{2n-1}^* = -\frac{1}{2}\left[\frac{(ab)^n}{d_o^* d_1^* \ldots d_{2n-1}^*}\right]^3 \tag{8'}$$

For the spheres, the three-dimensional form of the added-mass formula must be used. In terms of the masses of displaced fluid of the spheres, $M_1 = \frac{4}{3}\pi\rho a^3$ and $M_2 = \frac{4}{3}\pi\rho b^3$, where $\rho$ is the mass density of the fluid, we obtain

$$A_{11} = 4\pi\rho \sum_0^\infty \delta_{2n} - M_1 = 4\pi\rho\left(\sum_1^\infty \delta_{2n} + \frac{1}{6}a^3\right) = \frac{M_1}{2}\left(1 + \frac{6}{a^3}\sum_1^\infty \delta_{2n}\right) \tag{9'}$$

$$A_{22} = \frac{M_2}{2}\left(1 + \frac{6}{b^3}\sum_1^\infty \delta_{2n}^*\right) \tag{10'}$$

$$A_{12} = 4\pi\rho \sum_1^\infty \delta_{2n-1} = 4\pi\rho \sum_1^\infty \delta_{2n-1}^* \tag{11'}$$

Because the subsequent derivations of the d's and $\delta$'s for the circular cylinders and the spheres are very similar, only those for the former will be presented, and the corresponding results for spheres will be collected in a separate section.

## 2. Forces; added-mass derivatives

Once the added masses are known, the interaction forces $F_1$ and $F_2$ on the bodies can be obtained from Lagrange's form of the equations of motion

$$\frac{d}{dt}\frac{\partial T}{\partial U_1} - \frac{\partial T}{\partial x_1} = -F_1 \tag{12}$$

$$\frac{d}{dt}\frac{\partial T}{\partial U_2} - \frac{\partial T}{\partial x_2} = -F_2 \tag{13}$$

as is shown in Ref. [1]. Here T denotes the kinetic energy of the fluid,

$$2T = A_{11}U_1^2 + 2A_{12}\,U_1U_2 + A_{22}U_2^2 \tag{14}$$

Expressions for $F_1$ and $F_2$ given in [1] reduce, for the special case that will be considered in the present paper, that $U_1$ and $U_2$ are constants, to

$$F_1 = \frac{1}{2}\dot{A}_{11}U_1^2 - \dot{A}_{11}U_1U_2 - (\dot{A}_{12} + \frac{1}{2}\dot{A}_{22})\,U_2^2 \tag{15}$$

$$F_2 = (\frac{1}{2}\dot{A}_{11} + \dot{A}_{12})\,U_1^2 + \dot{A}_{22}\,U_1U_2 - \frac{1}{2}\dot{A}_{22}\,U_2^2 \tag{16}$$

where the dot over a symbol indicates differentiation with respect to c. In the more general formulas for $F_1$ and $F_2$, both the added masses and their derivatives appear.

In any case, the added-mass derivatives play an important role. These, obtained by differentiating (9), (10) and (11), are given by

$$\dot{A}_{11} = 2\pi\rho\Sigma_1^{\infty}\,\dot{\delta}_{2n} \qquad \dot{A}_{22} = 2\pi\rho\Sigma_1^{\infty}\,\dot{\delta}^{*}_{2n}$$

$$\dot{A}_{12} = 2\pi\rho\Sigma_1^{\infty}\,\dot{\delta}_{2n-1} = 2\pi\rho\Sigma_1^{\infty}\,\dot{\delta}^{*}_{2n-1} \tag{17}$$

and recurrence formulas for obtaining successive values of the $\delta$'s can be derived by differentiating (3), (6), (7) and (8). This gives for circles

$$\dot{\delta}_{2n} = \frac{a^2}{d_{2n-1}^2}\left(\frac{2\delta_{2n-1}}{d_{2n-1}}\dot{d}_{2n-1} - \dot{\delta}_{2n-1}\right), \quad \dot{\delta}_{2n-1} = \frac{b^2}{d_{2n-2}^2}\left(\frac{2\delta_{2n-2}}{d_{2n-2}}\dot{d}_{2n-2} - \dot{\delta}_{2n-2}\right), \quad \dot{\delta}_o = 0$$

$$\dot{d}_{2n} = 1 + \left(\frac{a}{d_{2n-1}}\right)^2 \dot{d}_{2n-1}, \quad \dot{d}_{2n-1} = 1 + \left(\frac{b}{d_{2n-2}}\right)^2 \dot{d}_{2n-2}, \quad \dot{d}_o = 1 \qquad (18)$$

Similarly we obtain for spheres

$$\dot{\delta}_{2n} = \frac{a^3}{d_{2n-1}^3}\left(\frac{3\delta_{2n-1}}{d_{2n-1}} - \dot{\delta}_{2n-1}\right) \quad \dot{\delta}_{2n-1} = \frac{b^3}{d_{2n-2}^3}\left(\frac{3\delta_{2n-2}}{d_{2n-2}} - \dot{\delta}_{2n-2}\right) \quad \dot{\delta}_o = 0 \qquad (18')$$

with the same equation as in (18) for the $\dot{d}$'s. The formulas for the $\dot{\delta}^*$ and $\dot{d}^*$ are the same, except that a and b are interchanged.

## 3. Solutions for the locations and strengths of the doublets

We have, by (6),

$$d_o = c, \quad d_1 = c - \frac{b^2}{c} \qquad d_2 = c - \frac{a^2}{d_1} = c - \frac{a^2}{c - \frac{b^2}{c}} \qquad d_3 = c - \frac{b^2}{c - \frac{a^2}{c - b^2/c}}$$

and in general, in the usual notation for a continued fraction,

$$d_{2n-1} = c - \frac{b^2}{c_1 -}\frac{a^2}{c_2 -}\frac{b^2}{c_3 -} \cdots \frac{b^2}{c_{2n-1}} \qquad d_{2n} = c - \frac{a^2}{c_1 -}\frac{b^2}{c_2 -} \cdots \frac{b^2}{c_{2n}} \qquad (19)$$

where the subscripts on the c's serve only to count the number of fractions, i.e. $c_1 = c_2 = c_3 = \ldots = c$.

Put $$d_{2n-1} = c - \frac{p_{2n-1}}{q_{2n-1}} \qquad d_{2n} = c - \frac{p_{2n}}{q_{2n}} \qquad (20)$$

Since the p's and q's with odd and even indices are defined by different continued fractions in (19), these do not satisfy the usual recurrence relation for

successive convergents of continued-fraction theory. An alternative, simple recurrence formula is satisfied, however, and this will now be derived.

We have, by (19),

$$\frac{p_{2n-1}}{q_{2n-1}} = \frac{b^2}{c - \dfrac{a^2}{c - \dfrac{p_{2n-3}}{q_{2n-3}}}} = \frac{b^2(cq_{2n-3} - p_{2n-3})}{(c^2-a^2)q_{2n-3} - cp_{2n-3}}$$

Then we may put

$$p_{2n-1} = b^2(cq_{2n-3} - p_{2n-3}), \quad q_{2n-1} = (c^2-a^2)q_{2n-3} - cp_{2n-3}$$

Then

$$q_{2n-3} = \frac{1}{b^2c}(p_{2n-1} + b^2p_{2n-3})$$

and substituting this and the corresponding expression for $q_{2n-1}$ into the second of the previous equations, we obtain the recurrence formula

$$p_{2n+1} = \alpha^2 p_{2n-1} - \beta^4 p_{2n-3} \tag{21}$$

where

$$\alpha^2 = c^2 - a^2 - b^2, \quad \beta^2 = ab \tag{22}$$

Similarly, eliminating $p_{2n-1}$ and $p_{2n-3}$ from the same pair of equations, yields the same recurrence formula for the q's,

$$q_{2n+1} = \alpha^2 q_{2n-1} - \beta^4 q_{2n-3} \tag{23}$$

Since the coefficients $\alpha^2$ and $\beta^4$ are symmetric in a and b, this recurrence formula is also applicable to the p's and q's with even indices; i.e. we have

$$p_{2n} = \alpha^2 p_{2n-2} - \beta^4 p_{2n-4}, \quad q_{2n} = \alpha^2 q_{2n-2} - \beta^4 q_{2n-4} \tag{24}$$

With the initial values

$$p_0 = 0 \quad q_0 = 1 \quad p_2 = ca^2 \quad q_2 = c^2 - b^2$$

$$p_1 = b^2 \quad q_1 = c \quad p_3 = b^2(c^2-b^2) \quad q_3 = c\alpha^2 \tag{25}$$

the values of $d_{2n}$ and $d_{2n+1}$ can be successively calculated from the recurrence formula (24), although the formulas given in (6) are more convenient for this purpose. By means of the former, however, exact closed-form expressions for $d_{2n}$ and $d_{2n+1}$ can be derived.

It is shown, in the theory of recurring series, that a sequence such as $\{p_{2n+1}\}$ which is linearly related, with constant coefficients, to the two previous members of the sequence, has a generating function given by

$$\frac{p_1 + (p_3 - \alpha^2 p_1)x}{1 - \alpha^2 x + \beta^4 x^2} = \sum_{n=0}^{\infty} p_{2n+1} x^n$$

This is readily verified by multiplying the equation by $1-\alpha^2 x + \beta^4 x^2$. Then, by (25),

$$\frac{b^2(1 + a^2 x)}{1 - \alpha^2 x + \beta^4 x^2} = \sum_{n=0}^{\infty} p_{2n+1} x^n \tag{26}$$

Similarly we obtain for the other three sequences

$$\frac{c}{1-\alpha^2 x + \beta^4 x^2} = \sum_{n=0}^{\infty} q_{2n+1} x^n \tag{27}$$

$$\frac{ca^2 x}{1-\alpha^2 x+\beta^4 x^2} = \sum_{n=1}^{\infty} p_{2n} x^n \tag{28}$$

$$\frac{1+a^2 x}{1 - \alpha^2 x + \beta^4 x^2} = \sum_{n=0}^{\infty} q_{2n} x^n \tag{29}$$

The quadratic denominator may be written as

$$1 - \alpha^2 x + \beta^4 x^2 = (1 - \lambda_1 x)(1-\lambda_2 x) \tag{30}$$

where

$$\lambda_{1,2} = \frac{1}{2}(\alpha^2 \pm \sigma_1), \quad \sigma_1 = \lambda_1 - \lambda_2 = (\alpha^4 - 4\beta^4)^{1/2} \tag{31}$$

Here $\lambda_{1,2}$ are real since

$$c^2 \geq (a+b)^2$$

and then $$c^2 - a^2 - b^2 = \alpha^2 \geq 2\beta^2.$$

Hence writing

$$\frac{1}{(1-\lambda_1 x)(1-\lambda_2 x)} = \frac{1}{\lambda_1-\lambda_2}\left(\frac{\lambda_1}{1-\lambda_1 x} - \frac{\lambda_2}{1-\lambda_2 x}\right) = \frac{1}{\sigma_1}\Sigma_0^{\infty}\sigma_{n+1}x^n, \quad \sigma_n = \lambda_1^n - \lambda_2^n$$

and

$$\frac{x}{(1-\lambda_1 x)(1-\lambda_2 x)} = \frac{1}{\sigma_1}\Sigma_1^{\infty}\sigma_n x^n$$

we obtain from (26, 27, 28, 29, 30)

$$p_{2n+1} = \frac{b^2}{\sigma_1}(\sigma_{n+1} + a^2\sigma_n), \quad q_{2n+1} = \frac{c\sigma_{n+1}}{\sigma_1} \tag{32}$$

$$p_{2n} = \frac{ca^2\sigma_n}{\sigma_1}, \quad q_{2n} = \frac{\sigma_{n+1} + a^2\sigma_n}{\sigma_1} \tag{33}$$

Then, by (20),

$$d_{2n} = \frac{c\sigma_{n+1}}{\sigma_{n+1} + a^2\sigma_n} \qquad d_{2n+1} = \frac{(c^2-b^2)\sigma_{n+1} - \beta^4\sigma_n}{c\sigma_{n+1}} = \frac{\sigma_{n+2}+a^2\sigma_{n+1}}{c\sigma_{n+1}} \tag{34}$$

since $c^2 - b^2 = \alpha^2 + a^2$ and by (31),

$$\lambda_i^2 = \alpha^2\lambda_i - \beta^4, \quad i = 1,2$$

This gives the locations of the successive doublets.

In order to find their strengths, we see from (4) and (5) that the products of the d's are required. From (34), we obtain

$$d_{2n-2}\, d_{2n-1} = \frac{\sigma_{n+1} + a^2\sigma_n}{\sigma_n + a^2\sigma_{n-1}}$$

Hence

$$d_0 d_1 d_2 \ldots d_{2n-1} = \frac{\sigma_{n+1} + a^2\sigma_n}{\sigma_1}$$

Also, by (34),

$$(d_0 d_1 \ldots d_{2n-3}) d_{2n-2} = \frac{\sigma_n + a^2\sigma_{n-1}}{\sigma_1} \cdot \frac{c\sigma_n}{\sigma_n + a^2\sigma_{n-1}} = \frac{c\sigma_n}{\sigma_1}$$

Hence (4) and (5) give

$$\delta_{2n} = \left[\frac{a\beta^{2n}\sigma_1}{\sigma_{n+1}+a^2\sigma_n}\right]^2, \quad \delta_{2n-1} = -\left[\frac{\beta^{2n}\sigma_1}{c\sigma_n}\right]^2 \tag{35}$$

The corresponding results for the case that $U_1 = 0$ and $U_2 = 1$ can be obtained from (34) and (35) by substituting $d^*_{2n}$ and $d^*_{2n+1}$ for $d_{2n}$ and $d_{2n+1}$, $\delta^*_{2n}$ and $\delta^*_{2n-1}$ for $\delta_{2n}$ and $\delta_{2n-1}$, and interchanging a and b, i.e.

$$d^*_{2n} = \frac{c\sigma_{n+1}}{\sigma_{n+1}+b^2\sigma_n} \quad d^*_{2n+1} = \frac{\sigma_{n+2}+b^2\sigma_{n+1}}{c\sigma_{n+1}} \quad n = 0,1,2,\ldots \tag{36}$$

$$\delta^*_{2n} = \left[\frac{b\beta^{2n}\sigma_1}{\sigma_{n+1}+b^2\sigma_n}\right]^2 \quad \delta^*_{2n-1} = -\left[\frac{\beta^{2n}\sigma_1}{c\sigma_n}\right]^2 \tag{37}$$

Results (34) and (36) for the locations of the successive doublets were first derived by Herman [10] for a pair of spheres. With a slight modification of his derivation, one can obtain the results (35) and (37) for the strengths of the doublets for a pair of circular cylinders. Here only the derivation of the Herman formulas is new. These are also presented by Guo and Chwang [2], but without attribution or derivation.

## 4. Solutions for added-mass coefficients

The nondimensional added-mass coefficients are defined by

$$k_1 = A_{11}/M_2, \quad k_2 = A_{22}/M_2, \quad k_{12} = A_{12}/M_2; \quad M_2 = \pi\rho b^2 \tag{38}$$

Then, by (9), (10), (11), (35) and (37), the coefficients are given by

$$k_1 = \frac{a^2}{b^2}\left(1 + \frac{2}{a^2}\Sigma_1^{\infty}\delta_{2n}\right) = \frac{a^2}{b^2}\left[1 + 2\Sigma_1^{\infty}\left(\frac{\beta^{2n}\sigma_1}{\sigma_{n+1} + a^2\sigma_n}\right)^2\right] \tag{39}$$

$$k_2 = 1 + \frac{2}{b^2}\Sigma_1^{\infty}\overset{*}{\delta}_{2n} = 1 + 2\Sigma_1^{\infty}\left(\frac{\beta^{2n}\sigma_1}{\sigma_{n+1}+b^2\sigma_n}\right)^2 \tag{40}$$

$$k_{12} = \frac{2}{b^2}\Sigma_1^{\infty}\delta_{2n-1} = -\frac{2}{b^2}\Sigma_1^{\infty}\left[\frac{\beta^{2n}\sigma_1}{c\sigma_n}\right]^2 \tag{41}$$

In order to avoid very large numbers in computing $k_1$, $k_2$ and $k_{12}$, we define the nondimensional quantities

$$\eta = \alpha^2/\beta^2 \quad \sigma_n' = \sigma_n/\beta^{2n} \quad \lambda_1' = \lambda_1/\beta^2 \quad \lambda_2' = \lambda_2/\beta^2$$

Then (39), (40), and (41) become, in terms of $\tau_n = \sigma_n'/\sigma_1'$,

$$k_1 = \frac{a^2}{b^2}\left[1 + 2b^2\Sigma_1^{\infty}(b\tau_{n+1} + a\tau_n)^{-2}\right] \tag{39a}$$

$$k_2 = 1 + 2a^2\Sigma_1^{\infty}(a\tau_{n+1} + b\tau_n)^{-2} \tag{40a}$$

$$k_{12} = -\frac{2a^2}{c^2}\Sigma_1^{\infty}\tau_n^{-2} \tag{41a}$$

and from (31),

$$\sigma_1' = (\eta^2-4)^{1/2} \quad \lambda_{1,2}' = \frac{1}{2}\left[\eta \pm (\eta^2-4)^{1/2}\right] \tag{42}$$

The forms in (42) suggest the substitution

$$\eta = 2\cosh\zeta \tag{43}$$

which yields

$$\sigma_1' = 2\sinh\zeta \quad \lambda_{1,2}' = e^{\pm\zeta} \quad \sigma_n' = 2\sinh n\zeta \tag{44}$$

Since, hereafter, only the nondimensional forms of $\lambda_1, \lambda_2$ and $\sigma_n$ will be used, the primes on these quantities will be omitted. Then, since

$$\tau_n = \frac{\sinh n\zeta}{\sinh \zeta} \tag{45}$$

by (44), the added-mass coefficients may be written in the third form

$$k_1 = \frac{a^2}{b^2}\{1 + 2b^2 \Sigma_1^\infty \frac{\sinh^2\zeta}{[b \sinh(n+1)\zeta + a \sinh n\zeta]^2}\} \tag{39b}$$

$$k_2 = 1 + 2a^2\Sigma_1^\infty \frac{\sinh^2\zeta}{[a \sinh(n+1)\zeta + b \sinh n\zeta]^2} \tag{40b}$$

$$k_{12} = -\frac{2a^2}{c^2}\Sigma_2(\zeta) \quad \Sigma_2(\zeta) = \Sigma_1^\infty \frac{\sinh^2\zeta}{\sinh^2 n\zeta} \tag{41b}$$

It will be shown that the parametric forms, (39b, 40b, 41b), which appear to be new except for Shail's result described below, play an important role in summing the three infinite series and investigating their uniform convergence, and enable the asymptotic behavior of the added masses and their derivatives to be determined when the gap between the circles is very small.

The same parameter $\zeta$ was introduced by Mitra [11] and Shail [12] in their treatments of two-sphere problems by the method of successive approximations using correction potentials. Mitra solved only the electrostatic condenser problem. Shail applied Mitra's analytical method to the hydrodynamic problem of two spheres moving along their line of centers, but gave specific results only for the case of a sphere approaching or moving away from a wall along its normal. His result for $k_2$ agrees with that in (75a) when the wall is treated as a sphere of infinite radius.

We shall now show that, even when $\zeta$ is small, n need not be taken very large in evaluating the infinite series (39b, 40b, 41b). To illustrate the procedure to be used, let us apply it to evaluate numerically the series

$\Sigma_1^\infty 1/n^2$. We shall see that this series is related to the value of $k_{12}$ at impact. It is well known that

$$\Sigma_1^\infty \frac{1}{n^2} = \frac{\pi^2}{6} = 1.644934... \tag{46}$$

This may be written as

$$\Sigma_1^N \frac{1}{n^2} + R^*(N), \quad R^*(N) = \Sigma_{N+1}^\infty \frac{1}{n^2}$$

Interpreting the remainder R*(N) as the trapezoidal rule for the integral

$$R(N) = \int_{N+\frac{1}{2}}^{\infty} \frac{dn}{n^2} = \frac{1}{N+\frac{1}{2}}$$

we obtain the values for the error in truncating the series at N shown in Table 1.

Thus the sums from 1 to N have errors of one in the first, second, and third decimals for N = 10, 100 and 1000 respectively, but essentially agree to four decimals at N = 10, and to at least six decimals at N = 100 and 1000 when corrected by the "remainder" given by the trapezoidal integral. Since the added-mass series converge faster than the series (46), as will be shown, this suggests that adequate accuracy could be obtained with N = O(10), provided the n-th terms of the three added-mass series could be integrated into a closed form. That this is the case will now be shown.

Let us first consider $k_{12}$, which, by (41b) may be written as

$$-k_{12} \doteq \frac{2a^2}{c^2} \Sigma_1^N \frac{\sinh^2\zeta}{\sinh^2 n\zeta} + R_{12}(N), \quad R_{12}(N) = \frac{2a^2}{c^2} \int_{N+\frac{1}{2}}^{\infty} \frac{\sinh^2\zeta}{\sinh^2 n\zeta}\, dn \tag{47}$$

But

$$R_{12}(N) = -\frac{2a^2}{c^2\zeta} \sinh^2\zeta \coth n\zeta \Big|_{N+\frac{1}{2}}^{\infty} = \frac{2a^2}{c^2\zeta} \frac{\sinh^2\zeta}{\sinh(N+\frac{1}{2})\zeta} \exp[-(N+\tfrac{1}{2})\zeta] \tag{48}$$

As $\zeta$ approaches zero, we obtain from (48) the limiting value

$$k_{12}(0) = -\frac{2a^2}{c^2}\Sigma_1^{\infty}\frac{1}{n^2} = -\frac{\pi^2 a^2}{3s^2} = -3.289868\cdots\frac{a^2}{s^2} \qquad s = a+b \tag{49}$$

The limiting value of $[\partial k_{12}(\zeta)/\partial\zeta]_{\zeta=0}$ can also be obtained from (48). Since each term of the truncated series is an even function of $\zeta$, its derivative is zero at $\zeta = 0$. Also, as $\zeta \to 0$ for a fixed N,

$$\frac{2a^2}{c^2\zeta}\sinh^2\zeta\,[\coth(N+\tfrac{1}{2})\,\zeta - 1] \approx \frac{2a^2}{c^2}\left(\frac{1}{N+\frac{1}{2}} - \zeta\right)$$

Hence, indicating differentiation with respect to $\zeta$ hereafter by a prime, we have

$$k'_{12}(0) = \frac{2a^2}{s^2} \tag{50}$$

and

$$k_{12}(\zeta) \approx -\frac{2a^2}{s^2}\left(\frac{\pi^2}{6} - \zeta\right) \tag{51}$$

Next consider $k_2(\zeta)$, written in the form

$$k_2(\zeta) \doteq 1 + \Sigma_1^N \frac{2a^2\sinh^2\zeta}{[a\sinh(n+1)\zeta + b\sinh n\zeta]^2} + R_2(N,\zeta) \tag{52}$$

where

$$R_2 = \int_{N+\frac{1}{2}}^{\infty} \frac{2a^2\sinh^2\zeta\,dn}{[a\sinh(n+1)\zeta + b\sinh n\zeta]^2} = \frac{2a\sinh\zeta\sinh n\zeta}{\zeta[a\sinh(n+1)\zeta + b\sinh n\zeta]}\Big|_{N+\frac{1}{2}}^{\infty}$$

At the upper limit, we have

$$\frac{\sinh(n+1)\zeta}{\sinh n\zeta} \approx \frac{e^{(n+1)\zeta}}{e^{n\zeta}} = e^{\zeta}$$

Then

$$R_2 = \frac{2a \sinh \zeta}{\zeta(ae^{\zeta} + b)} - \frac{2a \sinh \zeta \sinh(N+\frac{1}{2})\zeta}{\zeta[a \sinh(N+\frac{3}{2})\zeta + b \sinh(N+\frac{1}{2})\zeta]}$$

$$= \frac{2a^2 \sinh^2\zeta \cdot \exp[-(N+\frac{1}{2})\zeta]}{\zeta(ae^{\zeta}+b)[a(\cosh \zeta + \coth(N+\frac{1}{2})\zeta \sinh\zeta) + b]} \tag{53}$$

Here also only the term from the upper limit of the integral contributes to the coefficient of $\zeta$ in the Taylor expansion of $k_2$ about $\zeta = 0$, since the other terms are even functions. As $\zeta \to 0$, we obtain

$$R_2(\zeta) \approx \frac{2a}{s+a\zeta} \approx \frac{2a}{s}(1 - \frac{a}{s}\zeta) \tag{54}$$

Then

$$k_2'(0) = -\frac{2a^2}{s^2} \tag{55}$$

We then have

$$k_2(\zeta) \approx k_2(0) - \frac{2a^2}{s^2}\zeta \tag{56}$$

where, by (52) with $N = \infty$ and $\zeta \to 0$, we obtain the convergent series

$$k_2(0) = 1 + \Sigma_1^{\infty} \frac{2a^2}{(sn+a)^2} \tag{57}$$

Similarly, we find

$$k_1(\zeta) = \frac{a^2}{b^2}\{1 + \Sigma_1^{\infty} \frac{2b^2 \sinh^2\zeta}{[b \sinh(n+1)\zeta + a \sinh n\zeta]^2}\} \approx k_1(0) - \frac{2a^2}{s^2}\zeta \tag{58}$$

where

$$k_1(0) = \frac{a^2}{b^2}[1 + \Sigma_1^{\infty} \frac{2b^2}{(sn+b)^2}] \tag{59}$$

The linear variation of $k_1$ and $k_{12}$ with $\zeta$ is shown graphically in Fig. 2 for the case a = b, for which (58) and (59) become

$$k_1(0) = k_2(0) = 1 + 2\Sigma_1^{\infty} \frac{1}{(2n+1)^2} = \frac{\pi^2}{4} - 1 = 1.467401... \tag{60}$$

The results for $k_1(0)$, $k_2(0)$ and $k_{12}(0)$, corresponding to c = a+b, were given by Guo and Chwang [2]. The expressions for $k_1'(0)$, $k_2'(0)$ and $k_{12}'(0)$, however, are believed to be new. We see that the three added-mass coefficients have slopes of the same magnitude at $\zeta$=0. The remainder $R_1(\zeta)$, obtained from (53) by interchanging a and b and multiplying by $a^2/b^2$, becomes

$$R_1(\zeta) = \frac{2a^2 \sinh^2\zeta \cdot \exp[-(N+\frac{1}{2})\zeta]}{\zeta(be^{\zeta}+a)[b(\cosh\zeta+\coth(N+\frac{1}{2})\zeta\ \sinh\zeta)+a]} \tag{61}$$

## 5. Asymptotic formulas for small gaps

The principal mathematical parameter in the foregoing equations is $\zeta$, which was defined in (43). The principal physical parameter is the gap g between the circles, given by c = s+g. When g/b and a/b are given, then $\eta$ and $\sigma_1 = (\eta^2-4)^{1/2}$ are also known, and $\zeta$ can be found by (43) or (44) by inverting either the hyperbolic cosine or sine. When g is relatively small, however, the relation between these parameters becomes very simple and useful. This relation will now be derived.

We define the nondimensional quantities $\gamma$ and $\mu$ by

$$\gamma = (\frac{2sg}{\beta^2})^{1/2} \quad \mu = \frac{\beta}{s} \quad \mu^2\gamma^2 = \frac{2g}{s} \tag{62}$$

Then, we obtain

$$\alpha^2 = (a + b + g)^2 - a^2 - b^2 = 2\beta^2 + 2sg + g^2 = 2\beta^2(1 + \frac{1}{2}\gamma^2 + \frac{1}{8}\mu^2\gamma^4)$$

and, by (43),

$$\cosh \zeta = 1 + \frac{1}{2}\gamma^2 + \frac{1}{8}\mu^2\gamma^4 \tag{63}$$

Since $\cosh \zeta = 1 + 2\sinh^2 (\zeta/2)$, then

$$\zeta = 2\sinh^{-1}Z = 2\left[Z - \frac{1}{6}Z^3 + \frac{3}{40}Z^5 - \cdots\right], \quad Z \le 1 \tag{64}$$

where, by (63),

$$Z = \frac{\gamma}{2}(1 + \frac{1}{4}\mu^2\gamma^2)^{1/2} = \frac{\gamma}{2}(1 + \frac{1}{8}\mu^2\gamma^2 - \frac{1}{128}\mu^4\gamma^4 + \cdots), \quad \mu^2\gamma^2 = \frac{2g}{s} \le 1$$

Substituting the series for Z into (64), we now obtain the asymptotic formula

$$\zeta \approx \gamma\left[1 - \frac{1}{24}(1 - 3\mu^2)\gamma^2 + \frac{1}{640}(3 - 10\mu^2 - 5\mu^4)\gamma^4\right] \tag{65}$$

Of the two convergence conditions, $Z \le 1$ and $2g/s \le 1$, the former is more stringent. The latter restricts g to the mean of the radii, $g = (a + b)/2$. The former can be expressed as

$$\frac{g}{s} \le \left(1 + \frac{4ab}{s^2}\right)^{1/2} - 1$$

in which the right member has a maximum value of $\sqrt{2} - 1$ when a = b, and is zero when the ratio of the radii, a/b, is zero or infinity. Even at the maximum value, we have $g/a \le 2(\sqrt{2} - 1) = 0.828...$ versus 1.0 from the other condition. Yet, as we shall see, (65) yields a useful approximation at g/a = 1. Although the infinite series, of which (65) is a truncation, diverges, that series belongs to the class of divergent series in which the error in using a partial sum is less than the next term of the series. Thus the partial sum is useful if the next term is very small.

According to (62) and (65), $\zeta$ is proportional to the square root of the gap g when the gap is very small. For example, (58) gives

$$k_1(\zeta) \approx k_1(0) - \frac{2a^2}{s^2}\left(\frac{2sg}{\beta^2}\right)^{1/2} \tag{66}$$

Then

$$\frac{dk_1}{dg} \approx \frac{a^2}{s^2}\left(\frac{2s}{\beta^2 g}\right)^{1/2} \to \infty \text{ as } g \to 0$$

in agreement with the known property that the slopes of the added-mass coefficients versus g become infinite as the gap approaches zero. That the asymptotic slope varies inversely as the square root of the gap, however, is believed to be a new result.

For small values of the gap, the asymptotic formula (65) yields highly accurate values of $\zeta$. For example, with a = b, we have $\mu = 1/2$ and $\gamma = 2\sqrt{g/a}$. Then, at $g/a = 0.25$, ($\gamma = 1$), (65) gives $\zeta = 0.989876$ and $\sinh \zeta/2 = 0.515394$ versus the exact value from (64), 0.515388. The agreement is even better at smaller gaps. At $g/a = 1$, (65) gives $\zeta = 1.92604$ and $\sinh \zeta/2 = 1.1189$ versus the exact value 1.1180. Thus the asymptotic formula for $\zeta(\gamma)$ is sufficiently accurate for values of $g/a \leq 1$.

Equations (62) through (65) are also valid for two spheres. The asymptotic law for that case, given in (78), differs from that for the circles in (66).

## 6. Derivatives of the added-mass coefficients

Recurrence formulas for calculating the derivatives of the added masses were given in (18). Since the accuracy may be improved by applying (39a), (40a) and (41a), expressions for the derivatives will now be derived on the basis of these equations. Derivatives with respect to $\zeta$ will now be indicated by the prime of a quantity; e.g., $d\tau/d\zeta = \tau'$. Then, from (39a, 40a and 41a), we obtain

$$k_1' = -4a^2 \Sigma_1^{\infty} (b\tau_{n+1} + a\tau_n)^{-3} (b\tau_{n+1}' + a\tau_n') \tag{67}$$

$$k_2' = -4a^2 \Sigma_1^{\infty} (a\tau_{n+1} + b\tau_n)^{-3} (a\tau_{n+1}' + b\tau_n') \tag{68}$$

$$k_{12}' = 4a^2 \Sigma_1^{\infty} (c\tau_n)^{-3} (c\tau_{n+1} + c\tau_n'), \quad c' = \frac{ab}{c} \sinh \zeta \tag{69}$$

in which c′ is obtained by differentiating $\alpha^2 = 2\beta^2 \cosh \zeta$. Also, by (45), we have

$$\tau_n' = \operatorname{csch} \zeta \, (n \cosh n\zeta - \tau_n \cosh \zeta) \tag{70}$$

with which the k′'s can be computed.

The trapezoidal-integral procedure for evaluating the remainder of a truncated infinite series may also be applied to the series of derivatives of the added-mass coefficients. To apply the method, it was necessary that the n-th term of the series be integrable in closed form with respect to n, as was shown to be the case for the parametric forms of the coefficients. Hence the n-th term of the series of their derivatives must also be so integrable since the order of performing differentiation with respect to $\zeta$ and integration with respect to n may be reversed; i.e., the integral of the derivative is given by the derivative of the integral that has already been obtained for the parametric form of the added-mass coefficients.

The method will now be demonstrated by evaluating $\Sigma_2'(\zeta)$. We obtain by (49)

$$\Sigma_2' \doteq \Sigma_1^N \frac{d}{d\zeta}\left(\frac{\sinh^2\zeta}{\sinh^2 n\zeta}\right) - \frac{d}{d\zeta}\frac{\sinh^2\zeta \coth n\zeta}{\zeta}\Bigg|_{N+\frac{1}{2}}^{\infty}$$

$$\doteq \Sigma_1^N \frac{2}{\tau_n^2}(\coth\zeta - n \coth n\zeta) - \frac{\sinh^2\zeta}{\zeta^2} \cdot$$

$$\cdot \left\{(2\,\zeta \coth \zeta - 1)\,[1 - \coth (N + \tfrac{1}{2})\zeta] + (N + \tfrac{1}{2})\,\zeta \operatorname{csch}^2(N + \tfrac{1}{2})\zeta\right\}$$

## 7. Convergence of the series for the added masses and their derivatives

In summing the series for the added-mass coefficients, it was observed that the terms of the series were even functions of $\zeta$, so that the derivative of each term with respect to $\zeta$ is zero at $\zeta = 0$. Thus, if the series of derivatives were uniformly convergent, its sum would also be zero at $\zeta = 0$, contrary to the results given in (51), (55) and (58). It is important, then to investigate the

convergence of the series for the added-mass coefficients in (39a), (40a) and for their derivatives in (67), (68) and (69).

This topic was treated by Guo and Chwang [2], but their treatment was flawed by several errors. One is that they refer to proving the uniform convergence of the sequence of the terms of a series $\{a_n\}$, instead of the sequence of partial sums $\{\Sigma_1^n a_r\}$. A second is that the simple ratio test $a_{n+1}/a_n < 1$ was used to "prove" uniform convergence, although that criterion is only a necessary condition for convergence; for example, it is satisfied by the divergent series $\Sigma_1^\infty (1/n)$. Thirdly, no attempt was made to prove uniform convergence of the original series in the closed region $0 \leq g \leq \infty$. Its convergence at $g = 0$, and uniform convergence in the open region $0 < g \leq \infty$, does not assure uniform convergence in $0 \leq g \leq \infty$ since the series may be discontinuous at $g = 0$. Lastly, although they are aware of the need to prove uniform convergence of the series of derivatives, the reason for undertaking to prove that the original series is uniformly convergent is not mentioned. Hence a reconsideration of this subject appears to be necessary.

First consider the series for $k_{12}$ in (41b). Since $\sinh n\zeta \geq n \sinh \zeta$, $0 \leq \zeta \leq \infty$, (as is seen from their Taylor expansions), then by (45), $\tau_n \geq n$ and $\tau_n^{-2} \leq 1/n^2$ for $0 \leq \zeta \leq \infty$. Since also $c \geq s$, then

$$\Sigma_1^\infty (c\tau_n)^{-2} \leq \Sigma_1^\infty (s\tau_n)^{-2} \leq s^{-2} \Sigma_1^\infty 1/n^2$$

Application of the Weierstrass comparison test with the series $\Sigma_1^\infty 1/n^2$ then shows that the series for $k_{12}$ is uniformly convergent in $0 \leq \zeta \leq \infty$.

Next consider the series for $k_2$ in (40a). We have

$$(a\tau_{n+1} + b\tau_n)^{-2} < (b\tau_n)^{-2} \leq (bn)^{-2}$$

Hence, by the same comparison test, the series for $k_2$ is uniformly convergent in $0 \leq \zeta \leq \infty$. Similarly, by interchanging a and b, we can show that the series for $k_1$ has the same property.

Since the terms of the three series are continuous functions, and the series are uniformly convergent in $0 \leq \zeta \leq \infty$, we conclude that the added-mass coefficients, as given by their series, are continuous functions. This was not obvious since the terms of the series involve sinh $n\zeta$ which is zero when $\zeta = 0$, no matter how large n may be, but becomes infinite as n approaches infinity no matter how small $\zeta$ may be.

To investigate the convergence of the series for $k_2'$, we consider its form given in (40b). For n very large, we have

$$\frac{\sinh \zeta}{a \sinh (n+1)\zeta + b \sinh n\zeta} \approx \frac{2e^{-n\zeta}\sinh \zeta}{ae^{\zeta} + b}$$

Then

$$\frac{d}{d\zeta}\left(\frac{e^{-n\zeta} \sinh \zeta}{ae^{\zeta} + b}\right)^2 \approx -\frac{2ne^{-2n\zeta} \sinh^2\zeta}{(ae^{\zeta} + b)^2} \qquad (71)$$

Put $\rho = e^{-2\zeta}$, and let N be a large value of n at which (71) is valid. Then (71) is seen to be proportional to the derivative of the power series $\Sigma_N^{\infty} \rho^n$ which, together with all its derivatives, is uniformly convergent within its 'circle of convergence', i.e., $0 < \zeta < \infty$, or $\rho < 1$. A similar proof verifies that the series for $k_1'$ in (39b) is uniformly convergent in the same open range.

For $k_{12}$ in (41a), the n-th term of the series is

$$a_n = -\frac{d}{d\zeta}\left(\frac{\sigma_1}{c\sigma_n}\right)^2 = \frac{2\sigma_1^2\sigma_n'}{c^2\sigma_n^2} + \frac{2c'\sigma_1^2}{c^3\sigma_n^2} - \frac{2\sigma_1\sigma_1'}{c^2\sigma_n^2}$$

where c' is given in (69). Since $\sigma_n = \tau_n\sigma_1$ and the series $\Sigma_1^{\infty}(1/\tau_n^2)$ has already been shown to converge uniformly in the closed region, we see that the series of the second and third terms also converge uniformly in that region. The first term, however, becomes asymptotically

$$\frac{2\sigma_1^2 n \cosh n\zeta}{c^2 \sinh^2 n\zeta} \approx \frac{4\sigma_1^2}{c^2} ne^{-n\zeta}$$

proportional to that in (71), for which uniform convergence in the open region has already been proved. Hence the series for $k'_{12}$ is also uniformly convergent in the open region $0 < \zeta \leq \infty$.

If the derivative series were uniformly convergent in the closed region, then $k'_1$ (0) (say) would have been zero since all the terms of the series are even functions; but this would contradict the results in (58). Hence there is a discontinuity in slope as $\zeta$ passes through zero from positive to (physically meaningless) negative values, with $k_1(\zeta) = k_1(-\zeta)$ and a sharp peak at $\zeta = 0$.

## 8. Results for spheres

Basic iteration formulas for the locations and strengths of successive doublets for a pair of spheres were given in eqs. (3') to (11'). These show that the only changes in the expressions for the doublet strengths from those for a pair of circles are a factor of 1/2 and changes from squares to cubes, correlated with the changes from $\delta_0 = a^2$ to $a^3/2$ and $\delta^*_0 = b^2$ to $b^3/2$. The formulas for the positions of the doublets remain the same. Thus we obtain

$$\delta_{2n} = \frac{1}{2}\left[\frac{ab\sigma_1}{b\sigma_{n+1}+a\sigma_n}\right]^3 = \frac{1}{2}\left[\frac{ab \sinh\zeta}{b \sinh(n+1)\zeta + a \sinh n\zeta}\right]^3 \qquad (72)$$

$$\delta_{2n-1} = -\frac{1}{2}\left[\frac{ab\sigma_1}{c\sigma_n}\right]^3 = -\frac{1}{2}\left[\frac{ab \sinh\zeta}{c \sinh n\zeta}\right]^3 = \delta^*_{2n-1} \qquad (73)$$

The expressions for $\delta^*_{2n}$ and $\delta^*_{2n-1}$ can be obtained from (72) and (73) by interchanging a and b.

The added-mass coefficients can now be obtained by substitution into [9'], [10'] and [11'] and dividing by $M_2 = \frac{4}{3}\pi\rho b^3$. This gives

$$k_1 = \frac{a^3}{2b^3}\{1 + 3\,\Sigma_1^{\infty}[\frac{b\sinh\zeta}{b\sinh(n+1)\zeta + a\sinh n\zeta}]^3\} \tag{74}$$

$$k_2 = \frac{1}{2}\{1 + 3\,\Sigma_1^{\infty}[\frac{a\sinh\zeta}{a\sinh(n+1)\zeta + b\sinh n\zeta}]^3\} \tag{75}$$

$$k_{12} = -\frac{3a^3}{2c^3}\Sigma_3(\zeta) \quad \Sigma_3 = \Sigma_1^{\infty}\frac{\sinh^3\zeta}{\sinh^3 n\zeta} \tag{76}$$

The general terms of the series (74, 75, 76) can also be integrated into closed-form expressions, so that the technique of applying the integral to evaluate the remainder after the N-th term may be used to obtain high accuracy with a moderate value of N. For (76), the integral to be evaluated is of the form

$$\int \sinh^r x\,dx$$

for which a reduction formula for positive or negative integral values of r is given in tables of integrals. In the present case, r = - 3, and the reduction formula reduces it to the known integral for r = - 1. The denominators of the terms of (74) and (75) can be expressed in the same form by writing that in (75), for example, in the form

$$a\sinh(n+1)\zeta + b\sinh n\zeta = (A\sinh n\zeta + B\cosh n\zeta) = \sqrt{A^2-B^2}\sinh(n\zeta+\mu)$$

$$A = a\cosh\zeta + b,\ B = a\sinh\zeta,\quad \coth\mu = A/B.$$

The actual integrals will be presented here only for (76) since we are mainly interested in the numerical results for pairs of cylinders in the present paper.

As in (49), we write

$$-k_{12} = \frac{3a^3}{2c^3}[\Sigma_1^N\frac{\sinh^3\zeta}{\sinh^3 n\zeta} + R_{12}(N)],\quad R_{12}(N) = \int_{N+\frac{1}{2}}^{\infty}\frac{\sinh^3\zeta}{\sinh^3 n\zeta}\,dn$$

and we find

$$R_{12}(N) + \frac{\sinh^3\zeta}{2\zeta}\left[\operatorname{csch}\left(N+\frac{1}{2}\right)\zeta\coth\left(N+\frac{1}{2}\right)\zeta + \ln\tanh\frac{2N+1}{4}\zeta\right] \quad (77)$$

As in the derivation of (51), the limiting value of $(dk_{12}/d\zeta)_{\zeta=0}$ can be obtained from (76) and (77). Again we see that all the terms of the truncated series and the first term of $R_{12}(N)$ are even functions of $\zeta$, so that only the ln-term can contribute to the derivative at $\zeta=0$. Then, for small values of $\zeta$, as $\zeta$ approaches zero for a fixed N, we obtain

$$k_{12}(\zeta) \approx k_{12}(0) - \frac{3a^3}{4s^3}\zeta^2\ln\zeta \quad (78)$$

$$k_{12}' \approx -\frac{3a^3}{2s^3}\zeta\ln\zeta \approx -\frac{3a^3}{2s^3}\gamma\ln\gamma \quad (78a)$$

since $\zeta\approx\gamma$ according to (65). This shows that $k_{12}'$ approaches zero as $\zeta$ approaches zero. The derivative with respect to c, however, is infinite since, by (69),

$$\frac{d}{dc}\left(\frac{1}{2}\zeta^2\ln\zeta\right) = \frac{d}{d\zeta}\left(\frac{1}{2}\zeta^2\ln\zeta\right)/c' \approx \frac{s}{\beta^2}\ln\zeta \to -\infty \text{ as } \zeta \to 0. \quad (79)$$

Similarly it can be shown that the derivatives of $k_1$ and $k_2$ with respect to $\zeta$ are zero, and with respect to c are infinite. Again, this implies that the spheres would never meet.

The series for the added-mass coefficients, given in (74), (75) and (76), converge for all values of $\zeta$, $0 \le \zeta \le \infty$. At $\zeta = 0$, we obtain

$$k_1(0) = \frac{a^3}{2b^3}\left\{1 + 3\Sigma_1^{\infty}\frac{b^3}{[na+(n+1)b]^3}\right\} \quad (80)$$

$$k_2(0) = \frac{1}{2}\left\{1 + 3\Sigma_1^{\infty}\frac{a^3}{[(n+1)a+nb]^3}\right\} \quad (81)$$

$$k_{12}(0) = -\frac{3a^3}{2s^3}\Sigma_1^{\infty}\frac{1}{n^3} = -\ 1.2020569...\frac{3a^3}{2s^3} \quad (82)$$

When a = b, we get

$$k_1(0) = k_2(0) = \frac{1}{2}[1 + 3\Sigma_1^{\infty} \frac{1}{(2n+1)^3}] = 0.5776997... \qquad (83)$$

The results in (80) to (83) were given by Hicks [13].

The proofs of uniform convergence of the series for $k_1(\zeta)$, $k_2(\zeta)$ and $k_{12}(\zeta)$ in the closed region $0 \leq \zeta \leq \infty$ for the two spheres are similar to those for the two circles, with the convergent series in (82) serving for the comparison test. The proofs of the uniform convergence of the series for $dk_1/d\zeta$, $dk_2/d\zeta$ and $dk_{12}/d\zeta$ in the open region $0 < \zeta \leq \infty$ are also similar, with $\rho$ defined as $\rho = e^{-3\zeta}$, the proof then depending on the uniform convergence of a power series in $\rho$, and its derivatives within its 'circle of convergence.'

## Part II: Solution by Means of Integral Equations

### 1. Derivation of integral equations

The developments described in Part 1 were undertaken to evaluate the accuracy of the integral-equation procedures described in References [1], [2], [3], and [6], and used to obtain added masses for body pairs of various shapes. Among these procedures, the two that most affected numerical accuracy are the treatment of the sharp peaks of the integrands of the integral equations when the gap between the bodies is very small, and, secondly, the procedure for computing the derivatives of the added masses.

The unknown functions in these integral equations are taken to be the source distributions $\sigma_1$ and $\sigma_2$ on the surfaces of bodies, moving with velocities $U_1$ and $U_2$ along the line joining their centroids. When $U_1 = 1$ and $U_2 = 0$, the solutions $\sigma_1$ and $\sigma_2$ of the pair of integral equations, derived from the associated boundary conditions, give the added masses by applying the generalized Taylor formulas [4], [5] or [6]. The x-axis is taken along the line joining the centroids and the bodies are assumed to have an x-z plane of symmetry so that they can move without rotation along the x-axis; see Fig. 3.

For the two-dimensional case, the velocity potential $\phi(P)$ at a point P exterior to both bodies or on their bounding contours, is given by

$$\phi(P) = \oint_{c1} \sigma_1(Q_1) \ln r_{PQ1}\, ds_{Q1} + \oint_{c2} \sigma_2(Q_2) \ln r_{PQ2}\, ds_{Q2} \qquad (84)$$

in which $Q_1$ and $Q_2$ denote points on the closed contours $c_1$ and $c_2$ of bodies 1 and 2 respectively, $r_{PQ1}$ and $r_{PQ2}$ are distances to P from $Q_1$ and $Q_2$, and $ds_{Q1}$ and $ds_{Q2}$ are elements of arc along $c_1$ and $c_2$. The boundary conditions to be satisfied are

$$\frac{\partial \phi}{\partial n_{P1}} = U_1 \frac{\partial x}{\partial n_{P1}} \qquad \frac{\partial \phi}{\partial n_{P2}} = U_2 \frac{\partial x}{\partial n_{P2}} \qquad (85)$$

where $n_{P1}$ and $n_{P2}$ denote distances along the outward normal to $c_1$ and $c_2$, and the point P lies on the boundary of body 1 or 2. These give the pair of integral equations

$$\pi\sigma_1(P_1) + \oint_{c1} \sigma_1(Q_1) \frac{\partial}{\partial n_{P1}} \ln r_{P1Q1}\, ds_{Q1} +$$

$$\oint_{c2} \sigma_2(Q_2) \frac{\partial}{\partial n_{P1}} \ln r_{P_1Q_2}\, ds_{Q2} = U_1 \frac{\partial x}{\partial n_{P1}} \qquad (86)$$

$$\pi\sigma_2(P_2) + \oint_{c2} \sigma_2(Q_2) \frac{\partial}{\partial n_{P2}} \ln r_{P2Q2}\, ds_{Q2} +$$

$$\oint_{c1} \sigma_1(Q_1) \frac{\partial}{\partial n_{P2}} \ln r_{P_2Q_1}\, ds_{Q1} = U_2 \frac{\partial x}{\partial n_{P2}} \qquad (87)$$

Here the additional terms $\pi\sigma_1(P_1)$ and $\pi\sigma_2(P_2)$ appear in differentiating the integrals in (84) which are singular when $Q_1$ passes through $P_1$, or $Q_2$ passes through $P_2$. In (86) and (87), however, the kernels

$$K(P_1,Q_1) = \frac{\partial}{\partial n_{P1}} (\ln r_{P1Q1}), \quad K(P_2,Q_2) = \frac{\partial}{\partial n_{P2}} (\ln r_{P2Q2}) \qquad (88)$$

become indeterminate and, at smooth points of the contours, have the limiting values

$$K_1(P_1,P_1) = \frac{1}{2} C_1(P_1), \quad K_2(P_2,P_2) = \frac{1}{2} C_2(P_2) \tag{89}$$

where $C_1$ and $C_2$ are the curvatures of contours $c_1$ and $c_2$; see ref. [15].

When $c_1$ and/or $c_2$ are not defined analytically, there would be a loss of accuracy in determining $C_1$ and $C_2$. This can be avoided by taking advantage of the well known property of the integral of the transpose of the kernel,

$$\oint_{C_i} K_i(Q_i,P_i)\, ds_i = \pi, \quad i = 1,2 \tag{90}$$

Then (86) and (87) may be written as

$$2\pi\sigma_1(P_1) + \oint_{C_1} [\sigma_1(Q_1) \frac{\partial}{\partial n_{P1}} \ln r_{P1Q1} - \sigma_1(P_1) \frac{\partial}{\partial n_{Q1}} \ln r_{P1Q1}]\, ds_{Q1}$$

$$+ \oint_{C_2} \sigma_2(Q_2) \frac{\partial}{\partial n_{P1}} \ln r_{P1Q2}\, ds_{Q2} = U_1 \frac{\partial x}{\partial n_{P1}} \tag{91}$$

$$2\pi\sigma_2(P_2) + \oint_{C_2} [\sigma_2(Q_2) \frac{\partial}{\partial n_{P2}} \ln r_{P2Q2} - \sigma_2(P_2) \frac{\partial}{\partial n_{Q2}} \ln r_{P2Q2}]\, ds_{Q2}$$

$$+ \oint_{C_1} \sigma_1(Q_1) \frac{\partial}{\partial n_{P2}} \ln r_{P2Q1}\, ds_{Q1} = U_2 \frac{\partial x}{\partial n_{P2}} \tag{92}$$

We see from (91) and (92) that the integrands with the indeterminacies vanish when P and Q coincide.

The integral equations for the three-dimensional case are derived in a similar manner. The potential at a point P exterior to the bodies or on their bounding surfaces is

$$\phi(P) = - \int_{S_1} \sigma_1(Q_1) \frac{1}{r_{PQ1}}\, dS_{Q1} - \int_{S_2} \sigma_2(Q_2) \frac{1}{r_{PQ2}}\, dS_{Q2} \tag{93}$$

where $S_1$ and $S_2$ denote the surfaces of bodies 1 and 2, and $dS_{Q1}$ and $dS_{Q2}$ their area elements. The boundary conditions are the same as in (85), and applying these, we obtain the pair of integral equations

$$2\pi\sigma_1(P_1) - \int_{S_1} \sigma_1(Q_1) \frac{\partial}{\partial n_{P1}} \frac{1}{r_{P1Q1}} dS_{Q1} - \int_{S_2} \sigma_2(Q_2) \frac{\partial}{\partial n_{P1}} \frac{1}{r_{P1Q2}} dS_{Q2} = U_1 \frac{\partial x}{\partial n_{P1}} \quad (94)$$

$$2\pi\sigma_2(P_2) - \int_{S_2} \sigma_2(Q_2) \frac{\partial}{\partial n_{P2}} \frac{1}{r_{P2Q2}} dS_{Q2} - \int_{S_1} \sigma_1(Q_1) \frac{\partial}{\partial n_{P2}} \frac{1}{r_{P2Q1}} dS_{Q1} = U_2 \frac{\partial x}{\partial n_{P2}} \quad (95)$$

In this case, the kernels

$$K_i(P_i,Q_i) = -\frac{\partial}{\partial n_{Pi}} \frac{1}{r_{PiQi}}, \quad i = 1,2 \quad (96)$$

remain singular, and it is more important than in the two-dimensional case to remove the singularity. This can be accomplished by applying the property of the transpose of the kernel at a smooth point,

$$\int_{S_i} K_i (Q_i, P_i)\, dS_{Qi} = 2\pi, \quad i = 1,2 \quad (97)$$

to write (94) and (95) in the form

$$4\pi\sigma_1(P_1) - \int_{S_1} [\sigma_1(Q_1) \frac{\partial}{\partial n_{P1}} \frac{1}{r_{P1Q1}} - \sigma_1(P_1) \frac{\partial}{\partial n_{Q1}} \frac{1}{r_{P1Q1}}] dS_{Q1}$$

$$-\int_{S_2} \sigma_2(Q_2) \frac{\partial}{\partial n_{P1}} \frac{1}{r_{P1Q2}} dS_{Q2} = U_1 \frac{\partial x}{\partial n_{P1}} \quad (98)$$

$$4\pi\sigma_2(P_2) - \int_{S_2} [\sigma_2(Q_2) \frac{\partial}{\partial n_{P2}} \frac{1}{r_{P2Q2}} - \sigma_2(P_2) \frac{\partial}{\partial n_{Q2}} \frac{1}{r_{P2Q2}}] dS_{Q2}$$

$$-\int_{S_1} \sigma_1(Q_1) \frac{\partial}{\partial n_{P2}} \frac{1}{r_{P2Q1}} dS_{Q1} = U_2 \frac{\partial x}{\partial n_{P2}} \quad (99)$$

It was shown by Landweber and Macagno [16] that the singularity of the kernel is removed by the foregoing procedure.

After the integral equations have been solved for the source strengths $\sigma_{11}$ and $\sigma_{12}$ when $U_1 = 1$ and $U_2 = 0$, and for $\sigma_{21}$ and $\sigma_{22}$ when $U_1 = 0$ and $U_2 = 1$, where $\sigma_{ij}$ denotes the source distribution on the j-th body due to the

motion of the i-th, then, for the 2-D case, the added masses can be obtained from the generalized Taylor formulas. For the 2-D case, we obtain

$$A_{11} = 2\pi\rho\phi_{c_1} \times \sigma_{11} ds_1 - \rho A_1, \quad A_{22} = 2\pi\rho\phi_{c_2} \times \sigma_{22} ds_2 - \rho A_2$$

where $A_1$ and $A_2$ are the areas bounded by $c_1$ and $c_2$, and

$$A_{12} = A_{21} = 2\pi\rho\phi_{c_2} \times \sigma_{12} ds_2 = 2\pi\rho\phi_{c_1} \times \sigma_{21} ds_2$$

and for the 3-D case,

$$A_{11} = 4\pi\rho\phi_{S_1} \times \sigma_{11} ds_1 - \rho \forall_1, \quad A_{22} = 4\pi\rho\phi_{S_2} \times \sigma_{22} ds_2 - \rho \forall_2$$

where $\forall 1$ and $\forall 2$ are the volumes of the interiors of $S_1$ and $S_2$, and

$$A_{12} = A_{21} = 4\pi\rho\phi_{S_2} \times \sigma_{12} dS_2 = 4\pi\rho\phi_{S_1} \times \sigma_{21} dS_1$$

2. Elimination of peaks of integrands

When the gap between the bodies is small, then, at points $P_1Q_2$ and $P_2Q_1$ in the neighborhood of the gap, $r_{PQ}$ will also be small and the integrand will have a sharp peak. There are two ways to evaluate such an integral accurately. One is to eliminate or reduce the magnitude of the peak, the other is to use a quadrature formula which concentrates enough points in the neighborhood of the peak to yield the desired accuracy. A combination of these two procedures was used in [2] for the case of a pair of circles, and the resulting values of the added masses agreed very well with those from the method of images; but the procedure for modulating the peak depended upon the exact integral of the kernel for a circle, which is not available with other shapes and removed only the peak associated with the points P at $\theta_1 = 0$ or $\theta_2 = \pi$ for a pair of circles.

A procedure suitable for arbitrary shapes is based on the property of the transpose of the 2-D kernel $K(P_1,Q_2)$,

$$\phi_{c_2} K(Q_2,P_1)\, ds_{Q2} = \phi_{c_2} \frac{\partial}{\partial n_{Q2}} \ln r_{P1Q2}\, ds_{Q2} = 0 \qquad (100)$$

since the integral may be interpreted as the flux through a closed curve $c_2$ due to a unit point source at the exterior point $P_1$. Similarly we have

$$\int_{c_1} K(Q_1,P_2)\, ds_{Q1} = 0 \tag{101}$$

and for the 3-D kernels

$$\int_{S_1} K(Q_1,P_2)\, dS_{Q1} = \int_{S_2} K(Q_2,P_1)\, dS_{Q2} = 0 \tag{102}$$

Thus, for the integral over $c_1$ in (87) and (92), we may write

$$\oint_{c_1} \sigma_1(Q_1) \frac{\partial}{\partial n_{P2}} \ln r_{P2Q1}\, ds_{Q1} = \oint_{c_1} [\sigma_1(Q_1) \frac{\partial}{\partial n_{P2}} \ln r_{P2Q1} -$$

$$\sigma_1(P_1') \frac{\partial}{\partial n_{Q1}} \ln r_{P2Q1}] ds_{Q1} \tag{103}$$

where $P_1'$ is the point on $c_1$ closest to $P_2$, which is such the line $P_1' P_2$ lies along the outward unit vector $\hat{n}_{P1'}$, normal to $c_1$ at $P_1'$; see Fig. 4. Then, when $Q_1$ coincides with $P_1'$, the last integrand becomes

$$\frac{\sigma_1(P_1')}{r_{P2P1'}} (\frac{\partial}{\partial n_{P2}} - \frac{\partial}{\partial n_{P1'}}) r_{P2P1'} = \frac{\sigma_1(P_1')}{r_{P2P1'}} \hat{n}_{P1'} \cdot (\hat{n}_{P2} + \hat{n}_{P1'})$$

$$= \frac{\sigma_1(P_1')}{r_{P2P1'}} (1 + \hat{n}_{P1'} \cdot \hat{n}_{P2}) = \frac{\sigma_1(P_1')}{r_{P2P1'}} (1 + \cos \psi)$$

where $\hat{n}_{P2}$ is the outward unit normal vector at $P_2$ on $c_2$ and $\psi$ is the angle between the normals. In the range in which $r_{P2P1'}$ is very small, $\pi - \psi$ is also small, and hence $1 + \cos \psi$ appears to be small of second order, with $r_{P2P1'}$ considered as small of first order. Hence the introduction of the transpose in (103) reduces the magnitude of the peak to first order of smallness. Similarly, the second integrals of (86), (95) and (94) may be written as

$$\oint_{c_2} \sigma_2(Q_2) \frac{\partial}{\partial n_{P1}} \ln r_{P1Q2}\, ds_{Q2} = \oint_{c_2} [\sigma_2(Q_2) \frac{\partial}{\partial n_{P1}} \ln r_{P1Q2} -$$

$$\sigma_2(P_2') \frac{\partial}{\partial n_{Q2}} \ln r_{P1Q2}] \, ds_{Q2} \tag{104}$$

$$\int_{S_1} \sigma_1(Q_1) \frac{\partial}{\partial n_{P2}} \frac{1}{r_{P2Q1}} dS_{Q1} = \int_{S_1} [\sigma_1(Q_1) \frac{\partial}{\partial n_{P2}} \frac{1}{r_{P2Q1}} -$$

$$\sigma_1(P_1') \frac{\partial}{\partial n_{Q1}} \frac{1}{r_{P2Q1}}] \, dS_{Q1} \tag{105}$$

$$\int_{S_2} \sigma_2(Q_2) \frac{\partial}{\partial n_{P1}} \frac{1}{r_{P1Q2}} dS_{Q2} = \int_{S_2} [\sigma_2(Q_2) \frac{\partial}{\partial n_{P1}} \frac{1}{r_{P1Q2}} -$$

$$\sigma_2(P_2') \frac{\partial}{\partial n_{Q2}} \frac{1}{r_{P1Q2}}] \, dS_{Q2} \tag{106}$$

in which $P_2'$ is the point on $c_2$ closest to $P_1$.

3. The MAQF with nonuniform intervals

The second phase of treating the peak of the integrand was to select a quadrature formula which concentrates points in its neighborhood. For this purpose, a transformation was introduced which permitted the MAQF to be applied with nonuniform integrals, such that the desired concentration of points about the peaks was obtained. This will now be presented.

Let $F(\theta)$ be a periodic function, with period $2\pi$, which has a sharp peak for small values of $\theta$. We wish to evaluate the integral

$$I = \int_0^{2\pi} F(\theta) \, d\theta$$

If the MAQF were applied directly, a very large number of abscissas would be needed to obtain enough points over the range of the peak, since uniform intervals are required. To resolve this dilemma, we define a variable $\omega$ by

$$\theta = \omega - \sin \omega, \quad 0 \leq \omega \leq 2\pi \tag{107}$$

Then $$d\theta = (1 - \cos \omega) \, d\omega = 2 \sin^2 \frac{\omega}{2} d\omega$$

Hence

$$I = 2\int_0^{2\pi} G(\omega)\sin^2\frac{\omega}{2}\,d\omega, \quad G(\omega) \equiv F(\theta) \tag{108}$$

Clearly, the new integrand is also cyclic. Hence we may apply the MAQF (the trapezoidal rule) by using uniform intervals $\Delta\omega$. This concentrates many intervals near $\theta = 0$ and $2\pi$ where $\Delta\theta = \frac{1}{2}\omega^2\Delta\omega$, and fewer near $\theta = \omega = \pi$, where $\Delta\theta = 2\Delta\omega$, as was desired. Here we assumed that $\theta = 0$ and $2\pi$ at the points of minimum distance on both bodies. For the two-circle case, where the points of minimum distance are at $\theta_1 = 0$ and $\theta_2 = \pi$, we define $\theta_2' = \pi - \theta_2$ with which the above formulas may be directly applied.

For small values of $\omega$, (107) gives $\theta \approx \omega^3/6$. This suggests that the concentration of points near $\theta = 0$ and $2\pi$ could be increased by removing the $\omega^3$-term. This can be accomplished simply by modifying the $\theta(\omega)$ function in (107) by subtracting $\omega^3/6$, but that would violate the MAQF condition that the integrand be cyclic. Instead, we define $\theta(\omega)$ as

$$\theta = \omega - \sin\omega - \frac{1}{6}\sin^3\omega \tag{107a}$$

Then
$$d\theta = \left(2\sin^2\frac{\omega}{2} - \frac{1}{2}\sin^2\omega\cos\omega\right)d\omega$$

$$= 2\sin^4\frac{\omega}{2}(2 + \cos\omega)\,d\omega$$

and hence

$$I = 2\int_0^{2\pi} G(\omega)(2 + \cos\omega)\sin^4\frac{\omega}{2}\,d\omega \tag{108a}$$

which also has a cyclic integrand. At small values of $\omega$, we now have $\Delta\theta \approx \frac{3}{8}\omega^4\Delta\omega$, so that the concentration of $\theta$-intervals near $\theta = 0$ is greatly increased when $\Delta\omega$ is constant. At $\theta = \omega = \pi$, both (107) and (107a) give $d\theta = 2d\omega$. The asymptotic form of (107a) is $\theta \approx 3\omega^5/40$, which can also be eliminated by subtracting $(3/40)\sin^5\omega$. This yields the third transformation

$$\theta = \omega - \sin\omega - \frac{1}{6}\sin^3\omega - \frac{3}{40}\sin^5\omega \qquad (107b)$$

and
$$I = \int_0^{2\pi} G(\omega)(8 + 9\cos\omega + 3\cos^2\omega)\sin^6\frac{\omega}{2}\,d\omega \qquad (108b)$$

The procedures for obtaining a succession of nonuniform intervals, with which the MAQF can be applied, is now evident.

Since $\theta = 0$ when $\omega = 0$ and $\theta = \pi$ when $\omega = \pi$, and the $\omega$-intervals are uniform, an indication of the point concentration is given by the value $\theta = \theta_c$ when $\omega = \pi/2$, i.e. at half the number of points between 0 and $\pi$. Substitution of $\omega = \pi/2$ in (107) and (107a) gives $\theta_c = 33°$, 23°, and 19° respectively. Also, at these values of $\omega$ and $\theta_c$ we have $d\theta = d\omega$, indicating that the increments $\Delta\theta$ change from concentration to dispersion at $\theta = \theta_c$.

With any member of this family of modified MAQF transformations, the integrand vanishes at $\theta = 0$ and $2\pi$, thus eliminating the peak of the original integrand $F(\theta)$ at that point. This property also reduces the amplitude of the peaks occurring at small, nonzero values of $\theta$, but, as will be seen, not sufficiently so that the transpose correction for eliminating peaks of the kernel would become unnecessary.

When $\omega$ is small, significant figures may be lost in computing $\theta$ directly from (107, 107a, 107b). For (107), this can be avoided by writing

$$\theta = \frac{\omega^3}{3!} - \frac{\omega^5}{5!} + \frac{\omega^7}{7!} - \ldots = \frac{\omega^3}{6}\left(1 - \frac{\omega^2}{20} + \frac{\omega^4}{840} - \frac{\omega^6}{60{,}480}\right) + \varepsilon(\omega)$$

where $|\varepsilon(\omega)|$ is less than the next term of the series,

$$|\varepsilon| < \omega^{11}/11! < 1.6 \times 10^{-7}\omega^{11}$$

and $\omega^3/6$ is computed in scientific notation. For (107a) and (107b), we apply

$$\sin^3\omega = \frac{1}{4}(3\sin\omega - \sin 3\omega), \qquad \sin^5\omega = \frac{1}{16}(10\sin\omega - 5\sin 3\omega + \sin 5\omega)$$

and the Taylor series of sines of $\omega$, $3\omega$ and $5\omega$ to obtain, respectively,

$$\theta = \frac{3\omega^5}{40}\left[1 - 15\,\Sigma_3^{\infty}\,(-1)^n\,\frac{\omega^{2n-4}}{(2n+1)!}\,(3^{2n-2}-1)\right] \qquad (107c)$$

$$\theta = \frac{5\omega^7}{112}\left[1 - \frac{105}{8}\,\Sigma_4^{\infty}\,(-1)^n\,\frac{\omega^{2n-6}}{(2n+1)!}\,(2\cdot 3^{2n-1} + 5^{2n-2})\right] \qquad (107d)$$

4. Evaluation of derivatives of added mass

Both added masses and their derivatives with respect to the gap g between the cylinders occur in the expressions for the forces on the bodies. In Ref. [1], these derivatives were obtained by numerical differentiation of the smoothed added-mass data, with unsatisfactory results at small gaps, because the derivatives were approaching infinity and small errors in the data were amplified.

The accuracy of the results from numerical differentiation of the added-mass coefficients has been greatly improved by a simple and important change. Since the error depends on the magnitude of the second derivative, this suggests that the asymptotic law of the added-mass be applied to reduce the error. For example, according to (66), $k_1(g)$ varies linearly with $\sqrt{g}$ (or the parameter $\zeta$ or $\gamma$ of (62)) at small values of g, as is shown in Fig. 2. Then $dk_1/d\gamma$ can be obtained by numerical differentiation with greatly reduced error, with which, by (62), we get

$$\frac{dk_1}{dg} = \frac{dk_1}{d\gamma}\frac{d\gamma}{dg} = \frac{1}{2}\left(\frac{2s}{\beta^2 g}\right)^{1/2}\frac{dk_1}{d\gamma} \qquad (109)$$

without further loss of accuracy.

The parameter $\gamma$ is also useful for improving the accuracy of the added-mass derivatives for spheres. This is not indicated directly by the asymptotic formula (78), since the rate of variation of the added masses at very small values of $\zeta$ or $\gamma$ is much greater than at its moderately small values corresponding to the practical range for $g/a \geq 0.01$ (for equal spheres) due to the factor $\ln \gamma$. Since $dk_1/d\gamma$ varies slowly in that range, it could be evaluated

with sufficient accuracy from the computed values of the added masses. Their derivatives with respect to g were then obtained from (109).

To obtain the numerical results for the derivatives (other than the 'exact' ones) shown in the following tables, Lagrange's five-point interpolation formula was used, without smoothing the calculated values of the added-mass coefficients.

## 5. Numerical results for pairs of circles

### a) Exact results

All the numerical results were obtained on an IBM RISC/6000 minicomputer. First, an accurate set of added masses for a pair of equal circles was obtained by summing infinite series of doublet strengths. These were calculated by means of the basic recurrence formulas, such as (3) and (6), and by the various forms of the Herman formulas. Of these, the parametric forms in (39b, 40b, 41b) were found to be most efficient and their efficiency was greatly enhanced by applying the truncation corrections given in (49, 53, 61) in summing the series for the added-mass coefficients. This is demonstrated in Table 2 by calculations of $k_{12}$ for equal circles, where $R_{12}$ is given by the trapezoidal integral (49). This table supplements Table 1 which corresponds to the zero gap. We see that the approximate ratios of the number of terms N which give the same accuracy without and with the truncation correction are 10 at $g/a = 0.0001$, 4 at 0.001, and 2.5 at 0.01. This shows that the truncation correction is very effective at very small gaps, and that its effectiveness diminishes with increasing gaps. By (62), the parameter $\zeta$ is related to these gaps by $\zeta \approx 2\sqrt{g/a} = 0.02, .0632, 0.20$, respectively. Thus $\zeta$ is not very small at $g/a = 0.01$, and the series for $k_{12}$ at larger gaps (say $g/a \geq 0.10$) converge fast enough so that little is gained by applying the truncation correction.

It was found that, for $g/a \geq 0.01$, the added-mass coefficients obtained from the recurrence and the various forms of the Herman formulas were identical to the sixth decimal place. This would not be the case at much smaller gaps, corresponding to very small values of $\zeta$, when N is very large, because of accumulation of round-off errors in using the recurrence formulas.

For applications requiring accurate calculations at very small gaps, we observe that

$$\tau_n = \frac{\sinh n\zeta}{\sinh\zeta} = 2[\cosh(n-1)\zeta + \cosh(n-3)\zeta + \ldots + \cosh\zeta],\ n \text{ even}$$

$$\tau_n = 2[\cosh(n-1)\zeta + \cosh(n-3)\zeta + \ldots + \cosh 2\zeta] + 1,\ n \text{ odd} \qquad (110)$$

which can be readily derived by expressing the hyperbolic functions in their exponential forms. This would be useful when $\zeta$ is so small that $\tau_n$ could not be calculated accurately from its definition, even with double precision.

Values of $\dot{k}_1, \dot{k}_{12}$ for $g/a \geq 0.01$, designated as 'exact', will be given in Table 4. 'Exact' values of $k_1$ and $k_2$ are not listed separately in the table because these were identical to the calculated values to the six decimals shown. The columns for $\dot{k}_1$ and $\dot{k}_{12}$ are actually $b\dot{k}_1$ and $b\dot{k}_{12}$, but it is convenient to take b=1 hereafter. The 'exact' added-mass derivatives given in this table were also computed both by the recurrence formulas (18) and by the derivatives of the Herman formulas given in (67, 68, 69). These agreed to the six decimals shown in Table 4.

It is also of interest to show the variation of $k_1$ and $k_{12}$ with $\zeta$. This is depicted in Fig. 3 in which the asymptotic linearity with $\zeta$ or $\gamma$, according to (52, 58, 66), is clearly shown.

b) Computed results

For the case of two circles of radii a and b, the kernels of (88) are constant and, according to (89), the constants are given by

$$K(P_1,Q_1) = \frac{1}{2a} \qquad K(P_2,Q_2) = \frac{1}{2b}$$

The first integrals in (86) and (87) are then proportional to the total source strength on each circle, which is zero by the Gauss flux theorem. The kernel of the second integral of (86) is given by

$$K(P_1,Q_2) = \frac{\partial}{\partial n_{P1}} \ell n\, r_{P1Q2} = \frac{1}{r_{P1Q2}} \frac{\partial r_{P1Q2}}{\partial n_{P1}}$$

Here

$$r_{P1Q2} = [a^2 + b^2 + c^2 + 2bc \cos\theta_{Q2} - 2ca \cos\theta_{P1} - 2ab \cos(\theta_{Q2}-\theta_{P1})]^{1/2}$$

and $\partial r_{P1Q2}/\partial n_{P1}$, the cosine of the angle between the vector from $Q_2$ to $P_1$ and $\hat{n}_1$, can be obtained by differentiating $r_{P1Q2}$ with respect to a. This gives

$$K(P_1,Q_2) = \frac{1}{r_{P1Q2}^2}[a - c \cos\theta_{P1} - b \cos(\theta_{Q2} - \theta_{P1})] \tag{111}$$

Similarly, we obtain

$$K(P_2,Q_1) = \frac{\partial}{\partial n_{P2}} \ell n\, r_{P2Q1} = \frac{1}{r_{P2Q1}^2}[b + c \cos\theta_{P2} - a \cos(\theta_{P2} - \theta_{Q1})] \tag{112}$$

and for their transposes,

$$K(Q_2,P_1) = \frac{\partial}{\partial n_{Q2}} \ell n\, r_{P1Q2} = \frac{1}{r_{P1Q2}^2}[b + c \cos\theta_{Q2} - a \cos(\theta_{P1} - \theta_{Q2})] \tag{113}$$

$$K(Q_1,P_2) = \frac{\partial}{\partial n_{Q1}} \ell n\, r_{P2Q1} = \frac{1}{r_{P2Q1}^2}[a - c \cos\theta_{P2} - b \cos(\theta_{Q1} - \theta_{P2})] \tag{114}$$

The integral equations (86) and (87), with the transposes of the kernels applied to eliminate the peaks as shown in (103) and (104), now become

$$\pi\sigma_1(P_1) + \int_{c_2} [\sigma_2(Q_2)\, K(P_1,Q_2) - \sigma(P_2')\, K(Q_2,P_1)]\, b\,d\theta_2 = U_1 \frac{\partial x}{\partial n_{P1}} \tag{115}$$

$$\pi\sigma_2(P_2) + \int_{c_1} [\sigma_1(Q_1)\, K(P_2,Q_1) - \sigma(P_1')\, K(Q_1,P_2)]\, a\,d\theta_1 = U_2 \frac{\partial x}{\partial n_{P2}} \tag{116}$$

Here the point $P_1'$ is such that $r_{P2P1'}$ is the minimum distance from the point $P_2$ on one body to the other; see Fig. 4. For this case, $P_1'$ is the point of intersection of the line from $P_2$ to the center of the other circle, and one can readily show that $\theta_{P1}'$ and $\theta_{P2}'$ are given by

$$\tan\theta_{P1}' = \frac{b\sin\theta_{P2}}{c + b\cos\theta_{P2}} \qquad \tan\theta_{P2}' = \frac{a\sin\theta_{P1}}{c - a\cos\theta_{P1}} \tag{117}$$

The integrals were discretized by applying the modified MAQF of (107) and (108) to obtain a set of 2N linear equations for the $\sigma$'s. For integration over circle A, in which the peak occur near $\pi$ instead of zero, $\theta_2$ in (107) must be replaced by its supplement $\theta_2'$ i.e., $\theta_2' = \pi - \theta_2 = \omega - \sin\omega$. Then $\theta_2'$ and $\omega$ vary from 0 to $2\pi$ as $\theta_2$ varies from $\pi$ to $-\pi$. The discretized forms of (115) and (116) then become, in the form of an iteration formula,

$$\pi\sigma_{1i}^{(n+1)} = U_1\frac{\partial x}{\partial n_{1i}} - \frac{4\pi b}{N}\sum_{j=1}^{N}[\sigma_{2j}^{(n)}\,K_{1i2j} - \sigma_{2i'}^{(n)}\,K_{2j1i}]\sin^2\frac{\omega_j}{2}$$

$$\pi\sigma_{2i}^{(n+1)} = U_2\frac{\partial x}{\partial n_{2i}} - \frac{4\pi b}{N}\sum_{j=1}^{N}[\sigma_{1j}^{(n)}\,K_{2i1j} - \sigma_{1i'}^{(n)}\,K_{1j2i}]\sin^2\frac{\omega_j}{2} \tag{118}$$

where the superscripts (n) and (n+1) indicate the nth and the (n+1)th iterations. The values $\sigma_{1i}'$ and $\sigma_{2i}'$, corresponding to $\sigma(P_1')$ and $\sigma(P_2')$, were obtained by linear interpolation between the values of $\sigma$ at the extremities of the $\omega$-interval in which $P_1'$ or $P_2'$ lies. The initial approximations to start the iteration were taken to be

$$\sigma_{1i}^{(0)} = \frac{1}{\pi}U_1\frac{\partial x}{\partial n_{1i}} \qquad \sigma_{2i}^{(0)} = \frac{1}{\pi}U_2\frac{\partial x}{\partial n_{2i}} \tag{119}$$

Graphs of the source strengths $\sigma_1(\theta_1)$ and $\sigma_2(\theta_2')$ and of the original integrand $\sigma_2(\theta_2)\,K(P_1,Q_2)$ of (115) are given in Figs. 5 and 6 for the case $U_1 = 1$, $U_2 = 0$, and $a = b$. Results for three gaps, $g/b = 0.01, 0.05, 0.10$ in Fig. 5 show that both $\sigma_1$ and $\sigma_2$ peak sharply at $\theta_1 = \theta_2' = 0$, with peak maxima of $\sigma_1(0) \doteq 1.7$ and $\sigma_2(0) \doteq 1.5$ at $g/b = 0.01$ and the smaller values $\sigma_1(0) \doteq 0.80$, $\sigma_2(0) \doteq 0.64$ at $g/b = 0.05$, and $\sigma_1(0) \doteq 0.60$, $\sigma_2(0) = 0.44$ at 0.10, although the peaks of $\sigma_2$ are consistently sharper than those of $\sigma_1$. As the gap approaches infinity, the

source distributions become $\sigma_1 \approx \frac{1}{\pi}\cos\theta$, $\sigma_1(0) \approx 1/\pi$ and $\sigma_2 \approx 0$. At $\theta_1 = \theta_2' = \pi$, the limiting source strengths are $\sigma_1(\pi) \approx -1/\pi$ and $\sigma_2(\pi) \approx 0$, and the values at the small gaps are negative but deviate little from the limiting values at $g = \infty$.

Figures 6a, 6b, 6c show curves for $g/b = 0.01$ corresponding to three fixed points $\theta_{P1}$ which give $\theta'_{P2'} = 0, 6.5, 11.9$ degrees. We see that the peaks of the original integrands are an order of magnitude higher than those of the source strengths at this gap. For example, the maximum value of the kernel $K(P_1,Q_2)$ at $\theta_1 = 0$ occurs at $\theta_2' = 0$ and has the value $1/g = 100$ versus the peak $\sigma_2(0) \doteq 1.5$, in good agreement with the calculated peak value, $\sigma_2(0)\, K(P_1,Q_2) = 151.6$. At $\theta'_{P2'} = 6.5$ and 11.9 degrees, the peak values of the original integrand are 27.1 and 4.0, much less than the magnitude of the central peak.

With the transpose correction and the associated source strength $\sigma_2(\theta'_{2P'})$, the peaks were essentially eliminated. When $\sigma_2(\pi)$ was used instead of $\sigma_2(\theta'_{2P'})$, as is done in Ref. [2] for all points $P_1$, the peaks were overcorrected and the peaks of greater magnitude but of opposite sign shown in Figs. 6b and 6c were obtained. This is a direct consequence of the sharp peak of the $\sigma_2$-curve in Fig. 5a, which shows that $\sigma_2(0)$ is more than twice the values of $\sigma_2$ at $\theta'_{2P'} = 6.5$ and 11.9 degrees. This shows that, although the kernel peaks are much larger than those of the source distributions, the latter play an important role in the elimination of the peaks of the integrand.

In Fig. 7, the ordinate scales of Fig. 6 are magnified to show the fine structure of the nearly flat curves of the integrand when its peaks have been removed. The initial dip of the curve for $\theta'_{2P'} = 0$ is due to a combination of the small value of the gap, $g/b = 0.01$, and the associated very sharp peak of $\sigma_2(\theta_2')$; this was verified analytically by applying the expressions for the kernel in (111) and its transpose in (113). For the other two values of $\theta'_{2P'}$, many

more points would have been needed to show smooth curves of their oscillations; but since these curves were not used quantitatively, and the purpose of the figure was to show the need to concentrate many points of a quadrature formula in the gap region to take this fine structure into account, the present figure sufficed. This was accomplished by using the modified MAQF (107) to concentrate points in the regions of the peaks and increasing the number of points as the gap decreases. In Ref. [2], three Gauss quadrature formulas of order 20, two of which extended over the peak region, were used for the same purpose.

The foregoing hypotheses were tested by running the numerical experiments of Table 3. Condition 1 gave 'exact' values; comparison of conditions 1 and 4 confirms the importance of removing integrand peaks, although the accuracy of 4 improved greatly at N = 100. Condition 2 simulates the above-described technique of Ref. [2], in which $\sigma_1(0)$ and $\sigma_2(0)$ are used instead of $\sigma_1(\theta_{1P}')$ and $\sigma_2(\theta_{2P}')$. The accuracy improved greatly by increasing N from 40 to 100 and the latter result agrees very well with that of Ref. [2] given in Table 5. Condition 5 is the procedure used in Ref. [1], which required N = 600 to obtain acceptable accuracy. Thus it appears to be most efficient and accurate to remove all the peaks of the integrand and to use some means of concentrating points in the peak regions.

The present results are compared with the 'exact' ones in Table 4 and with those of Ref. [2] in Table 5. The latter shows that the values of $k_1$ and $k_{12}$ given by the present methods agree with the exact values to six decimals. In Ref. [2], the results were correct to only two decimals at gaps of 0.01 and 0.02, three decimals at 0.03 and 0.04, and to at least four decimals at 0.05 and beyond. The greater accuracy with the present methods is evident.

The need for high accuracy becomes apparent when the data are used to obtain the derivatives of the added masses by numerical differentiation, which depend upon differences between successive values. From Table 5, we see that the differences between values at gaps of 0.01 and 0.02 for $k_1$, 0.0313 from Ref. [2], versus the exact value of 0.0337, is in error by 7 percent. Clearly, then, numerical differentiation could not be used in Ref. [2]. Instead, the derivatives of the original integral equations were solved for the derivatives of the source strengths, which then yielded the derivatives of the added-

masses directly. This procedure gave the values shown in Table 6, which have an error of 2.5 percent at g/a = 0.01, but are very accurate of gaps of 0.02 and beyond. Since the peaks of the integrands of the differentiated integral equations were much higher, the order of the two Gauss quadrature formulas in the symmetrical peak regions was increased from 20 to 40. The values of $k_1$ and $k_{12}$, obtained with the four Gauss quadrature formulas, each of order 40, are not listed in Ref. [2]. The present method gives more accurate results at g/b = 0.01 and 0.02, but at 0.03 and beyond, both are highly accurate. The present method, however, attains the accuracy with a much simpler computer program, requiring the simultaneous solution of two, instead of four, integral equations, with the kernels of the two additional equations having peak magnitudes of order 1/g2 versus 1/g for the original pair. The numerical results by the present method were obtained with a minicomputer; those of Ref. [2] for $\dot{k}_1$ and $\dot{k}_{12}$ required a supercomputer.

Results for unequal circles are given in Tables 7, 8 and 9 for a/b = 4, 16,∞. 'Exact' results are not shown separately since these agreed exactly with the computed results to the number of digits shown. This was accomplished by using the modified MAQF (107) on both circles and taking $N(\frac{a}{b}) = \frac{a}{b} N(1)$. Actually, it was necessary to increase the number of points only on $c_1$, and there only in the peak regions, as we have verified by using (107b) to increase the point concentration there for a/b = 16, with a smaller value of $N_1$. The results in Table 7, however, were obtained with N = 120 on both circles, and those in Table 8 with N = 600 on both at g/b = 0.01, although 40 points on the smaller circle would have matched the accuracy attained with a/b = 1. Fewer points were required at larger gaps.

The coefficients $k_1$ in Tables 7 and 8 are seen to be given approximately by $(a/b)^2$ followed by six decimals. As is seen from (39b), however, $(a/b)^2$ is a known additive constant, and the remaining terms need to be calculated accurately to only the usual number of seven significant figures. Similarly, in solving the integral equations for the source distribution on the larger circle, the known contribution to the distribution from the doublet of strength $a^2$ at the center of the large circle, $\sigma_o = (1/\pi) \cos \theta_1$, would also subtract out the additive constant $(a/b)^2$ from the values of $k_1$ and require only the same seven-digit accuracy for the remainder. This procedure can be generalized to

apply to a noncircular cylinder by obtaining first the source distribution $\sigma_o$ on the surface of that cylinder when the other cylinder is not present, and then solving the pair of integral equations for the interaction source distribution $\sigma$-$\sigma_o$.

Graphs of the force-coefficient data in Tables 4, 7, 8 and 9 are shown in Figs. 8a to 8d. Here $C_{F1}$ denotes the coefficient of the force on the circle of radius a when that circle has the velocity $U_1$ and the circle of radius b is at rest, and $C_{F2}$ that for the force on the circle of radius b. These coefficients are defined by

$$C_{F1} = \frac{F_1}{\rho b U_1^2} \qquad C_{F2} = \frac{F_2}{\rho b U_1^2}$$

where the subscript '1' corresponds to the a-circle and '2' to the b-circle. Similarly, when the a-circle is at rest and the b-circle is moving with velocity $U_2$, the forces are designated as $F_1^*$ and $F_2^*$ and the coefficients are defined by

$$C_{F1}^* = \frac{F_1^*}{\rho b U_2^2} \qquad C_{F2}^* = \frac{F_2^*}{\rho b U_2^2}$$

For these special cases, we obtain from (15) and (16) with b = 1

$$C_{F1} = \frac{1}{2}\pi \dot{k}_1,\ C_{F2} = \pi(\frac{1}{2}\dot{k}_1 + \dot{k}_{12}),\ C_{F1}^* = -\pi(\dot{k}_{12} + \frac{1}{2}\dot{k}_2),\ C_{F2}^* = -\pi\dot{k}_2 \quad (120)$$

Although the procedures for computing the results for a = $\infty$ are not presented until the next section, it is convenient here to consider this case as the limit of the sequence of circles of increasing radii. Curves of $C_{F1}$ and $C_{F2}$ do not appear in Figs. 8a and 8b since motion of the wall towards a stationary cylinder would require an infinite added mass. We see that the forces are always repulsive and approach infinity as the gap approaches zero. Values of $C_{F1}^*$ and $C_{F2}^*$ are not shown explicitly in Table 4 for a/b = 1 since, by symmetry,

we have $C^*_{F1} = - C_{F2}$ and $C^*_{F2} = - C_{F1}$. The graphs show that $C_{F1}$ and $C^*_{F2}$ vary monotonically with a/b for all values of g/b. $C_{F2}$ and $C^*_{F1}$ also vary monotonically, but only for values of g/b from 0 to 0.16 and 0.04 respectively.

When a/b = 1, Figs. 8a and 8b and Table 4 show that the force on the stationary cylinder is about five times larger than that on the moving one at g/b = 1, and about 50 percent larger at g/b = 0.10. This indicates that it would be easier to detect hydrodynamic interaction effects experimentally on the stationary cylinder, for which the predicted value $C_{F2} = 0.75$ at g/b = 0.50 is large enough to be readily measured. For other diameter ratios at g/b = 0.50, the force coefficient on the large cylinder is greater no matter which of the cylinders is moving.

6. Results for a circular cylinder (or a sphere) and a wall.

The case of a circular cylinder moving along the normal to an impervious wall is the limiting case of a pair of circles as the radius of one of the circles approaches infinity. Each of these large circles is taken to be at rest as $a \to \infty$, so that $g/a \to 0$, in contrast to the results for a/b = 16 in Table 8, which are given to g/a = 6.25. Thus results for the present case, given in Table 9, should resemble those of Table 8 only for small gaps, say $g/b \leq 1.0$, at which $g/a \leq 1/16$.

As is well known, an alternative approach is to replace the wall by the mirror image of the circle in it. This method transforms the problem to the case of a pair of equal circles for which results are given in Table 4. Both approaches will now be treated.

As a approaches infinity in (40b) and (41b), we obtain in the limit

$$k_2 = 1 + 2 \Sigma_1^{\infty} \frac{\sinh^2\zeta}{\sinh^2(n+1)\zeta} = 2\Sigma_2(\zeta) - 1, \qquad \dot{k}_2 = 2\dot{\Sigma}_2 \tag{121}$$

$$k_{12} = - 2\Sigma_2(\zeta), \qquad \dot{k}_{12} = - \dot{k}_2 \tag{122}$$

Then, by (15) and (16),

$$F_1 = -(\dot{A}_{12} + \tfrac{1}{2}\dot{A}_{22})\,U_2^2 = -\pi\rho b^2(\dot{k}_{12} + \tfrac{1}{2}\dot{k}_2)U_2^2 = \pi\rho b^2\dot{\Sigma}_2 U_2^2 \qquad (123)$$

$$F_2 = -\tfrac{1}{2}\dot{A}_{22}\,U_2^2 = -\tfrac{1}{2}\pi\rho b^2\dot{k}_2 = -\pi\rho b^2\dot{\Sigma}_2 U_2^2 \qquad (124)$$

With b = 1, these give the force coefficients

$$C_{F1} = \frac{F_1}{\rho b U_2^2} = \pi\dot{\Sigma}_2(\zeta) \qquad C_{F2} = -\pi\dot{\Sigma}_2(\zeta) \qquad (125)$$

The value of $\zeta$ for given values of a, b, and c can be obtained from (63), which may be written as

$$\cosh\zeta = 1 + \frac{g}{b} + \frac{b}{a}\left(\frac{g}{b} + \frac{1}{2}\frac{g^2}{b^2}\right)$$

In the present case of $a = \infty$, we get

$$\cosh\zeta - 1 = 2\sinh^2\frac{\zeta}{2} = \frac{g}{b} \qquad \zeta = 2\sinh^{-1}\left(\frac{g}{2b}\right)^{1/2} \qquad (126)$$

To obtain $\dot{\Sigma}_2$, we first apply (69) for $a \to \infty$ to get

$$\Sigma_2' = \Sigma_1^{\infty}\frac{d}{d\zeta}\tau_n^{-2} = -2\,\Sigma_1^{\infty}\tau_n^{-3}\tau_n'$$

As a and c approach infinity in (69), this gives

$$\dot{\Sigma}_2(\zeta) = \Sigma_2'(\zeta)/c' = -\frac{2}{b}\,\mathrm{csch}\,\zeta\,\Sigma_1^{\infty}\tau_n^{-3}\tau_n'$$

The force coefficients (125), for the case of a cylinder moving normal to a wall then become

$$C_{F1} = - C_{F2} = - 2\pi \operatorname{csch} \zeta \, \Sigma_1^{\infty} \tau_n^{-3} \tau_n' \tag{127}$$

Next consider the two-equal-circle approach. By (14), the kinetic energy of the fluid, with $U_1 = - U_2$ and $A_{11} = A_{22}$, is

$$T_c = [A_{22c}(g_c) - A_{12c}(g_c)]U_2^2, \qquad g_c = 2g$$

and that for the half space with $U_1 = 0$ is given by $2T = A_{22}(g)\, U_2^2$. Here the subscript c indicates values for the pair of equal circles, and the other quantities refer to the half space when the wall is present. Since Tc = 2T, we obtain the simple relation $A_{22} = A_{22c} - A_{12c}$ or, in nondimensional form,

$$k_2\left(\frac{g}{b}\right) = k_{2c}\left(\frac{g_c}{b}\right) - k_{12c}\left(\frac{g_c}{b}\right) \tag{128}$$

Hence, differentiating with respect to g, we obtain

$$k_2\left(\frac{g}{b}\right) = 2\left[\dot{k}_{2c}\left(\frac{g_c}{b}\right) - k_{12c}\left(\frac{g_c}{b}\right)\right] \tag{129}$$

The derivation of the results $F_1 = - F_2$ in (123) and (124) was based on the formulas for $k_1$ and $k_{12}$ for a circular cylinder in (121) and (122). We shall now show that $F_1$, the force on the wall, is also given by $F_1 = - F_2$ for bodies of arbitrary shape.

According to the Lagally theorem [5], the force on a nonrotating body in an irrotational flow can be expressed in terms of the strength and location of the singularities within it, the velocities due to external mechanisms at their locations, and the acceleration of the displaced fluid (which is zero in the present case). Since the image body and the wall (considered as a circle of infinite radius) contain the same set of singularities, the force must be the same on both. But, by symmetry, the force on the image body is equal and opposite to that on the actual one. Hence that is also true for the force on the wall, as we wished to show.

Also valid for bodies of arbitrary shape are equations (123, 124, 128, 129), the derivation of which did not depend on the body shape. Since $F_1 + F_2 = 0$,

we now find, from (123) and (124), that the relation $\dot{A}_{22} = -\dot{A}_{12}$, given in (129) for a circular cylinder, also applies to arbitrary shapes. Thus, the determination of the forces $F_1$ and $F_2$ on a body, approaching a wall at constant speed requires only that the added masses be determined by the integral-equation procedure that has already been described, applied to the body and its mirror image.

For the case of a sphere moving away from a wall, we treat the wall as a sphere of infinite radius. Then, as a approaches infinity in (75) and (76), we obtain in the limit

$$k_2 = \frac{1}{2}\left[1 + 3\,\Sigma_1^{\infty}\frac{\sinh^3\zeta}{\sinh^3(n+1)\zeta}\right] = \frac{3}{2}\Sigma_3(\zeta) - 1 \tag{130}$$

$$k_{12} = -\frac{3}{2}\Sigma_3(\zeta) \tag{131}$$

Then, by (15) and (16),

$$F_1 = -\left(\dot{A}_{12} + \frac{1}{2}\dot{A}_{22}\right)U_2^2 = -\frac{4}{3}\pi\rho b^3\left(\dot{k}_{12} + \frac{1}{2}\dot{k}_2\right) = \pi\rho b^3\dot{\Sigma}_3(\zeta)U_2^2$$

$$F_2 = -\frac{1}{2}\dot{A}_{22}\,U_2^2 = -\frac{2}{3}\pi\rho b^3\,\dot{k}_2\,U_2^2 = -\,\pi\rho b^3\dot{\Sigma}_3(\zeta)U_2^2$$

These give the force coefficients

$$C_{F1} = \frac{2F_1}{\pi\rho b^2 U_2^2} = 2b\dot{\Sigma}_3(\zeta) = -\,C_{F2} \tag{132}$$

As for the case of a circle and a wall, $\dot{\Sigma}_3(\zeta)$ can be expressed in terms of $k_{12}$ and $\dot{k}_{12}$. From (76), we obtain $\Sigma_3(\zeta) = \Sigma_1^{\infty} \tau_n^{-3}$, $\Sigma_3' = -3\Sigma_1^{\infty} \tau_n^{-4}\tau'$ and then

$$\dot{\Sigma}_3 = \Sigma_3'/c' = -\frac{3}{b}\,\mathrm{csch}\zeta\cdot\Sigma_1^{\infty} \tau_n^{-4}\,\tau_n' \tag{133}$$

where $c'$ and $\tau_n'$ are given in (69) and (70).

7. Ellipse-circle combinations

The procedure developed for pairs of circular cylinders will now be applied to the case of an elliptical cylinder approaching a circular one along their line of centers. Since an exact solution is not available for this case, we proceed immediately to the integral-equation for the source distributions $\sigma_1(Q_1)$ and $\sigma_2(Q_2)$ formulated in (86) and (87), in which the first integral of (87) over the circle $c_2$ vanishes, as was shown in Section 5.

The peaks of the integrands when the gap is small were eliminated by introducing the transposes of the kernels and locating the points $P_1'$ and $P_2'$ defined in (103) and (104). Since $c_2$ is a circle, the point $P_2'$ is again given by (117); but to find $P_1'$, one must determine the point on the ellipse at which the distance from an exterior point $P_2$ on the circle is a minimum. This can be found from the condition that the line normal to the ellipse at $P_1'$ passes through the point $P_2(x_2,y_2)$. In terms of the parametric form of the equation of the ellipse, $x = a_1 \cos\psi$, $y = a_2 \sin\psi$, this gives

$$\tan\psi(P_1') = y_2/[a_1x_2 - (a_1^2 - a_2^2)\cos\psi\,(P_1')]$$

Since $\psi$ is small in the region of the peaks, this equation can readily be solved by iteration, with $\psi = 0$ in the right member as the first approximation.

Results for an ellipse approaching a circle are given in Tables 10 and 11. In the former $a_1 = 2b$ and $a_2 = b$, in the latter $a_1 = b$, $a_2 = 2b$, where b is the

radius of the circle, in terms of which the added masses and forces are nondimensionalized. Comparison of Tables 4 and 10 shows that, although the transverse dimensions and the asymptotic added masses as $g \to \infty$ are the same, the added mass and forces are appreciably less for the ellipse-circle pair. On the other hand when Tables 4 and 11 are compared, it is seen that the interaction effects are considerably greater for the ellipse-circle pair. These results are reasonable since, with $a_1/a_2 = 2$, the radius of curvature at the leading edge of the ellipse is $b/2$, and with $a_1/a_2 = 1/2$, is $4b$. The accuracy of the results in Tables 10 and 11 was judged by the effects of increasing the number of points on each body. To obtain the indicated accuracy, $N = 300$ was used on both bodies in both cases.

8. Results for two spheres by method of integral equations

Two spheres of radii a and b are moving with velocities $U_1$ and $U_2$ along their line of centers. We shall use two spherical coordinate systems, $(R_1, \theta_1, \psi_1)$ and $(R_2, \theta_2, \psi_2)$, with origins at the centers of the spheres at $x = x_1$ and $x = x_2$ for the spheres of radii a and b respectively. With the x-axis as the polar axis, the spherical coordinates are related to a fixed rectangular coordinate system by

$$x - x_i = R_i \cos\theta_i,\ y = R_i \sin\theta_i \cos\psi_i,\ z = R_i \sin\theta_i \sin\psi_i,\ i = 1,2$$

with

$$x_2 - x_1 = c.$$

Relative to the center of one of the spheres of radius a, we have

$$r_{PQ}^2 = R_P^2 + R_Q^2 - 2 R_P R_Q G(P,Q)$$

where

$$G(P,Q) = \cos\theta_P \cos\theta_Q + \sin\theta_P \sin\theta_Q \cos(\psi_P - \psi_Q)$$

we see that $G(P,Q) = G(Q,P)$. Then the kernels of the integral equation (98) become

$$K(P,Q) = -\left[\frac{\partial}{\partial R_P}\frac{1}{r_{PQ}}\right]_{R_P = a} = \frac{a}{r_{PQ}^3}[1 - G(P,Q)] = \frac{[1 - G(P,Q)]^{-1/2}}{2\sqrt{2}\,a^2} \qquad (134)$$

We see that the kernel is symmetric; i.e. K (P,Q) = K(Q,P).

Next, when the points P and Q are on different spheres of radii a and b, we obtain

$$r^2_{P1Q2} = (c - x_{P1} + x_{Q2})^2 + (y_{P1} - y_{Q2})^2 + (z_{P1} - z_{Q2})^2$$

$$= a^2 + b^2 + c^2 - 2c\,(a \cos\theta_{P1} + b \cos\theta'_{Q2}) - 2abG\,(P_1,Q_2),\ \theta' = \pi - \theta$$

where

$$G(P_1,Q_2) = -\cos\theta_{P1}\cos\theta'_{Q2} + \sin\theta_{P1}\sin\theta'_{Q2}\cos(\psi_{P1} - \psi_{Q2})$$

$$K(P_1,Q_2) = -\frac{\partial}{\partial a}\frac{1}{r_{P1Q2}} = \frac{1}{r^3_{P1Q2}}[a - c\cos\theta_{P1} - bG(P_1,Q_2)] \qquad (135)$$

$$K(Q_2,P_1) = -\frac{\partial}{\partial b}\frac{1}{r_{P1Q2}} = \frac{1}{r^3_{P1Q2}}[b - c\cos\theta'_{Q2} - aG(P_1,Q_2)] \qquad (136)$$

and similarly

$$r^2_{P2Q1} = a^2+b^2+c^2 - 2c(a\cos\theta_{Q1} + b\cos\theta'_{P2}) - 2abG\,(P_2,Q_1)$$

$$G(P_2,Q_1) = -\cos\theta'_{P2}\cos\theta_{Q1} + \sin\theta'_{P2}\sin\theta_{Q1}\cos(\psi_{P2} - \psi_{Q1})$$

$$K(P_2,Q_1) = -\frac{\partial}{\partial b}\frac{1}{r_{P2Q1}} = \frac{1}{r^3_{P2Q1}}[b - c\cos\theta'_{P2} - aG\,(P_2,Q_1)] \qquad (137)$$

$$K(Q_1,P_2) = -\frac{\partial}{\partial a}\frac{1}{r_{P2Q1}} = \frac{1}{r^3_{P2Q1}}[a - c\cos\theta_{Q1} - bG\,(P_2,Q_1)] \qquad (138)$$

The integral equations then become, by (105) and (106),

$$4\pi\sigma_1(P_1) + \int_{S_1}[\sigma_1(Q_1) - \sigma_1(P_1)]\,K(P_1,Q_1)\,dS_1$$

$$+ \int_{S_2} [\sigma_2(Q_2)\, K(P_1,Q_2) - \sigma_2(P_2')\, K(Q_2,P_1)]\, dS_{Q2} = U_1 \frac{\partial x}{\partial n_{P1}} \qquad (139)$$

$$4\pi\sigma_2(P_2) + \int_{S_2} [\sigma_2(Q_2) - \sigma_2(P_2)]\, K(P_2,Q_2)\, dS_{Q2}$$

$$+ \int_{S_1} [\sigma_1(Q_1)\, K(P_2,Q_1) - \sigma_1(P_2')\, K(Q_1,P_2)]\, dS_{Q1} = U_2 \frac{\partial x}{\partial n_{P2}} \qquad (140)$$

in which $\theta_{P1'}$ and $\theta_{P2'}$ at $P_1'$ and $P_2'$ are given by (117), so that (139, 140) are in the form for removing both the singularities of the kernels and the peaks of the integrands.

Because of the axial symmetry, the $\sigma$'s are not functions of $\psi$. We may then integrate first with respect to $\psi_Q$, and since the integration extends over the entire circular section, we may take $\psi_P = 0$. For bodies of revolution moving in the direction of their axes of symmetry, it is known that the integration over the polar angle $\psi$ in the plane of transverse section can be expressed in terms of elliptic integrals. We shall take advantage of this property to reduce the computing effort required to obtain accurate results on a 3-D problem, and will treat only the case of equal spheres, i.e., a = b.

First, then, we need to integrate the kernels of (139) and (140) with respect to $\psi$. For the cases $K(P_1,Q_1)$ and $K(P_2,Q_2)$, consider (with i = 1 or 2)

$$1 - G(P_i,Q_i) = 1 - \cos\theta_{Pi}\cos\theta_{Qi} - \sin\theta_{Pi}\sin\theta_{Qi}\,(2\cos^2\frac{\psi}{2} - 1)$$

$$= 1 - \cos(\theta_{Pi} + \theta_{Qi}) - 2\sin\theta_{Pi}\sin\theta_{Qi}\sin^2\nu, \quad \nu = \frac{1}{2}(\pi - \psi)$$

$$= 2\sin^2\frac{1}{2}(\theta_P + \theta_Q)\,[1 - \xi^2(\theta_P,\theta_Q)\sin^2\nu], \quad \xi^2_{PiQi} = \frac{\sin\theta_{Pi}\sin\theta_{Qi}}{\sin^2\frac{1}{2}(\theta_P + \theta_Q)}$$

Then by (134),

$$\int_0^{2\pi} K(P_i,Q_i)\, d\psi = \frac{1}{a^2} \csc\frac{1}{2}(\theta_{Pi} + \theta_{Qi}) \int_0^{\pi/2} (1 - \xi^2_{PiQi} \sin^2\nu)^{-1/2}\, d\nu$$

$$= \frac{1}{a^2} \csc\frac{1}{2}(\theta_{Pi} + \theta_{Pi})\ K(\xi^2_{PiQi}) \tag{141}$$

where $K(\xi_{PiQi})$ is the complete elliptic integral of the first kind.

For the case a = b, the other four kernels, given in (135, 136, 137, 138), are of the form

$$K(P,Q) = \frac{a[1-G(\theta,\theta',\nu)] - c\cos\{^{\theta}_{\theta'}\}}{\{2a^2[1-G(\theta,\theta',\nu)] - 2ac\,(\cos\theta + \cos\theta') + c^2\}^{3/2}} \tag{142}$$

where $\theta = \theta_1$ and $\theta' = \pi - \theta_2$, and

$$1-G(\theta,\theta',\nu) = 1 + \cos(\theta - \theta') - 2\sin\theta\sin\theta'\sin^2\nu \tag{143}$$

The numerator of (142) may then be expressed as

$$\frac{1}{2a}(r^2_{PQ} + 2ac\cos\{^{\theta'}_{\theta}\} - c^2) = \frac{1}{2a}[r^2_{PQ} - c(g + 4a\sin^2\frac{1}{2}\{^{\theta'}_{\theta}\})]$$

and since the denominator is $r^3_{PQ}$, we obtain

$$K(P,Q) = \frac{1}{2a}[\frac{1}{r_{PQ}} - \frac{c}{r^3_{PQ}}(g + 4a\sin^2\frac{1}{2}\{^{\theta'}_{\theta}\})] \tag{144}$$

Also one can show that

$$r^2_{PQ} = D^2[1 - \xi^2(\theta,\theta')\sin^2 v] \tag{145}$$

where

$$D^2 = [g + 2a(\sin^2\frac{\theta}{2} + \sin^2\frac{\theta'}{2})]^2 + a^2(\sin\theta + \sin\theta')^2 \tag{146a}$$

$$\xi^2(\theta,\theta') = \frac{4a^2}{D^2} \sin\theta \sin\theta' \qquad (146b)$$

We see from (144) and (145) that the integral of the first term of the kernel is immediately expressible in terms of an elliptic integral. To verify that the integral of the second term is also so expressible, we now show that

$$\int_0^{\pi/2} (1 - \xi^2)(1 - \xi^2 \sin^2\nu)^{-3/2}\, d\nu = E(\xi) \qquad (147)$$

where $E(\xi)$ is the complete elliptic integral of the second kind,

The integrand of (147) may be written as

$$(1-\xi^2 \sin^2\nu)^{-1/2} - \xi^2\cos^2\nu(1-\xi^2\sin^2\nu)^{-3/2} \qquad (148)$$

Integrating the second term by parts, we obtain

$$\int_0^{\pi/2} \xi^2\cos^2\nu\,(1-\xi^2\sin^2\nu)^{-3/2}\, d\nu = \int_0^{\pi/2} \xi^2\sin^2\nu\,(1-\xi^2 \sin^2\nu)^{-1/2}\, d\nu$$

which, combined with the integral of the first term of (148), gives

$$E(\xi) = \int_0^{\pi/2} (1 - \xi^2\sin^2\nu)^{1/2}\, d\nu$$

as stated.

The integral of the kernel (144) with respect to $\psi$ when P and Q lie on different spheres may now be written in terms of elliptic integrals. We obtain, by (145),

$$\int_0^{2\pi} K(P,Q)\, d\psi = 4 \int_0^{\pi/2} K(P,Q)\, d\nu = \frac{2}{aD} K[\xi(\theta,\theta')] - \frac{2c(g + 4a\sin^2 \frac{1}{2}\{^{\theta'}_{\theta}\})}{aD^3[1-\xi^2(\theta,\theta')]} E(\xi) \qquad (149)$$

The four integrals in (139, 140) can now be evaluated by multiplying the results in (141) and (149) by $a^2\sin\theta_{Q1}$ or $a^2\sin\theta'_{Q2}$ and integrating with respect to $\theta_{Q1}$ or $\theta'_{Q2}$ from 0 to $\pi$. These become

$$I_{PiQi} = \int_0^{\pi} [\sigma_i(Q_i) - \sigma_i(P_i)] \sin\theta_{Qi} \csc\frac{1}{2}(\theta_{Qi} + \theta_{Pi})\, K(\xi_{PiQi})\, d\theta_{Qi};\ i = 1,2 \qquad (150)$$

$$I_{P1Q2} = \int_0^{\pi} \{[\sigma_2(Q_2) - \sigma_2(P'_2)] \frac{2a}{D_{P1Q2}} K(\xi_{P1Q2}) - \frac{acE(\xi_{P1Q2})}{D^3_{P1Q2}(1 - \xi^2_{P1Q2})} \cdot$$

$$\cdot [\sigma_2(Q_2)(g + 4a\sin^2\frac{1}{2}\theta'_{Q2}) - 2\sigma_2(P'_2)(g + 4a\sin^2\frac{1}{2}\theta_{P1})]\} \sin\theta'_{Q2}\, d\theta'_{Q2} \qquad (151)$$

where, by (146),

$$D^2_{P1Q2} = [g + 2a(\sin^2\frac{1}{2}\theta_{P1} + \sin^2\frac{1}{2}\theta'_{Q2})]^2 +$$

$$a^2(\sin\theta_{P1} + \sin\theta'_{Q2})^2 = D^2_{Q2P1} \qquad (152)$$

and

$$\xi^2_{PiQi} = \frac{\sin\theta_{Pi}\sin\theta_{Qi}}{\sin^2\frac{1}{2}(\theta_{Pi} + \theta_{Qi})} = \xi^2_{QiPi},\ i = 1,2 \qquad (153)$$

$$\xi^2_{P1Q2} = \frac{4a^2}{D^2_{P1Q2}} \sin\theta_{P1} \sin\theta'_{Q2} = \xi^2_{Q2P1} \qquad (154)$$

Expressions for $I_{P2Q1}$, $D^2_{P2Q1}$ and $\xi^2_{P2Q1}$ can be obtained from (151, 152, 154) by interchanging subscripts 1 and 2.

$K(\xi)$ has a logarithmic singularity at $\xi = 1$ or $\xi' = (1 - \xi^2)^{1/2}) = 0$. When $\xi'^2$ is less than 1/2, $K(\xi)$ and $E(\xi)$ can be computed accurately and efficiently by the expansions

$$K(\xi) = \ell n \frac{4}{\xi'} + \sum_{n=1}^{\infty} a_n^2 \, (\ell n \frac{4}{\xi'} - b_n) \, \xi'^{2n} \tag{155}$$

$$E(\xi) = 1 + \frac{1}{2} (\ell n \frac{4}{\xi'} - \frac{1}{2}) \, \xi'^2 + \sum_{n=1}^{\infty} a_n \, a_{n+1} \, [\ell n \frac{4}{\xi'} - \frac{1}{(2n+1)(2n+2)} - b_n] \, \xi'^{2n+2}$$

$$a_n = \frac{2n-1}{2n} a_{n-1} = \frac{1.3.5...(2n-1)}{2.4.6...2n} \qquad b_n = b_{n-1} + \frac{1}{n(2n-1)} = \sum_{i=1}^{n} \frac{1}{i(2i-1)} \tag{156}$$

For $\xi^2$ less than 1/2, the series expansions

$$K(\xi) = \frac{\pi}{2} (1 + \sum_{n=1}^{\infty} a_n^2 \, \xi^{2n}), \qquad E = \frac{\pi}{2} (1 - \sum_{n=1}^{\infty} \frac{a_n^2}{2n-1} \xi^{2n}) \tag{157}$$

converge rapidly.

Since the integrands $F(\theta)$ of (150) and (151) are not cyclic in $0 < \theta < \pi$, where $\theta$ represents $\theta_Q$ or $\theta_Q'$, the MAQF cannot be used directly to evaluate their integrals. We could generate a continuous cyclic function by defining $F(\theta) = F(2\pi - \theta)$ for $\pi < \theta < 2\pi$ and then repeating this combination for successive $2\pi$-intervals to the left and right of the 0 to $2\pi$ range; but the derivatives at the junction points $\theta = 0, \pi, 2\pi$ would have opposite signs since $F'(\theta) = - F'(2\pi - \theta)$. Hence the MAQF, which requires a smooth function, may not be applied unless the slopes are zero there.

We have seen that the nonuniform MAQF transformation (107) introduces the factor $\sin^2 \omega/2$ in the integrand, which gives zero derivatives with respect to $\omega$ at $\omega = 0$ and $2\pi$, but not at $\omega = \pi$. By replacing $\theta$ and $\omega$ in (107) by $2\theta$ and $2\omega$, the transformation and its differential become

$$\theta = \omega - \frac{1}{2} \sin 2\omega, \qquad d\theta = 2\sin^2 \omega d\omega \tag{158}$$

and then

$$\int_0^{\pi} F(\theta)\, d\theta = 2 \int_0^{\pi} F(\theta) \sin^2 \omega d\omega \qquad (159)$$

Since $\sin \theta$ is a factor of $F(\theta)$, the zeros of the integrand of (159) at $\omega = 0, \pi, 2\pi$ are seen to be of third order. Hence not only the slopes but also the curvatures of the extended integrands are zero at the junction points as a consequence of the transformation (158). If a higher concentration of points near $\theta = 0$ than that given by (158) is required, the transformations (107a) and (107b) may be used, again with $\theta$ and $\omega$ replaced by $2\theta$ and $2\omega$.

Results for $k_1$, $k_{12}$, $\dot{k}_1$, $\dot{k}_{12}$ are given in Table 12, where calculated values are compared with the exact ones. The derivatives were obtained by the same procedure as for the circles, i.e., numerical differentiation with respect to the parameter $\gamma$ by a five point central-difference formula, followed by the exact derivative of $\gamma$ with respect to g, as is shown in (109). The results for $k_1$ and $k_{12}$ practically agree to five decimals from $g/b = 0.01$ to 0.04, and to six decimals at larger gaps; $\dot{k}_1$ and $\dot{k}_{12}$ agree to three decimals up to $g/b = 0.03$ to four decimals up to 0.07, and to five decimals at larger gaps.

Results for $k_1$ and $k_{12}$ are compared with those of Ref. [2] in Table 13. The deviation from the 'exact' values is seen to be much less with the present procedures, which were accurate enough for application of numerical differentiation to obtain the added-mass derivatives given in Table 12. Only exact values of these derivatives are presented in Ref. [2], indicating that their procedure of solving the pair of differentiated integral equations could not give adequate accuracy at small gaps, probably because the peaks of their differentiated kernels are of the order of $1/g^3$.

## SUMMARY AND CONCLUSIONS

The motivation for undertaking the present work was to evaluate the accuracy of the interaction forces computed by the integral-equation approach. For this purpose, the classical theory of successive images, for central impact of pairs of circles or spheres, is available for obtaining highly accurate numerical solutions, against which results from integral equations could be compared. In the course of applying these approaches, new and significant

advances in both areas were made and have been described. These will now be summarized.

On the method of successive images, the following has been accomplished:

1. A new and more rational derivation of Herman's formulas for the doublet strengths than that given in his paper [10] is presented.

2. A parametric form of these formulas has been applied to derive new truncation-correction formulas, with which the infinite series for the added masses can be summed to a desired accuracy with many fewer terms.

3. A new asymptotic formula equating the mathematical parameter $\zeta$ of the aforementioned parametric form to a polynomial in the nondimensional physical parameter $\gamma$ (which is proportional to the square-root of the gap g between the bodies) is derived, and shown to be highly accurate at small gaps, and for equal circular cylinders or spheres, to be usefully accurate up to $g/b = 1$.

4. Combining the truncation and asymptotic formulas yielded the results that the series for the added masses, and those for their derivatives with respect to the parameter $\zeta$, both converge at $g = 0$, and asymptotic Taylor expansions about $g = 0$, which display the added masses and their derivatives at $g = 0$, are given. These properties led to the new results that the derivatives of the added masses with respect to g, for small values of $\gamma$, vary as $g^{-1/2}$ for circular cylinders and as $-\ell n\, g$ for spheres. In both cases, this implies that the repulsive forces approach infinity, verifying the well-known irrotational-flow paradox that the bodies would never meet.

5. The need for considering the property of uniform convergence of the series for the added masses and their derivatives is discussed in the text. It is proved that these series are uniformly convergent in the closed region $0 \leq g \leq \infty$, indicating that the added masses are continuous functions of g at $g = 0$; and that the series for their derivatives with respect to $\zeta$ are uniformly convergent in the open region $0 < g \leq \infty$, i.e., although this derivative series converges at $g = 0$, the convergence is not uniform. This implies that the

derivatives of the added masses may be discontinuous at $\zeta = 0$, as is shown in the text for a pair of circular cylinders.

On the method of integral equations, three new procedures were developed to obtain more accurate solutions. The first of these was required at small gaps to eliminate the peaks of the four kernels of the two integral equations. It was shown that the transposes of these kernels eliminate not only their singularities but also their peaks, which are of the order of $1/g$ for two-dimensional and of $1/g^2$ for three-dimensional bodies of general shape. This left a residue of much smaller peaks due to the rapid variation of the source distribution in the gap region when the gap is small. These were treated by applying a quadrature formula, described in the next paragraph, which concentrates many points in the small neighborhood of the smaller peaks.

In the second procedure, the 'most accurate quadrature formula,' which requires a smooth, cyclic integrand and uniform intervals, was modified by changing the variable of integration, so that the integrand remains cyclic, uniform intervals are taken in the new variable, and many points of the original variable are concentrated in the desired region. A sequence of such transformations, of successively increasing point concentrations in a small region, is presented. With a slight modification, this nonuniform MAQF also served to evaluate accurately the noncyclic integrals of the two-sphere problem.

The third procedure was developed in order to improve the accuracy of the added-mass derivatives obtained by numerical differentiation of the added-mass data. As is described in the text, this procedure, which is suitable for general shapes, requires accurate solutions of the integral equations, and is suggested by the asymptotic formulas for the added masses at small gaps.

By means of these new procedures, the minimum gap at which accurate results could be obtained was reduced to about one-tenth of those reported in the original work on this problem for the Mobil Research and Development Corporation. Results for circle pairs of diameter ratios 1,4,16 and $\infty$, two ellipse-circle pairs and a pair of equal spheres are presented. The treatment of the infinite-diameter ratio (a circle approaching a wall), which is

also applied to a sphere and a wall, yields results for the added masses and forces on bodies of arbitrary shape. All the other applications were to two-dimensional and axisymmetric forms, for which the integral-equation approach yielded highly accurate solutions. An IBM RISC/6000 was used to obtain the numerical results.

## ACKNOWLEDGEMENT

This work was partly supported by the Office of Naval Research under Grant N00014-89-J-1581.

## REFERENCES

1. Landweber, L., Chwang, A.T., and Guo, Z., "Interaction between Two Bodies Translating in an Inviscid Fluid," Journal of Ship Research, accepted for publication.

2. Guo, Z. and Chwang, A.T., "Oblique Impact of Two Cylinders in a Uniform Flow," Journal of Ship Research, accepted for publication.

3. Guo, Z. and Chwang, A.T., "On the Planar Translation of Two Bodies in a Uniform Flow," IIHR Report No. 337, March 1990.

4. Landweber, L., "On a Generalization of Taylor's Virtual Mass Relation for Rankine Bodies," Quarterly of Applied Mathematics, Vol. 14, No. 1, 1956, pp. 51-56.

5. Landweber, L. and Yih, C.S., "Forces, Moments and Added Masses for Rankine Bodies," Journal of Fluid Mechanics, Vol. 1, Part 3, 1956, pp. 319-336.

6. Landweber, L. and Chwang, A.T., "Generalization of Taylor's Added Mass Formula for Two Bodies," Journal of Ship Research, Vol. 33, No. 1, March 1989, pp. 1-9.

7. Isaacson, M. and Chung, K.F., "Hydrodynamics of Ice Mass near Large Offshore Structure," Journal of Waterway, Port, Coastal, and Ocean Engineering, Vol. 114, No. 4, July 1988, pp. 487-502.

8. Atkinson, K.E., An Introduction to Numerical Analysis, 2nd ed., Wiley, 1988, pp. 285-289.

9. Miloh, T. and Landweber, L., "Ship Centerplane Source Distribution," Journal of Ship Research, Vol. 24, No. 1, March 1980, pp. 8-23.

10. Herman, R.A., "On the Motion of Two Spheres in Fluid and Allied Problems," Quarterly Journal of Mathematics, Vol. 22, 1887, pp. 204-262.

11. Mitra, S.K., "A New Method of Solution of the Boundary Value Problems of Laplace's Equation Relating to Two Spheres," Bulletin of the Calcutta Mathematics Society, Vol. 36, 1944, pp. 31-39.

12. Shail, R., "On Some Axisymmetrical Two Sphere Potential Problems," Mathematika, Vol. 9, 1962, pp. 57-70.

13. Hicks, W.M., "On the Motion of Two Spheres in a Fluid," Philosophical Transactions, Royal Society of London, Vol. 171-II, 1880, pp. 455-492.

14. Hicks, W.M., "On the Motion of Two Cylinders in a Fluid," Quarterly Journal of Mathematics, Vol. 16, 1879, pp. 113-140, 193-219.

15. Landweber, L., "Properties of the Neumann Kernel and Interior Irrotational Flow for a Nearly Closed Surface," Proceedings of Symposium on Fluid Dynamics in Honor of Theodore Yao-Tsu Wu, 1989, published by World Scientific Publishing Co., 1990.

16. Landweber, L. and Macagno, M., "Irrotational Flow about Ship Forms," IIHR Report No. 123, Iowa Institute of Hydraulic Research, University of Iowa, 1969.

Table 1. Example showing truncation correction by trapezoidal integral

| N | R(N) | $\Sigma_1^N \frac{1}{n^2} + R(N)$ |
|---|---|---|
| 10 | 0.095238 | 1.645006 |
| 100 | 0.009950 | 1.644934 |
| 1000 | 0.001000 | 1.644934 |

Table 2. Calculation of $-k_{12}$ with truncation correction $R_{12}$ for a=b.

| | g/a = 0.0001 | | g/a = 0.001 | | g/a = 0.01 | |
|---|---|---|---|---|---|---|
| N | $R_{12}$ | $-k_{12}$** | $R_{12}$ | $-k_{12}$ | $R_{12}$ | $-k_{12}$ |
| 10 | .0383183 | .8125634 | .0228071 | .7914781 | .0030591 | .7282811 |
| 20 | .0157424 | .8125323 | .0051146 | .7914469 | .0000553 | .7282603 |
| 30 | .0083784 | .8125290 | .0013646 | .7914436 | .0000010 | .7282599 |
| 40 | .0049347 | .8125281 | .0003793 | .7914429 | 0 | . |
| 50 | .0030590 | .8125278 | .0001066 | .7914427 | . | . |
| 70 | .0012677 | .8125276 | .0000085 | . | . | . |
| 100 | .0003656 | . | .0000002 | . | . | . |
| 200 | .0000066 | . | . | . | . | . |
| 300 | .0000001 | . | . | . | . | . |
| ∞ | 0 | .8125275 | 0 | .7914426 | 0 | .7282599 |

* $-k_{12} \doteq \frac{2}{b^2} \Sigma_1^N \delta_{2n-1} + R_{12}$

Table 3. Values of $k_1$ by various methods at g/b = 0.01 for a = b

| | | | $k_1$ | |
|---|---|---|---|---|
| | Integrand peaks removed? | Nonuniform MAQF | N = 40 | N = 100 |
| 1. | Yes | Yes | 1.375338 | 1.375338 |
| 2. | No, only kernel peaks removed* | Yes | 1.0177 | 1.3715 |
| 3. | Yes | uniform | 1.3790 | 1.3785 |
| 4. | No | Yes | 6.8110 | 1.3748 |
| 5. | No | uniform | diverged | diverged |

*Used $\sigma_1(0)$ and $\sigma_2(\pi)$ instead of $\sigma_1(\theta_{1P'})$ and $\sigma_2(\theta_{2P'})$

Table. 4. Comparison of 'exact' added masses and their derivatives for equal circles with results calculated using integral equations.

| g/a | $k_1$(calc) | $\dot{k}_1$(calc) | $\dot{k}_1$(exact) | $k_{12}$(calc) | $\dot{k}_{12}$(calc) | $\dot{k}_{12}$(exact) | $C_{F1} = -C^*_{F2}$ | $C_{F2} = -C^*_{F1}$ | N |
|---|---|---|---|---|---|---|---|---|---|
| 0.01 | 1.375338 | -4.22054 | -4.22048 | -0.728260 | 4.43439 | 4.43434 | -6.6296 | 7.3014 | 40 |
| 0.02 | 1.341620 | -2.77335 | -2.77335 | -0.692409 | 2.98609 | 2.98609 | -4.3564 | 5.0247 | 40 |
| 0.03 | 1.317390 | -2.13769 | -2.13769 | -0.666057 | 2.34931 | 2.34931 | -3.3579 | 4.0227 | 40 |
| 0.04 | 1.298030 | -1.76190 | -1.76190 | -0.644586 | 1.97240 | 1.97240 | -2.7676 | 3.4289 | 40 |
| 0.05 | 1.281755 | -1.50753 | -1.50753 | -0.626212 | 1.71691 | 1.71691 | -2.3680 | 3.0258 | 40 |
| 0.06 | 1.267655 | -1.32129 | -1.32129 | -0.610023 | 1.52955 | 1.52955 | -2.0755 | 2.7297 | 40 |
| 0.07 | 1.255188 | -1.17771 | -1.17771 | -0.595480 | 1.38485 | 1.38485 | -1.8499 | 2.5007 | 40 |
| 0.08 | 1.244005 | -1.06291 | -1.06291 | -0.582231 | 1.26892 | 1.26892 | -1.6696 | 2.3168 | 40 |
| 0.09 | 1.233862 | -0.96858 | -0.96858 | -0.570034 | 1.17347 | 1.17347 | -1.5214 | 2.1651 | 40 |
| 0.10 | 1.224583 | -0.88942 | -0.88942 | -0.558711 | 1.09319 | 1.09319 | -1.3971 | 2.0373 | 30 |
| 0.12 | 1.208116 | -0.76342 | -0.76342 | -0.538191 | 0.96494 | 0.96494 | -1.1992 | 1.8323 | 30 |
| 0.14 | 1.193850 | -0.66707 | -0.66707 | -0.519918 | 0.86634 | 0.86634 | -1.0478 | 1.6739 | 30 |
| 0.16 | 1.181301 | -0.59065 | -0.59065 | -0.503405 | 0.78767 | 0.78767 | -0.9278 | 1.5467 | 30 |
| 0.18 | 1.170130 | -0.52839 | -0.52839 | -0.488317 | 0.72315 | 0.72315 | -0.8300 | 1.4419 | 30 |
| 0.20 | 1.160096 | -0.47657 | -0.47657 | -0.474410 | 0.66908 | 0.66908 | -0.7486 | 1.3534 | 30 |
| 0.25 | 1.138879 | -0.37825 | -0.37825 | -0.443709 | 0.56512 | 0.56512 | -0.5942 | 1.1812 | 30 |
| 0.30 | 1.121797 | -0.30870 | -0.30870 | -0.417425 | 0.48991 | 0.48991 | -0.4849 | 1.0542 | 30 |
| 0.35 | 1.107715 | -0.25694 | -0.25694 | -0.394423 | 0.43252 | 0.43252 | -0.4036 | 0.9552 | 30 |
| 0.40 | 1.095906 | -0.21704 | -0.21704 | -0.373976 | 0.38700 | 0.38700 | -0.3409 | 0.8749 | 30 |
| 0.45 | 1.085873 | -0.18547 | -0.18547 | -0.355584 | 0.34985 | 0.34985 | -0.2913 | 0.8078 | 30 |
| 0.50 | 1.077258 | -0.15998 | -0.15998 | -0.338889 | 0.31885 | 0.31885 | -0.2513 | 0.7504 | 30 |
| 0.60 | 1.063293 | -0.12168 | -0.12168 | -0.309579 | 0.26978 | 0.26978 | -0.1911 | 0.6564 | 30 |
| 0.70 | 1.052548 | -0.09471 | -0.09471 | -0.284544 | 0.23248 | 0.23248 | -0.1488 | 0.5816 | 30 |
| 0.80 | 1.044109 | -0.07505 | -0.07505 | -0.262822 | 0.20304 | 0.20304 | -0.1179 | 0.5200 | 30 |
| 0.90 | 1.037374 | -0.06034 | -0.06034 | -0.243752 | 0.17915 | 0.17915 | -0.0948 | 0.4680 | 30 |
| 1.00 | 1.031926 | -0.04911 | -0.04911 | -0.226856 | 0.15936 | 0.15936 | -0.0771 | 0.4235 | 30 |
| 1.20 | 1.023785 | -0.03353 | -0.03353 | -0.198233 | 0.12850 | 0.12850 | -0.0527 | 0.3510 | 30 |
| 1.40 | 1.018137 | -0.02366 | -0.02366 | -0.174925 | 0.10565 | 0.10565 | -0.0372 | 0.2948 | 30 |
| 1.60 | 1.014101 | -0.01714 | -0.01714 | -0.155617 | 0.08817 | 0.08817 | -0.0269 | 0.2501 | 30 |
| 1.80 | 1.011145 | -0.01270 | -0.01270 | -0.139405 | 0.07448 | 0.07448 | -0.0199 | 0.2140 | 30 |
| 2.00 | 1.008935 | -0.00958 | -0.00958 | -0.125641 | 0.06356 | 0.06356 | -0.0151 | 0.1846 | 30 |
| 2.50 | 1.005414 | -0.00508 | -0.00508 | -0.099063 | 0.04432 | 0.04432 | -0.0080 | 0.1313 | 30 |
| 3.00 | 1.003479 | -0.00290 | -0.00290 | -0.080152 | 0.03219 | 0.03219 | -0.0046 | 0.0966 | 30 |
| 4.00 | 1.001634 | -0.00112 | -0.00112 | -0.055604 | 0.01857 | 0.01857 | -0.0018 | 0.0566 | 30 |
| 5.00 | 1.000868 | -0.00051 | -0.00051 | -0.040835 | 0.01168 | 0.01168 | -0.0008 | 0.0359 | 30 |
| 6.00 | 1.000504 | -0.00026 | -0.00026 | -0.031258 | 0.00782 | 0.00782 | -0.0004 | 0.0242 | 30 |
| 8.00 | 1.000204 | -0.00008 | -0.00008 | -0.020002 | 0.00400 | 0.00400 | -0.0001 | 0.0124 | 30 |
| 10.00 | 1.000098 | -0.00003 | -0.00003 | -0.013890 | 0.00231 | 0.00231 | -0.0001 | 0.0072 | 30 |

Table 5. Comparison with Ref [2] of values of $k_1$ and $k_{12}$ for equal circles.

| | $k_1$ | | | $-k_{12}$ | | |
|---|---|---|---|---|---|---|
| g/b | exact | present* int. eq. | Ref. [2]** int. eq. | exact | present int. eq. | Ref. [2] int. eq. |
| 0.01 | 1.375338 | 1.375338 | 1.3713 | 0.728260 | 0.728260 | 0.7214 |
| 0.02 | 1.341620 | 1.341620 | 1.3400 | 0.692409 | 0.692409 | 0.6901 |
| 0.03 | 1.317390 | 1.317390 | 1.3169 | 0.666057 | 0.666057 | 0.6653 |
| 0.04 | 1.298030 | 1.298030 | 1.2979 | 0.644586 | 0.644586 | 0.6443 |
| 0.05 | 1.281755 | 1.281755 | 1.2817 | 0.626212 | 0.626212 | 0.6261 |
| 0.06 | 1.267655 | 1.267655 | 1.2676 | 0.610023 | 0.610023 | 0.6100 |
| 0.07 | 1.255188 | 1.255188 | 1.2552 | 0.595480 | 0.595480 | 0.5955 |
| 0.08 | 1.244005 | 1.244005 | 1.2440 | 0.582231 | 0.582231 | 0.5822 |
| 0.09 | 1.233862 | 1.233862 | 1.2339 | 0.570034 | 0.570034 | 0.5700 |
| 0.10 | 1.224583 | 1.224583 | 1.2246 | 0.558711 | 0.558711 | 0.5587 |

*Calculated with a 40-point nonuniform MAQF, and all integrand peaks removed.

**Calculated with three Gauss quadrature formulas, of order 20 (see condition 2 of Table 3).

Table 6. Comparison with Ref [2] of values of $\dot{k}_1$ and $\dot{k}_{12}$ for a = b = 1.

| | $-\dot{k}_1$ | | | $\dot{k}_{12}$ | | |
|---|---|---|---|---|---|---|
| g/b | exact | present* int. eq. | Ref. [2] int. eq. | exact | present* int. eq. | Ref. [2] int. eq. |
| 0.01 | 4.220480 | 4.22054 | 4.10983 | 4.434339 | 4.43439 | 4.32371 |
| 0.02 | 2.773348 | 2.77335 | 2.77325 | 2.986088 | 2.98609 | 2.98597 |
| 0.03 | 2.137694 | 2.13769 | 2.13769 | 2.349315 | 2.34931 | 2.34931 |
| 0.04 | 1.761898 | 1.76190 | 1.76190 | 1.972399 | 1.97240 | 1.97240 |
| 0.05 | 1.507534 | 1.50753 | 1.50753 | 1.716914 | 1.71691 | 1.71691 |
| 0.06 | 1.321292 | 1.32129 | 1.32129 | 1.529551 | 1.52955 | 1.52955 |
| 0.07 | 1.177713 | 1.17771 | 1.17771 | 1.384850 | 1.38485 | 1.38485 |
| 0.08 | 1.062909 | 1.06291 | 1.06291 | 1.268923 | 1.26892 | 1.26892 |
| 0.09 | 0.968580 | 0.96858 | 0.96868 | 1.173472 | 1.17347 | 1.17347 |
| 0.10 | 0.889422 | 0.88942 | 0.88942 | 1.093190 | 1.09319 | 1.09319 |

*Calculated from a five-point central-difference formula, for which values of $k_1$ and $k_{12}$ at g/b = 0.005 and 0.007 were required and computed.

Table 7. Results for unequal circles; a = 4b.

| g/b | $k_1$ | $k_2$ | $k_{12}$ | $\dot{k}_1$ | $\dot{k}_2$ | $\dot{k}_{12}$ | $C_{F1}$ | $C_{F2}$ | $C^{\bullet}_{F1}$ | $C^{\bullet}_{F2}$ |
|---|---|---|---|---|---|---|---|---|---|---|
| 0.010 | 17.432850 | 1.758403 | -1.916832 | -8.85621 | -8.41063 | 8.78604 | -13.9113 | 13.6909 | -14.3908 | 13.2114 |
| 0.020 | 17.361419 | 1.691412 | -1.846095 | -5.93574 | -5.49313 | 5.86718 | -9.2942 | 9.0795 | -9.8037 | 8.6286 |
| 0.030 | 17.309123 | 1.643528 | -1.794476 | -4.65482 | -4.21516 | 4.58800 | -7.3118 | 7.1019 | -7.7925 | 6.6212 |
| 0.040 | 17.266634 | 1.605421 | -1.752647 | -3.89846 | -3.46161 | 3.83322 | -6.1237 | 5.9187 | -6.6049 | 5.4375 |
| 0.050 | 17.230353 | 1.573495 | -1.717011 | -3.38702 | -2.95290 | 3.32325 | -5.3034 | 5.1037 | -5.8019 | 4.6384 |
| 0.060 | 17.198442 | 1.545911 | -1.685730 | -3.01271 | -2.58147 | 2.95056 | -4.7324 | 4.5371 | -5.2145 | 4.0550 |
| 0.070 | 17.169815 | 1.521582 | -1.657716 | -2.72421 | -2.29582 | 2.66374 | -4.2792 | 4.0892 | -4.7621 | 3.6063 |
| 0.080 | 17.143766 | 1.499803 | -1.632264 | -2.49363 | -2.06798 | 2.43463 | -3.9045 | 3.7197 | -4.4002 | 3.2484 |
| 0.090 | 17.119806 | 1.480086 | -1.608887 | -2.30416 | -1.88125 | 2.24664 | -3.6194 | 3.4387 | -4.1030 | 2.9551 |
| 0.100 | 17.097582 | 1.462077 | -1.587230 | -2.14504 | -1.72494 | 2.08913 | -3.3694 | 3.1938 | -3.8537 | 2.7095 |
| 0.120 | 17.057338 | 1.430179 | -1.548073 | -1.89158 | -1.47702 | 1.83872 | -2.9618 | 2.7963 | -3.4564 | 2.3201 |
| 0.140 | 17.021527 | 1.402605 | -1.513290 | -1.69738 | -1.28827 | 1.64747 | -2.6662 | 2.5094 | -3.1521 | 2.0236 |
| 0.160 | 16.989179 | 1.378385 | -1.481911 | -1.54296 | -1.13924 | 1.49596 | -2.4237 | 2.2760 | -2.9102 | 1.7895 |
| 0.180 | 16.959622 | 1.356849 | -1.453265 | -1.41669 | -1.01832 | 1.37259 | -2.2182 | 2.0802 | -2.7126 | 1.5996 |
| 0.200 | 16.932374 | 1.337515 | -1.426870 | -1.31111 | -0.91808 | 1.26989 | -2.0595 | 1.9300 | -2.5474 | 1.4421 |
| 0.250 | 16.872176 | 1.296639 | -1.368559 | -1.10899 | -0.72907 | 1.07468 | -1.7420 | 1.6342 | -2.2310 | 1.1452 |
| 0.300 | 16.820542 | 1.263681 | -1.318474 | -0.96355 | -0.59640 | 0.93586 | -1.5087 | 1.4220 | -2.0033 | 0.9368 |
| 0.350 | 16.775244 | 1.236428 | -1.274401 | -0.85301 | -0.49832 | 0.83165 | -1.3399 | 1.2728 | -1.8300 | 0.7828 |
| 0.400 | 16.734858 | 1.213471 | -1.234930 | -0.76561 | -0.42308 | 0.75032 | -1.2026 | 1.1546 | -1.6926 | 0.6646 |
| 0.450 | 16.698414 | 1.193856 | -1.199105 | -0.69445 | -0.36377 | 0.68492 | -1.0874 | 1.0575 | -1.5803 | 0.5714 |
| 0.500 | 16.665216 | 1.176903 | -1.166246 | -0.63515 | -0.31598 | 0.63110 | -0.9977 | 0.9850 | -1.4863 | 0.4963 |
| 0.600 | 16.606622 | 1.149114 | -1.107539 | -0.54137 | -0.24423 | 0.54748 | -0.8504 | 0.8696 | -1.3363 | 0.3836 |
| 0.700 | 16.556201 | 1.127361 | -1.056045 | -0.47001 | -0.19358 | 0.48518 | -0.7359 | 0.7835 | -1.2202 | 0.3041 |
| 0.800 | 16.512128 | 1.109952 | -1.010045 | -0.41348 | -0.15642 | 0.43668 | -0.6495 | 0.7224 | -1.1262 | 0.2457 |
| 0.900 | 16.473159 | 1.095774 | -0.968395 | -0.36735 | -0.12839 | 0.39763 | -0.5770 | 0.6722 | -1.0475 | 0.2017 |
| 1.000 | 16.438403 | 1.084062 | -0.930295 | -0.32887 | -0.10674 | 0.36532 | -0.5166 | 0.6311 | -0.9800 | 0.1677 |
| 10.000 | 16.010208 | 1.000733 | -0.142275 | -0.00273 | -0.00021 | 0.01898 | -0.0043 | 0.0553 | -0.0593 | 0.0003 |
| 50.000 | 16.000056 | 1.000004 | -0.010579 | -0.00000 | 0.00000 | 0.00039 | -0.0000 | 0.0012 | -0.0012 | 0.0000 |

Table 8. Results for unequal circles; a = 16b.

| g/b | $k_1$ | $k_2$ | $k_{12}$ | $\dot{k}_1$ | $\dot{k}_2$ | $\dot{k}_{12}$ | $C_{F1}$ | $C_{F2}$ | $C^{\bullet}_{F1}$ | $C^{\bullet}_{F2}$ |
|---|---|---|---|---|---|---|---|---|---|---|
| 0.010 | 258.444846 | 1.951934 | -2.678140 | -10.88335 | -10.58338 | 10.75711 | -17.0955 | 16.6989 | -17.1701 | 16.6243 |
| 0.020 | 258.357764 | 1.867850 | -2.592318 | -7.17711 | -6.87754 | 7.05129 | -11.2379 | 10.8439 | -11.3491 | 10.8032 |
| 0.030 | 258.294924 | 1.808004 | -2.530735 | -5.55800 | -5.25868 | 5.43238 | -8.7305 | 8.3358 | -8.8060 | 8.2603 |
| 0.040 | 258.244458 | 1.760530 | -2.481524 | -4.60564 | -4.30664 | 4.48034 | -7.2345 | 6.8409 | -7.3105 | 6.7649 |
| 0.050 | 258.201795 | 1.720855 | -2.440112 | -3.96404 | -3.66540 | 3.83911 | -6.2069 | 5.8156 | -6.3033 | 5.7576 |
| 0.060 | 258.164604 | 1.686649 | -2.404169 | -3.49650 | -3.19815 | 3.37178 | -5.4923 | 5.1005 | -5.5691 | 5.0236 |
| 0.070 | 258.131506 | 1.656533 | -2.372317 | -3.13760 | -2.83954 | 3.01319 | -4.9285 | 4.5377 | -5.0059 | 4.4603 |
| 0.080 | 258.101610 | 1.629616 | -2.343663 | -2.85172 | -2.55397 | 2.72770 | -4.4652 | 4.0768 | -4.5576 | 4.0118 |
| 0.090 | 258.074299 | 1.605281 | -2.317591 | -2.61788 | -2.32043 | 2.49403 | -4.1122 | 3.7231 | -4.1903 | 3.6449 |
| 0.100 | 258.049125 | 1.583080 | -2.293655 | -2.42239 | -2.12526 | 2.29875 | -3.8051 | 3.4167 | -3.8834 | 3.3384 |
| 0.120 | 258.003928 | 1.543818 | -2.250922 | -2.11266 | -1.81627 | 1.98980 | -3.3080 | 2.9233 | -3.3982 | 2.8530 |
| 0.140 | 257.964126 | 1.509937 | -2.213571 | -1.87750 | -1.58177 | 1.75526 | -2.9492 | 2.5651 | -3.0297 | 2.4846 |
| 0.160 | 257.928498 | 1.480217 | -2.180382 | -1.69215 | -1.39711 | 1.57049 | -2.6580 | 2.2758 | -2.7393 | 2.1946 |
| 0.180 | 257.896207 | 1.453819 | -2.150518 | -1.54191 | -1.24766 | 1.42088 | -2.4143 | 2.0353 | -2.5040 | 1.9598 |
| 0.200 | 257.866650 | 1.430139 | -2.123375 | -1.41752 | -1.12404 | 1.29714 | -2.2266 | 1.8485 | -2.3095 | 1.7656 |
| 0.250 | 257.802008 | 1.380126 | -2.064711 | -1.18320 | -0.89161 | 1.06446 | -1.8586 | 1.4855 | -1.9436 | 1.4005 |
| 0.300 | 257.747180 | 1.339826 | -2.015779 | -1.01875 | -0.72922 | 0.90166 | -1.5952 | 1.2285 | -1.6872 | 1.1455 |
| 0.350 | 257.699428 | 1.306498 | -1.973839 | -0.89697 | -0.60955 | 0.78159 | -1.4090 | 1.0465 | -1.4980 | 0.9575 |
| 0.400 | 257.657019 | 1.278405 | -1.937155 | -0.80322 | -0.51802 | 0.68958 | -1.2617 | 0.9047 | -1.3527 | 0.8137 |
| 0.450 | 257.618784 | 1.254372 | -1.904558 | -0.72890 | -0.44601 | 0.61702 | -1.1413 | 0.7909 | -1.2378 | 0.7006 |
| 0.500 | 257.583896 | 1.233570 | -1.875220 | -0.66861 | -0.38808 | 0.55851 | -1.0503 | 0.7044 | -1.1450 | 0.6096 |
| 0.600 | 257.521886 | 1.199369 | -1.824038 | -0.57692 | -0.30130 | 0.47045 | -0.9062 | 0.5717 | -1.0047 | 0.4733 |
| 0.700 | 257.467675 | 1.172466 | -1.780291 | -0.51060 | -0.24009 | 0.40780 | -0.7995 | 0.4776 | -0.9040 | 0.3771 |
| 0.800 | 257.419231 | 1.150811 | -1.741943 | -0.46045 | -0.19519 | 0.36133 | -0.7233 | 0.4119 | -0.8285 | 0.3066 |
| 0.900 | 257.375225 | 1.133065 | -1.707665 | -0.42117 | -0.16125 | 0.32573 | -0.6616 | 0.3617 | -0.7700 | 0.2533 |
| 1.000 | 257.334744 | 1.118305 | -1.676545 | -0.38951 | -0.13501 | 0.29773 | -0.6118 | 0.3235 | -0.7233 | 0.2121 |
| 10.000 | 256.247598 | 1.002291 | -0.703140 | -0.03680 | -0.00052 | 0.05227 | -0.0576 | 0.1061 | -0.1634 | 0.0008 |
| 100.000 | 256.000700 | 1.000003 | -0.037402 | -0.00002 | 0.00000 | 0.00064 | -0.0000 | 0.0020 | -0.0020 | 0.0000 |

Table 9. Results for a circle and a wall; a = ∞.

| g/b | $k_2$ | $\dot{k}_2$ | $\dot{k}_{12}$ | $C^*_{F1}$ | $C^*_{F2}$ |
|---|---|---|---|---|---|
| 0.010 | 2.034029 | -11.51887 | -3.03403 | -18.09380 | 18.09380 |
| 0.020 | 1.942616 | -7.46859 | -2.94262 | -11.73164 | 11.73164 |
| 0.030 | 1.877678 | -5.70168 | -2.87768 | -8.95618 | 8.95618 |
| 0.040 | 1.826236 | -4.66366 | -2.82624 | -7.32567 | 7.32567 |
| 0.050 | 1.783295 | -3.96522 | -2.78330 | -6.22856 | 6.22856 |
| 0.060 | 1.746306 | -3.45672 | -2.74631 | -5.42980 | 5.42980 |
| 0.070 | 1.713768 | -3.06681 | -2.71377 | -4.81733 | 4.81733 |
| 0.080 | 1.684706 | -2.75665 | -2.68471 | -4.33014 | 4.33014 |
| 0.090 | 1.658447 | -2.50308 | -2.65845 | -3.93183 | 3.93183 |
| 0.100 | 1.634506 | -2.29131 | -2.63451 | -3.59919 | 3.59919 |
| 0.120 | 1.592194 | -1.95648 | -2.59219 | -3.07323 | 3.07323 |
| 0.140 | 1.555711 | -1.70265 | -2.55571 | -2.67452 | 2.67452 |
| 0.160 | 1.523729 | -1.50298 | -2.52373 | -2.36088 | 2.36088 |
| 0.180 | 1.495338 | -1.34151 | -2.49534 | -2.10724 | 2.10724 |
| 0.200 | 1.469882 | -1.20809 | -2.46988 | -1.89767 | 1.89767 |
| 0.250 | 1.416147 | -0.95764 | -2.41615 | -1.50426 | 1.50426 |
| 0.300 | 1.372872 | -0.78292 | -2.37287 | -1.22981 | 1.22981 |
| 0.350 | 1.337092 | -0.65439 | -2.33709 | -1.02791 | 1.02791 |
| 0.400 | 1.306931 | -0.55618 | -2.30693 | -0.87364 | 0.87364 |
| 0.450 | 1.281126 | -0.47898 | -2.28113 | -0.75238 | 0.75238 |
| 0.500 | 1.258781 | -0.41694 | -2.25878 | -0.65493 | 0.65493 |
| 0.600 | 1.222018 | -0.32407 | -2.22202 | -0.50905 | 0.50905 |
| 0.700 | 1.193062 | -0.25861 | -2.19306 | -0.40623 | 0.40623 |
| 0.800 | 1.169718 | -0.21062 | -2.16972 | -0.33084 | 0.33084 |
| 0.900 | 1.150550 | -0.17435 | -2.15055 | -0.27386 | 0.27386 |
| 1.000 | 1.134576 | -0.14628 | -2.13458 | -0.22977 | 0.22977 |
| 1.200 | 1.109603 | -0.10637 | -2.10960 | -0.16709 | 0.16709 |
| 1.400 | 1.091129 | -0.08006 | -2.09113 | -0.12576 | 0.12576 |
| 1.600 | 1.077037 | -0.06191 | -2.07704 | -0.09724 | 0.09724 |
| 1.800 | 1.066022 | -0.04893 | -2.06602 | -0.07685 | 0.07685 |
| 2.000 | 1.057238 | -0.03937 | -2.05724 | -0.06185 | 0.06185 |
| 2.500 | 1.041703 | -0.02435 | -2.04170 | -0.03825 | 0.03825 |
| 3.000 | 1.031762 | -0.01612 | -2.03176 | -0.02533 | 0.02533 |
| 4.000 | 1.020206 | -0.00814 | -2.02021 | -0.01279 | 0.01279 |
| 5.000 | 1.013987 | -0.00468 | -2.01399 | -0.00735 | 0.00735 |
| 6.000 | 1.010257 | -0.00294 | -2.01026 | -0.00461 | 0.00461 |
| 8.000 | 1.006192 | -0.00137 | -2.00619 | -0.00216 | 0.00216 |
| 10.000 | 1.004141 | -0.00075 | -2.00414 | -0.00118 | 0.00118 |

Table 10. Results for an ellipse and a circle; $a_1 = 2b$, $a_2 = b$.

| g/b | $k_1$ | $k_2$ | $k_{12}$ | $\dot{k}_1$ | $\dot{k}_2$ | $\dot{k}_{12}$ | $C_{F1}$ | $C_{F2}$ |
|---|---|---|---|---|---|---|---|---|
| 0.010 | 1.25049 | 1.24980 | -0.58373 | -2.4268 | -2.4463 | 2.6227 | -3.8120 | 4.4276 |
| 0.020 | 1.23092 | 1.23003 | -0.56220 | -1.6257 | -1.6446 | 1.8204 | -2.5536 | 3.1654 |
| 0.030 | 1.21662 | 1.21554 | -0.54595 | -1.2704 | -1.2887 | 1.4638 | -1.9955 | 2.6033 |
| 0.040 | 1.20505 | 1.20379 | -0.53246 | -1.0585 | -1.0762 | 1.2508 | -1.6627 | 2.2667 |
| 0.050 | 1.19523 | 1.19380 | -0.52072 | -0.9140 | -0.9312 | 1.1050 | -1.4357 | 2.0358 |
| 0.060 | 1.18664 | 1.18505 | -0.51023 | -0.8075 | -0.8241 | 0.9973 | -1.2684 | 1.8646 |
| 0.070 | 1.17900 | 1.17724 | -0.50069 | -0.7249 | -0.7409 | 0.9134 | -1.1386 | 1.7310 |
| 0.080 | 1.17209 | 1.17018 | -0.49191 | -0.6584 | -0.6738 | 0.8457 | -1.0342 | 1.6227 |
| 0.090 | 1.16579 | 1.16372 | -0.48374 | -0.6035 | -0.6184 | 0.7896 | -0.9480 | 1.5326 |
| 0.100 | 1.15999 | 1.15778 | -0.47609 | -0.5572 | -0.5715 | 0.7421 | -0.8752 | 1.4560 |
| 0.120 | 1.14962 | 1.14714 | -0.46205 | -0.4830 | -0.4963 | 0.6654 | -0.7587 | 1.3318 |
| 0.140 | 1.14056 | 1.13782 | -0.44936 | -0.4257 | -0.4380 | 0.6057 | -0.6687 | 1.2343 |
| 0.160 | 1.13252 | 1.12954 | -0.43774 | -0.3800 | -0.3913 | 0.5576 | -0.5969 | 1.1548 |
| 1.800 | 1.12531 | 1.12211 | -0.42700 | -0.3424 | -0.3528 | 0.5176 | -0.5379 | 1.0884 |
| 0.200 | 1.11878 | 1.11539 | -0.41700 | -0.3110 | -0.3205 | 0.4838 | -0.4885 | 1.0315 |
| 0.250 | 1.10483 | 1.10101 | -0.39455 | -0.2507 | -0.2582 | 0.4177 | -0.3939 | 0.9184 |
| 0.300 | 1.09343 | 1.08928 | -0.37494 | -0.2076 | -0.2132 | 0.3688 | -0.3261 | 0.8326 |
| 0.350 | 1.08390 | 1.07951 | -0.35749 | -0.1751 | -0.1792 | 0.3307 | -0.2751 | 0.7639 |
| 0.400 | 1.07580 | 1.07124 | -0.34175 | -0.1498 | -0.1527 | 0.2999 | -0.2353 | 0.7069 |
| 0.500 | 1.06277 | 1.05803 | -0.31425 | -0.1132 | -0.1140 | 0.2527 | -0.1778 | 0.6162 |
| 0.600 | 1.05278 | 1.04802 | -0.29080 | -0.0881 | -0.0877 | 0.2178 | -0.1384 | 0.5459 |
| 0.700 | 1.04492 | 1.04025 | -0.27043 | -0.0702 | -0.0688 | 0.1907 | -0.1102 | 0.4888 |
| 0.800 | 1.03860 | 1.03409 | -0.25249 | -0.0568 | -0.0550 | 0.1688 | -0.0893 | 0.4410 |
| 0.900 | 1.03344 | 1.02914 | -0.23654 | -0.0467 | -0.0445 | 0.1508 | -0.0734 | 0.4004 |
| 1.000 | 1.02918 | 1.02510 | -0.22224 | -0.0388 | -0.0365 | 0.1357 | -0.0610 | 0.3652 |

Table 11. Results for an ellipse and a circle; $a_1 = b$, $a_2 = 2b$.

| g/b | $k_1$ | $k_2$ | $k_{12}$ | $\dot{k}_1$ | $\dot{k}_2$ | $\dot{k}_{12}$ | $C_{F1}$ | $C_{F2}$ |
|---|---|---|---|---|---|---|---|---|
| 0.010 | 5.05016 | 1.73670 | -1.54440 | -8.7454 | -8.3825 | 8.8101 | -13.7372 | 13.9404 |
| 0.020 | 4.97982 | 1.66997 | -1.47340 | -5.8271 | -5.4679 | 5.8932 | -9.1531 | 9.3610 |
| 0.030 | 4.92860 | 1.62233 | -1.42152 | -4.5470 | -4.1919 | 4.6148 | -7.1423 | 7.3555 |
| 0.040 | 4.88719 | 1.58445 | -1.37942 | -3.7910 | -3.4400 | 3.8605 | -5.9550 | 6.1732 |
| 0.050 | 4.85198 | 1.55273 | -1.34351 | -3.2797 | -2.9327 | 3.3508 | -5.1518 | 5.3750 |
| 0.060 | 4.82114 | 1.52534 | -1.31195 | -2.9054 | -2.5623 | 2.9780 | -4.5638 | 4.7920 |
| 0.070 | 4.79359 | 1.50120 | -1.28367 | -2.6168 | -2.2776 | 2.6910 | -4.1104 | 4.3435 |
| 0.080 | 4.76862 | 1.47960 | -1.25794 | -2.3859 | -2.0506 | 2.4616 | -3.7478 | 3.9856 |
| 0.090 | 4.74574 | 1.46005 | -1.23430 | -2.1961 | -1.8646 | 2.2733 | -3.4496 | 3.6921 |
| 0.100 | 4.72459 | 1.44221 | -1.21238 | -2.0366 | -1.7089 | 2.1153 | -3.1991 | 3.4462 |
| 0.120 | 4.68653 | 1.41062 | -1.17271 | -1.7823 | -1.4621 | 1.8638 | -2.7996 | 3.0556 |
| 0.140 | 4.65291 | 1.38334 | -1.13744 | -1.5871 | -1.2742 | 1.6713 | -2.4930 | 2.7576 |
| 0.160 | 4.62278 | 1.35939 | -1.10559 | -1.4317 | -1.1260 | 1.5185 | -2.2488 | 2.5217 |
| 0.180 | 4.59546 | 1.33811 | -1.07651 | -1.3043 | -1.0057 | 1.3937 | -2.0488 | 2.3296 |
| 0.200 | 4.57047 | 1.31902 | -1.04971 | -1.1977 | -0.9061 | 1.2896 | -1.8814 | 2.1699 |
| 0.250 | 4.51600 | 1.27872 | -0.99050 | -0.9931 | -0.7182 | 1.0906 | -1.5600 | 1.8663 |
| 0.300 | 4.47022 | 1.24628 | -0.93972 | -0.8454 | -0.5864 | 0.9480 | -1.3279 | 1.6502 |
| 0.350 | 4.43088 | 1.21951 | -0.89513 | -0.7329 | -0.4890 | 0.8400 | -1.1512 | 1.4877 |
| 0.400 | 4.39654 | 1.19701 | -0.85534 | -0.6438 | -0.4143 | 0.7550 | -1.0113 | 1.3604 |
| 0.500 | 4.33920 | 1.16128 | -0.78655 | -0.5111 | -0.3080 | 0.6287 | -0.8028 | 1.1722 |
| 0.600 | 4.29307 | 1.13427 | -0.72841 | -0.4164 | -0.2368 | 0.5385 | -0.6541 | 1.0378 |
| 0.700 | 4.25515 | 1.11323 | -0.67811 | -0.3453 | -0.1866 | 0.4703 | -0.5423 | 0.9353 |
| 0.800 | 4.22349 | 1.09649 | -0.63387 | -0.2900 | -0.1499 | 0.4165 | -0.4555 | 0.8531 |
| 0.900 | 4.19678 | 1.08295 | -0.59448 | -0.2459 | -0.1222 | 0.3728 | -0.3863 | 0.7847 |
| 1.000 | 4.17403 | 1.07185 | -0.55908 | -0.2102 | -0.1008 | 0.3363 | -0.3302 | 0.7263 |

Table. 12. Comparison of 'exact' and calculated values of added masses and their derivatives for equal spheres.

| g/a | $k_1$(exact) | $k_1$(calc) | $\dot{k}_1$(exact) | $\dot{k}_1$(calc) | $k_{12}$(exact) | $k_{12}$(calc) | $\dot{k}_{12}$(exact) | $\dot{k}_{12}$(calc) | N |
|---|---|---|---|---|---|---|---|---|---|
| 0.010 | 0.570162 | 0.570146 | -0.57083 | -0.57062 | -0.216292 | -0.216276 | 0.72567 | 0.72541 | 100 |
| 0.020 | 0.565138 | 0.565129 | -0.44862 | -0.44806 | -0.209728 | -0.209719 | 0.60200 | 0.60137 | 100 |
| 0.030 | 0.561022 | 0.561018 | -0.37956 | -0.37935 | -0.204085 | -0.204080 | 0.53147 | 0.53099 | 100 |
| 0.040 | 0.557477 | 0.557474 | -0.33206 | -0.33190 | -0.199028 | -0.199025 | 0.48252 | 0.48242 | 100 |
| 0.050 | 0.554343 | 0.554341 | -0.29629 | -0.29621 | -0.194396 | -0.194394 | 0.44530 | 0.44521 | 100 |
| 0.060 | 0.551527 | 0.551526 | -0.26788 | -0.26782 | -0.190098 | -0.190097 | 0.41544 | 0.41533 | 100 |
| 0.070 | 0.548968 | 0.548967 | -0.24449 | -0.24444 | -0.186071 | -0.186070 | 0.39062 | 0.39057 | 100 |
| 0.080 | 0.546625 | 0.546625 | -0.22477 | -0.22478 | -0.182273 | -0.182273 | 0.36946 | 0.36947 | 100 |
| 0.090 | 0.544464 | 0.544464 | -0.20782 | -0.20782 | -0.178672 | -0.178672 | 0.35107 | 0.35107 | 100 |
| 0.100 | 0.542461 | 0.542461 | -0.19303 | -0.19303 | -0.175244 | -0.175244 | 0.33486 | 0.33486 | 100 |
| 0.120 | 0.538857 | 0.538857 | -0.16837 | -0.16837 | -0.168832 | -0.168832 | 0.30736 | 0.30736 | 100 |
| 0.140 | 0.535695 | 0.535695 | -0.14851 | -0.14851 | -0.162918 | -0.162918 | 0.28468 | 0.28468 | 100 |
| 0.160 | 0.532893 | 0.532893 | -0.13212 | -0.13212 | -0.157421 | -0.157421 | 0.26549 | 0.26549 | 100 |
| 0.180 | 0.530393 | 0.530393 | -0.11833 | -0.11833 | -0.152281 | -0.152281 | 0.24893 | 0.24893 | 100 |
| 0.200 | 0.528147 | 0.528147 | -0.10656 | -0.10656 | -0.147450 | -0.147450 | 0.23441 | 0.23441 | 100 |
| 0.250 | 0.523427 | 0.523427 | -0.08353 | -0.08353 | -0.136508 | -0.136508 | 0.20462 | 0.20462 | 100 |
| 0.300 | 0.519690 | 0.519690 | -0.06677 | -0.06678 | -0.126882 | -0.126882 | 0.18130 | 0.18130 | 100 |
| 0.350 | 0.516681 | 0.516681 | -0.05416 | -0.05416 | -0.118306 | -0.118306 | 0.16233 | 0.16233 | 80 |
| 0.400 | 0.514227 | 0.514227 | -0.04442 | -0.04443 | -0.110597 | -0.110597 | 0.14647 | 0.14647 | 80 |
| 0.500 | 0.510523 | 0.510523 | -0.03068 | -0.03068 | -0.097270 | -0.097270 | 0.12129 | 0.12129 | 80 |
| 0.600 | 0.507931 | 0.507931 | -0.02177 | -0.02177 | -0.086143 | -0.086143 | 0.10205 | 0.10205 | 80 |
| 0.700 | 0.506072 | 0.506072 | -0.01579 | -0.01579 | -0.076727 | -0.076727 | 0.08685 | 0.08685 | 80 |
| 0.800 | 0.504713 | 0.504713 | -0.01165 | -0.01165 | -0.068676 | -0.068676 | 0.07458 | 0.07458 | 80 |
| 0.900 | 0.503702 | 0.503702 | -0.00873 | -0.00873 | -0.061738 | -0.061738 | 0.06451 | 0.06451 | 80 |
| 1.000 | 0.502939 | 0.502939 | -0.00664 | -0.00664 | -0.055718 | -0.055718 | 0.05614 | 0.05614 | 80 |
| 10.000 | 0.500001 | 0.500001 | 0.00000 | 0.00000 | -0.000868 | -0.000868 | 0.00022 | 0.00022 | 80 |
| 20.000 | 0.500000 | 0.500000 | 0.00000 | 0.00000 | -0.000141 | -0.000141 | 0.00002 | 0.00002 | 80 |

Table 13. Comparison with Ref. [2] of values of $k_1$ and $k_{12}$ for equal spheres.

| | $k_1$ | | | $-k_{12}$ | | |
|---|---|---|---|---|---|---|
| g/b | 'exact' | calculated | Ref. [2] calc. | 'exact' | calculated | Ref. [2] calc. |
| 0.01 | 0.570162 | 0.570146 | – | 0.216292 | 0.216276 | – |
| 0.02 | 0.565138 | 0.565129 | 0.5614 | 0.209728 | 0.209719 | 0.2063 |
| 0.03 | 0.561022 | 0.561018 | 0.5591 | 0.204085 | 0.204080 | 0.2025 |
| 0.04 | 0.557477 | 0.557474 | 0.5562 | 0.199028 | 0.199025 | 0.1981 |
| 0.05 | 0.554343 | 0.554341 | 0.5540 | 0.194396 | 0.194394 | 0.1943 |
| 0.06 | 0.551527 | 0.551526 | 0.5512 | 0.190098 | 0.190097 | 0.1900 |
| 0.07 | 0.548968 | 0.548967 | 0.5486 | 0.186071 | 0.186070 | 0.1860 |
| 0.08 | 0.546625 | 0.546625 | 0.5464 | 0.182273 | 0.182273 | 0.1823 |
| 0.09 | 0.544464 | 0.544464 | – | 0.178672 | 0.178672 | – |
| 0.10 | 0.542461 | 0.542461 | 0.5421 | 0.175244 | 0.175244 | 0.1752 |

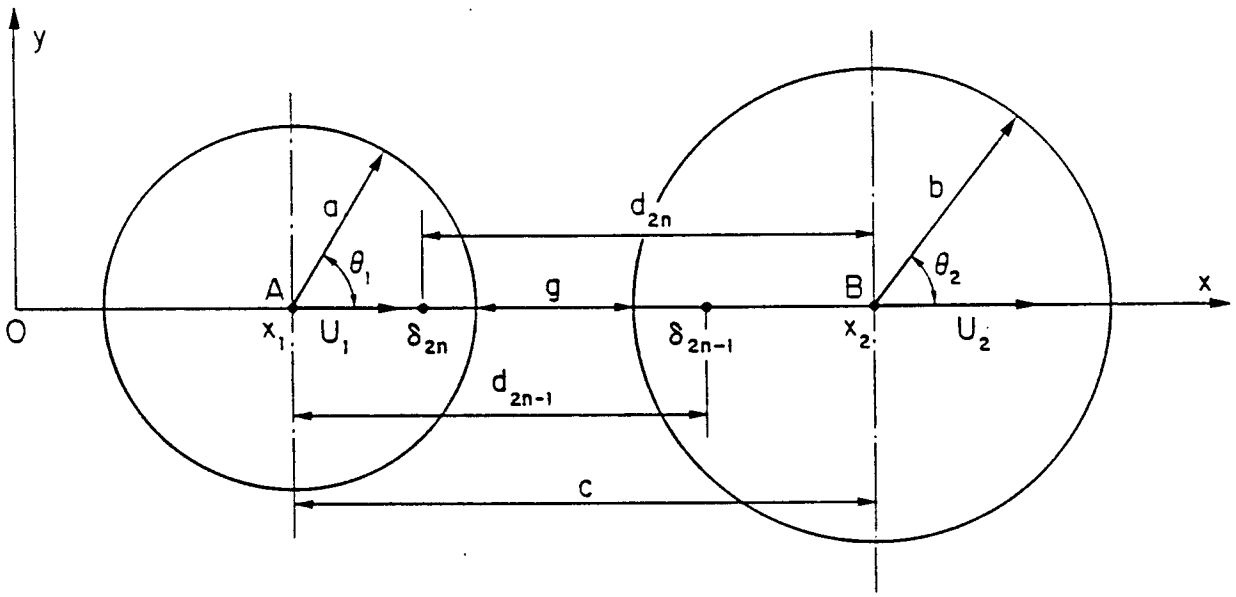


Figure 1. Definition sketch of two circles or spheres moving along their line of centers for method of successive images.

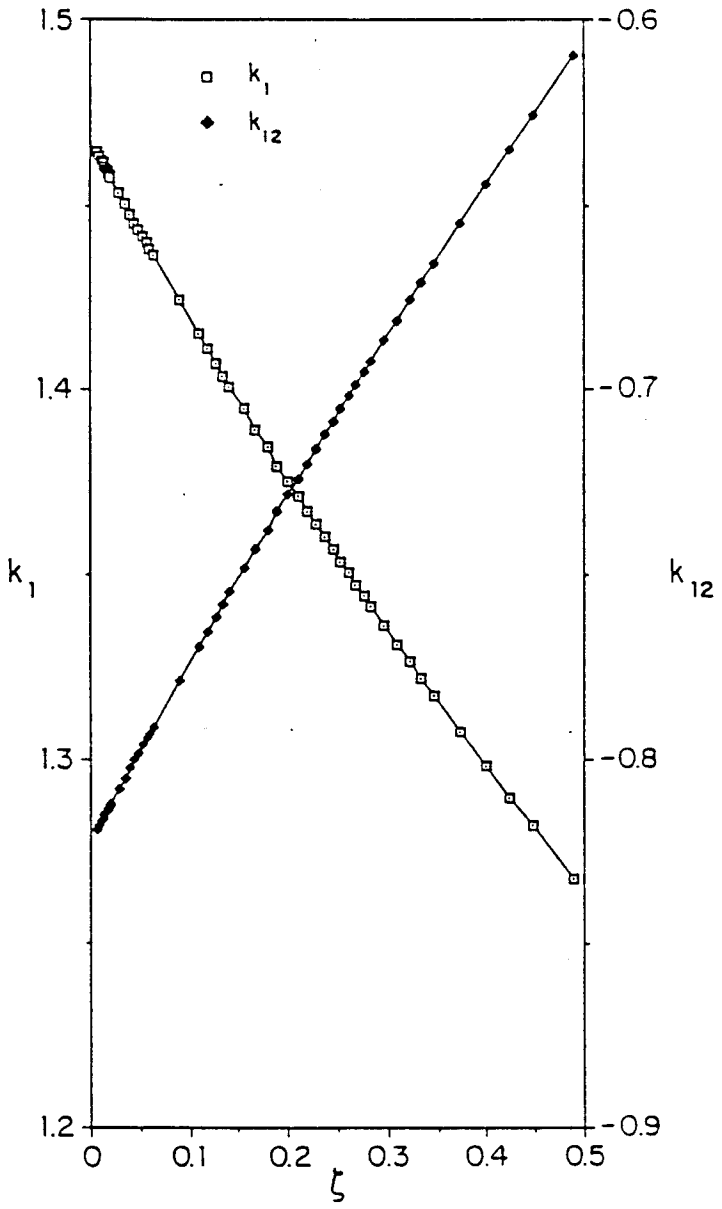


Figure 2. Graphs of added-mass coefficients against parameter $\zeta$.

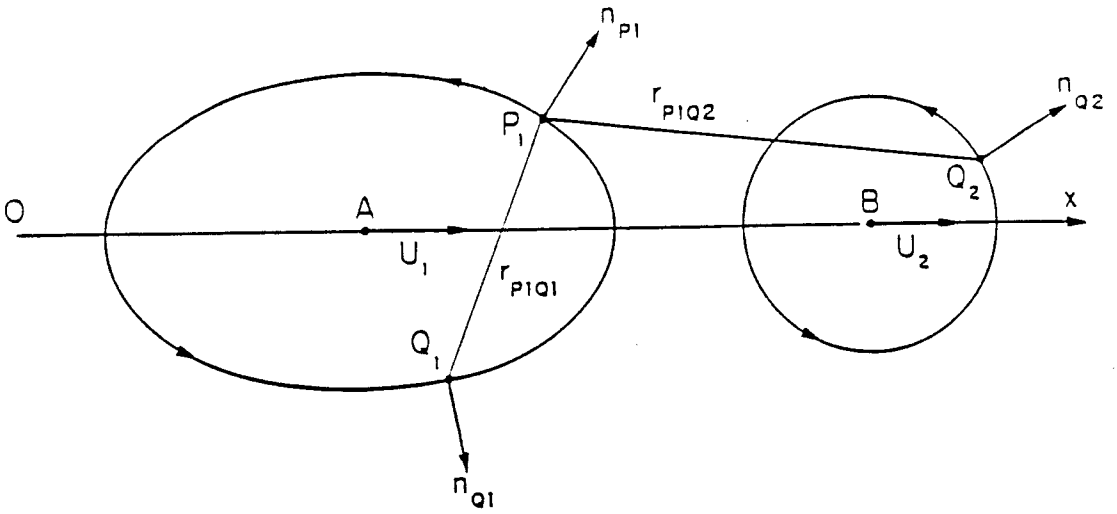


Figure 3. Sketch of two cylinders for method of integral equations.

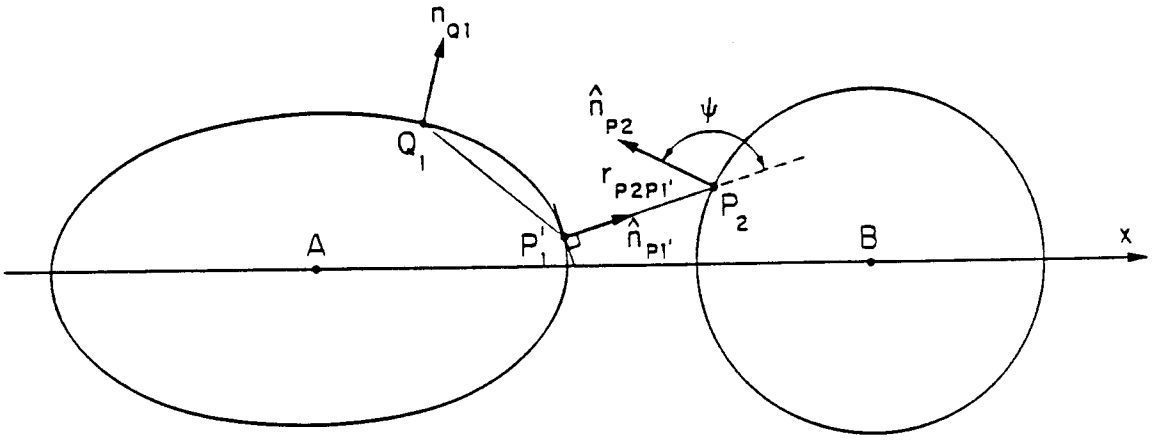


Figure 4. Illustration of procedure for eliminating peaks of integrand.

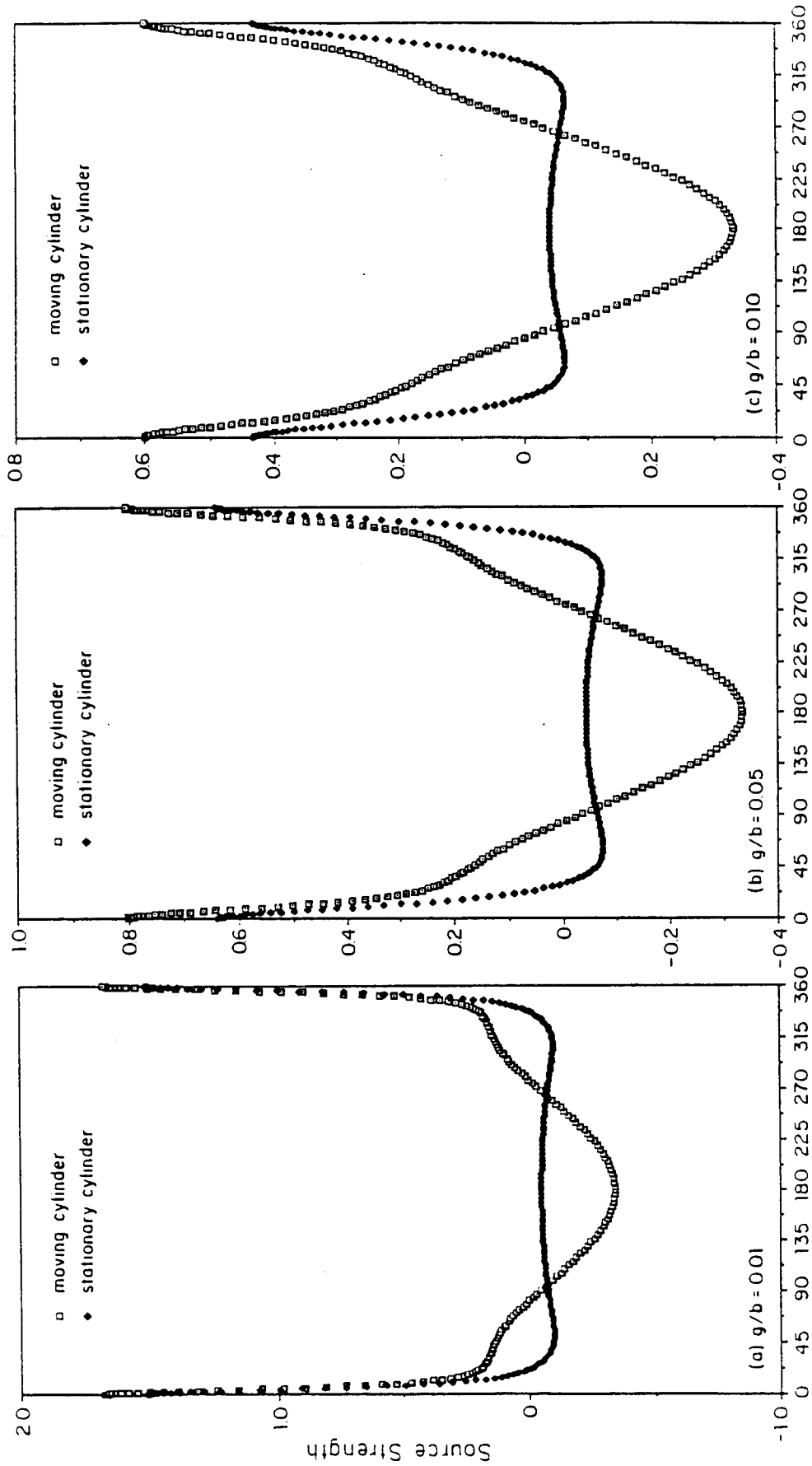


Figure 5. Source distributions on equal circles for $U_1 = 1$ and $U_2 = 0$.

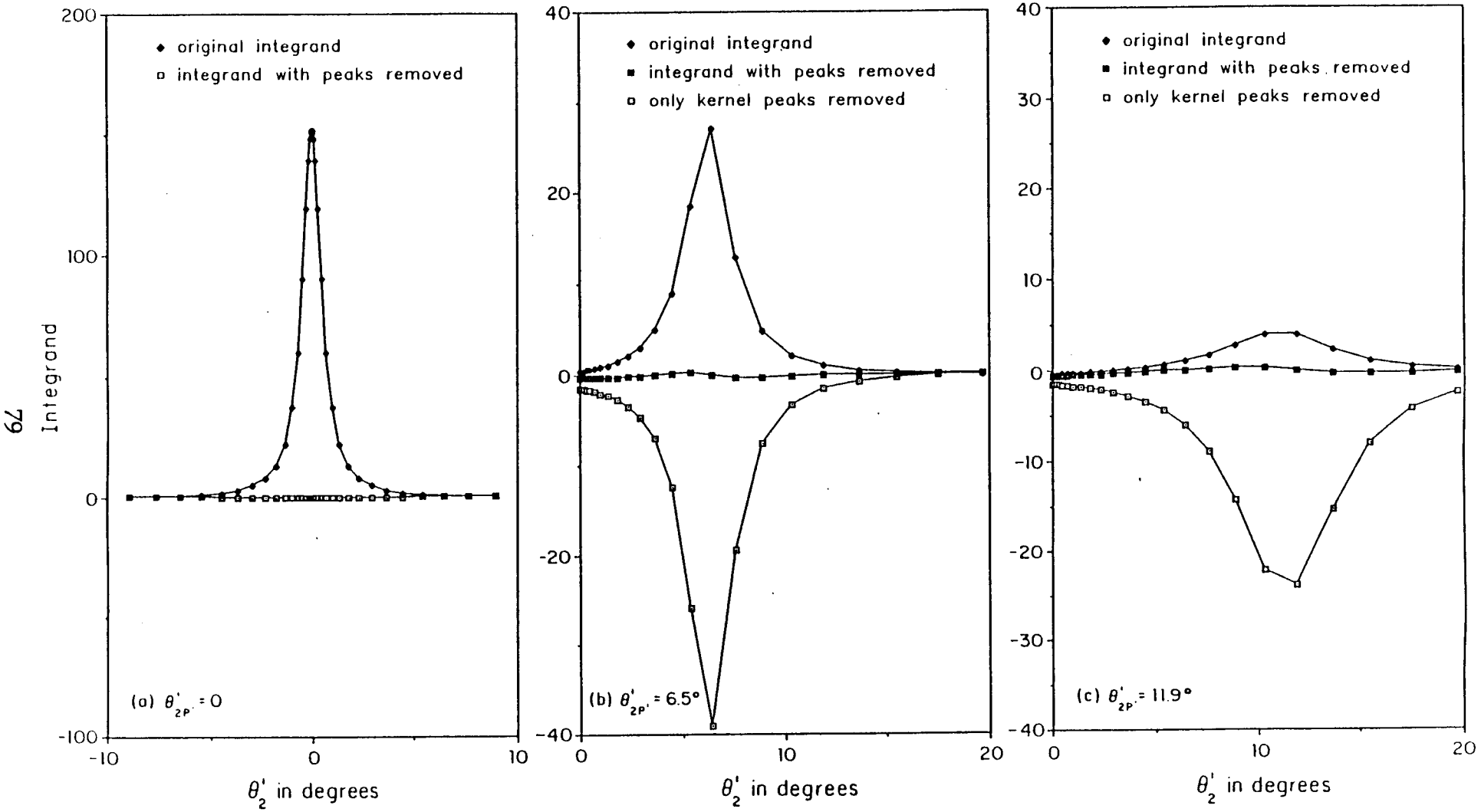


Figure 6. Integrands of moving circle for various fixed points on stationary one for a = b and g/b = 0.01.

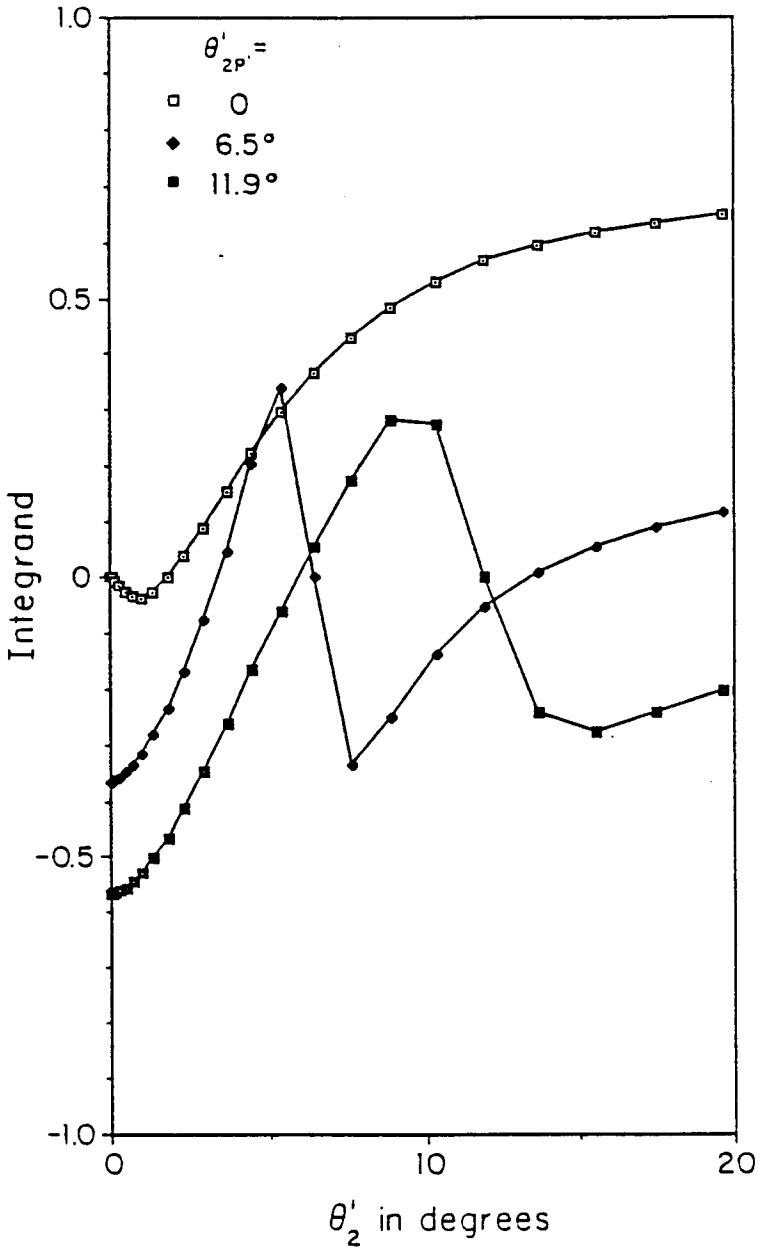


Figure 7. Magnified graphs of Fig. 6 with peaks of integrand removed.

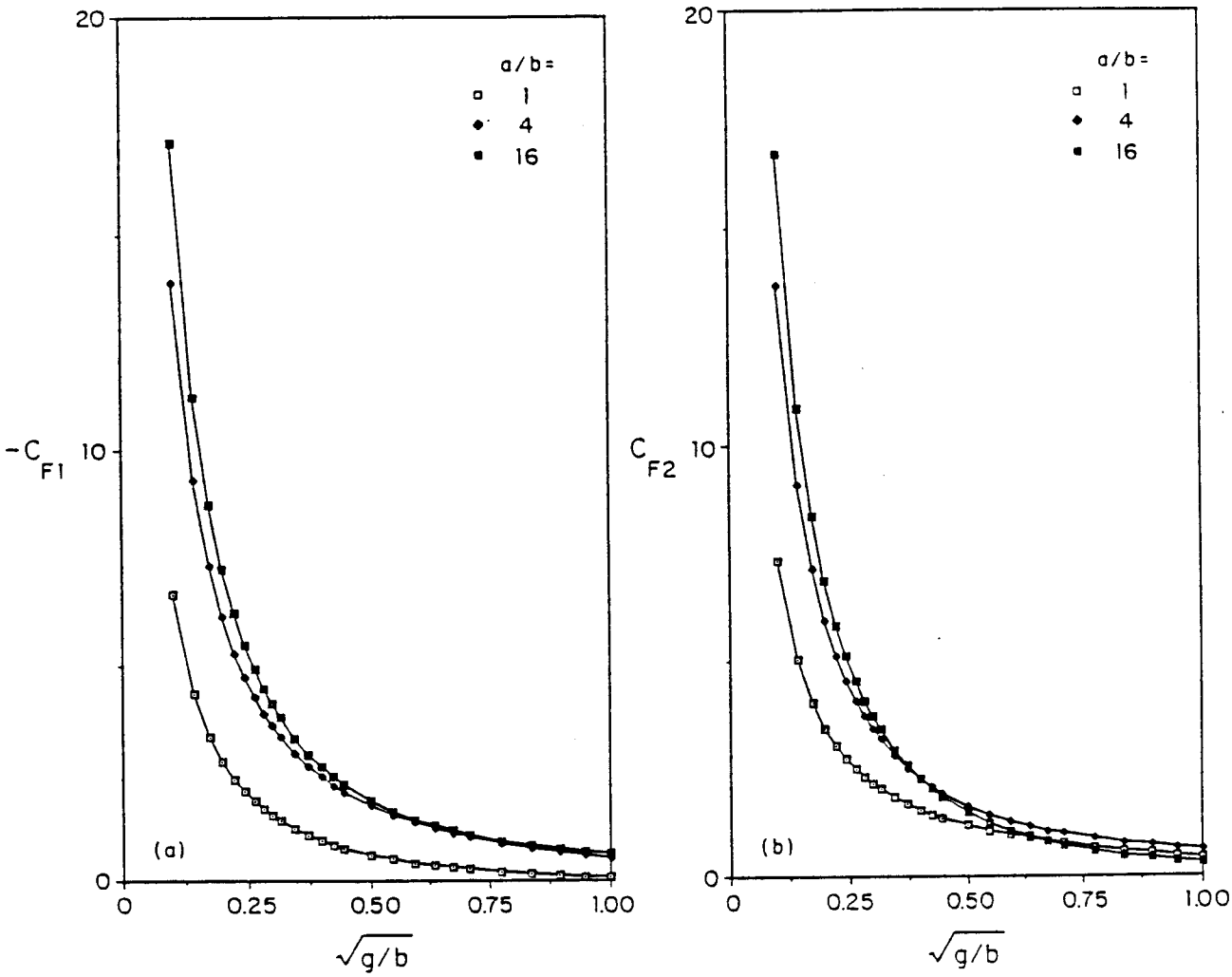


Figure 8. Force coefficients for a/b = 1, 4, 16 with smaller circle at rest.

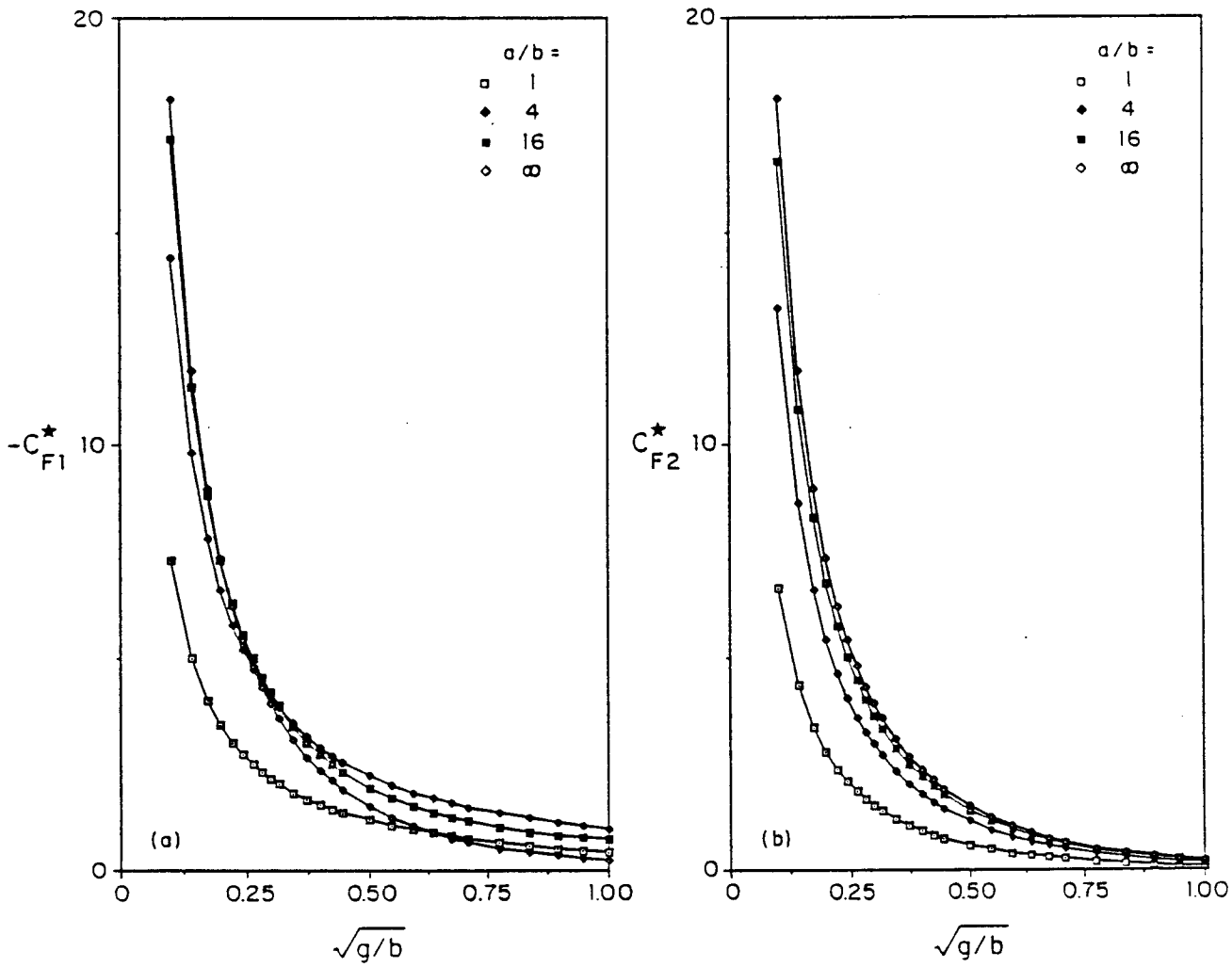


Figure 9. Force coefficients for a/b = 1, 4, 16, ∞ with larger circle at rest.